Terahertz Communications and Sensing for 6G and Beyond: A Comprehensive View

Wei Jiang, *Senior Member, IEEE,* Qiuheng Zhou, Jiguang He, *Senior Member, IEEE,* Mohammad Asif Habibi, *Member, IEEE,* Sergiy Melnyk, Mohammed El-Absi, *Member, IEEE,* Bin Han, *Senior Member, IEEE,* Marco Di Renzo, *Fellow, IEEE,* Hans Dieter Schotten, Fa-Long Luo, *Fellow, IEEE,* Tarek S. El-Bawab, *Fellow, IEEE,* Markku Juntti, *Fellow, IEEE,* Mérouane Debbah, *Fellow, IEEE,* Victor C. M. Leung, *Life Fellow, IEEE*

***Abstract*—The next-generation wireless technologies, commonly referred to as the sixth generation (6G), are envisioned to support extreme communications capacity and in particular disruption in the network sensing capabilities. The terahertz (THz) band is one potential enabler for those due to the enormous unused frequency bands and the high spatial resolution enabled by both short wavelengths and bandwidths. Different from earlier surveys, this paper presents a comprehensive treatment and technology survey on THz communications and sensing in terms of the advantages, applications, propagation characterization, channel modeling, measurement campaigns, antennas, transceiver devices, beamforming, networking, the integration of communications and sensing, and experimental testbeds. Starting from the motivation and use cases, we survey the development and historical perspective of THz communications and sensing with the anticipated 6G requirements. We explore the radio propagation, channel modeling, and measurements for THz band. The transceiver requirements, architectures, technological challenges, and approaches together with means to compensate for the high propagation losses by appropriate antenna and beamforming solutions. We survey also several system technologies required by or beneficial for THz systems. The synergistic design of sensing and communications is explored with depth. Practical trials, demonstrations, and experiments are also summarized. The paper gives a holistic view of the current state of the art and highlights the issues and challenges that are open for further research towards 6G**

***Index Terms*—6G, Beamforming, Imaging, Integrated Communications and Sensing, ICAS, Localization, Positioning, Sensing, Terahertz, THz Communications, THz channels**

I. Introduction

TODAY, the fifth generation (5G) mobile networks are still in the way of being massively deployed worldwide [1], but both academia and industry have shifted their focus to the next-generation technologies, commonly referred to as the sixth generation (6G) [2]. A collection of research groups, standardization bodies, regulatory organizations, and government agencies [3] has initiated a variety of programs to discuss the 6G vision [4] and develop key technologies [5], as we will elaborate later in Sec. II-A. To support disruptive applications, such as virtual and augmented reality [6], Internet of Things [7], Industry 4.0, connected and autonomous vehicles [8], and yet-to-be-conceived use cases like Metaverse, holographic-type telepresence [9], Tactile Internet [10], digital twin [11], full immersiveness [12], multi-sense experience, and blockchain [13], 6G requires significantly stringent performance, e.g., hyper rates on the order of terabits-per-second (Tbps) [14], ultra-reliability, near-zero latency, and massive connectivity density, far beyond what its predecessor can offer [15].

It is envisioned that the major mission of mobile networks needs to be transformed from *connected people and things* to *connected intelligence* [16]. In addition to enhanced communications capabilities including the evolution of enhanced mobile broadband (eMBB+), the evolution of ultra-reliable low-latency communications (URLLC+), and the evolution of massive machine-type communications (mMTC+) [17], as shown in Fig.1, wireless *sensing* along with networked artificial intelligence (AI) are expected to play critical roles in 6G and beyond to meet the demands of information and communications technology after 2030 [18]. Driven by the continuous improvement in frequency bands, bandwidths, antennas, devices, and signal processing, 6G and beyond are able to integrate sensing and communications into a unified system [19]. This integration enables 6G and beyond to *see* the physical world through electromagnetic (EM) waves [20]. It offers high-resolution sensing, localization, imaging, and environment reconstruction capabilities to improve communications performance. Also, it supports a wide range of

Manuscript received xxxx xx, 2023; (*Corresponding author: Wei Jiang (e-mail: wei.jiang@dfki.de)*)

W. Jiang, Q. Zhou, S. Melnyk, and H. D. Schotten are with the Intelligent Networking Research Group, German Research Centre for Artificial Intelligence (DFKI), Kaiserslautern, Germany.

J. He is with the Technology Innovation Institute, Abu Dhabi, United Arab Emirates, and also with Centre for Wireless Communications, University of Oulu, Oulu 90014, Finland (e-mail: jiguang.he@tii.ae).

M. El-Absi is with the Institue of Digital Signal Processing, University of Duisburg-Essen, Duisburg, Germany.

M. A. Habibi, B. Han, and H. D. Schotten are with the Department of Electrical and Computer Engineering, Rheinland-Pfalzische Technische Universitat Kaiserslautern-Landau (RPTU), Germany.

M. Di Renzo is with Université Paris-Saclay, CNRS, CentraleSupélec, Laboratoire des Signaux et Systèmes, 3 Rue Joliot-Curie, 91192 Gif-sur-Yvette, France. (marco.di-renzo@universite-paris-saclay.fr)

F. L. Luo is with the Electrical and Computer Engineering Department, University of Washington, Seattle, WA 98195, USA. (email: falong@uw.edu)

T. S. El-Bawab is with the School of Engineering at the American University of Nigeria (AUN), Nigeria.

M. Juntti is with Center for Wireless Communications (CWC) at the University of Oulu, Finland.

M. Debbah is with Khalifa University of Science and Technology, P O Box 127788, Abu Dhabi, UAE (email: merouane.debbah@ku.ac.ae).

Victor C. M. Leung is with the College of Computer Science and Software Engineering at Shenzhen University, China, and is also with the Laboratory for Wireless Networks and Mobile Systems at the University of British Columbia (UBC), Canada.

novel applications beyond communications such as object tracking, security screening, remote sensing, process monitoring, simultaneous localization and mapping (SLAM), gesture recognition, and activity detection [21].

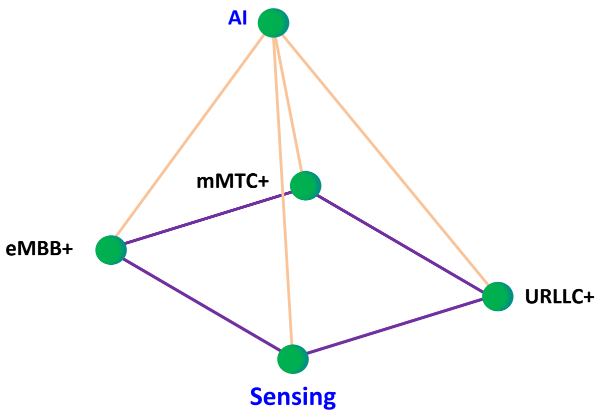

Fig. 1. Envision of 6G usage scenarios, where sensing and AI will be critical pillars in addition to enhanced communications services [17].

A. Why do 6G and beyond need the THz band?

The THz band has attracted a lot of interest in recent years and is recognized as a promising technique for 6G [22]. Prior to stepping into the technical details, the authors of this article would like to first clarify a fundamental question that might still have confusion or disputes in some prior literature. That is, *why do we need to exploit the THz band in 6G and beyond*? We try to address this concern from the perspectives of both THz communications and THz sensing, as well as their synergy.

1) THz Communications: At the World Radiocommunication Conference (WRC) held in 2019 a.k.a WRC-19, the International Telecommunication Union - Radiocommunication (ITU-R) assigned a total of 13.5 GHz spectrum, consisting of a group of high-frequency bands, for the deployment of 5G millimeter wave (mmWave) communications [1], see Sec. II-B. Despite the spectral redundancy of mmWave bands, it might not be sufficient to meet the growing need for bandwidth over the next decade. There are enormous spectral resources at higher frequencies that were already used for a wide variety of non-cellular applications such as remote sensing, radio astronomy, and radar [23], to name a few. With the advancement in antenna technology and radio-frequency components, these frequencies previously considered unsuitable for mobile communications due to their unfavorable propagation characteristics become technologically usable [24].

Fig. 2 illustrates the whole EM spectrum, consisting of radio, microwave, infrared (IR), visible light, ultraviolet, X-rays, and Gamma rays, from the lower to higher frequencies. It is noted that the definition of the EM spectrum in the general case differs from the naming of frequency bands from the perspective of wireless communications, as shown in this figure. Based on these considerations, THz is considered a suitable candidate to realize Tbps communications under the current level of hardware and signal-processing technologies. The reasons are explained as follows:

- **Spectrum scarcity of the sub-6 GHz band**: Favourable propagation characteristics of sub-6 GHz frequencies facilitate the use of sophisticated transmission technologies such as massive multi-input multi-output (MMIMO) [25], non-orthogonal multiple access (NOMA) [26], and high-order modulation like 1024-ary quadrature amplitude modulation (1024QAM) to achieve high spectral efficiency. However, spectrum scarcity and non-continuity pose a significant challenge to achieving higher rates. Even if the sub-6 GHz band ultimately determines a bandwidth of 1 GHz for International Mobile Telecommunications (IMT) services, a Tbps link can only be realized under extreme spectral efficiency of 1000 bps/Hz, as suggested by the Shannon capacity $R = B\log(1+S/N)$. Unfortunately, such a level of this performance metric is infeasible in the foreseeable future, as the peak spectral efficiency specified for 5G, see ITU-R M.2410 [27], is 30 bps/Hz (in ideal conditions).
- **Insufficient mmWave bandwidth for Tbps**: By far, there are a total of 13.5 GHz spectral resources available within the mmWave band below 100 GHz. A data rate of 1 Tbps can only be achieved with transmission schemes having a spectral efficiency of approaching 100 bps/Hz, which is currently infeasible for sub-6 GHz frequencies and more challenging to implement for mmWave signals. Therefore, *the only possibility for Tbps communications relies on massively abundant frequencies above 100 GHz*.
- **Constraints of the optical bands**: Despite the enormous available spectrum in optical bands at IR [28], visible-light [29], and ultraviolet frequencies [30], several issues limit the practicality of optical wireless communications (OWC). The restriction of low transmission power due to hardware constraints and eye-safety purposes, the effects of several types of atmospheric attenuation on the signal propagation (e.g., fog, rain, dust, or pollution), high diffuse reflection losses, and the impact of misalignment between transmitter and receiver lead to limited data rates and short transmission ranges [31], locking its feasibility of large-scale use for mobile systems in 6G and beyond.
- **Adverse health effects of extreme high bands**: Ionizing radiation, including ultraviolet, X-rays, and Gamma rays, poses a significant risk to human health as it has strong energy power to dislodge electrons and generate free radicals that can lead to cancer. The adverse health effects of ionizing radiation are controllable if used with care, so it is used in specific fields such as radiotherapy, photography, semiconductor manufacturing, and nuclear medicine, among others. However, it is still too dangerous for personal communications [22].

Unlike ionizing radiation, THz frequencies are non-ionizing because their photon energy is not sufficient (0.1 to 12.4meV, which is over three orders of magnitude weaker than ionizing photon energy levels) to release an electron from an atom or a molecule, where typically 12eV is required for ionization. The THz band offers abundant spectral resources, ranging from tens of gigahertz to several terahertz, depending on the transmission distance. This makes the available bandwidth

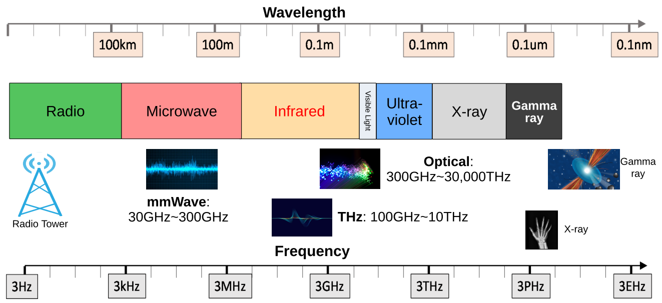

Fig. 2. The electromagnetic spectrum and the positions of mmWave, THz, and optical bands.

more than ten times greater than that of mmWave bands, while the operating frequency is at least one order of magnitude below the optical bands. In addition, the technology required to make Tbps transmission over the THz band a reality is rapidly advancing, and the development of new transceiver architectures and antennas built upon novel materials with remarkable properties are finally overcoming one of the significant challenges [32].

2) THz Sensing: As we know, the spatial resolution of a propagated signal becomes much finer with increasing frequencies, thereby enabling high-definition spatial differentiation [33]. In addition to THz communications, THz sensing (including positioning, imaging, and spectroscopy) exploit the tiny wavelength on the order of micrometers and the frequency-selective resonances of various materials over the measured environment to gain unique information based on the observed signal signature [34]. Compared with wireless sensing over other bands, THz sensing offers the following advantages:

- **High resolution and penetration capability**: Although low-frequency signals are able to sense, detect, and localize objects, as radar [23] and Global Navigation Satellite System (GNSS), THz sensing/positioning can improve the resolution due to tiny wavelengths, even for objects hidden from direct view. THz waves are able to penetrate a variety of non-conductive materials, e.g., plastics, fabrics, paper, ceramics, and dielectric substances. This allows THz sensing to detect hidden objects, structural defects, and layers beneath surfaces, making it useful in security screening, quality control, process monitoring, and material characterization [35].
- **Non-ionizing radiation**: Compared to X-rays and Gamma rays, THz waves have much lower photon energy, making them non-ionizing [36]. This means THz sensing is generally considered safe for biological samples and humans, allowing for non-destructive and non-invasive imaging and diagnosing.
- **Low environmental interference**: In contrast to visible or IR radiation [28], THz waves are less vulnerable to environmental factors such as ambient light, fog, or smoke. It allows THz sensing for outdoor or adverse conditions, expanding its usability in fields such as remote sensing, atmospheric monitoring, and outdoor security.
- **Spectroscopic analysis**: THz waves interact with molecules in a characteristic manner, leading to unique spectral fingerprints. THz spectroscopy provides valuable information about molecular vibrations and rotational transitions, enabling the identification and analysis of chemical substances, including explosives, drugs, and biomolecules [37]. It is particularly effective for identifying substances with distinct THz absorption or reflection properties.

3) Synergy between THz communications and THz sensing: As discussed above, the THz band offers not only massive spectral resources for wireless communications but also unique advantages in sensing, positioning, imaging, and spectroscopy [33]. Hence, it attracted a lot of interest recently as a key enabler for implementing integrated sensing and communications (ISAC) for 6G and beyond [38]. On top of implementing THz communications and THz sensing in a unified system, these dual-functional wireless networks offer a great synergy through **sensing-aided communication** [39], [40] and **communication-aided sensing** [41], as elaborated in Sec. IX.

Using sensing information in communications may be one of the significant benefits of ISAC, which enables a more deterministic and predictable propagation channel. It facilitates the design of efficient communications algorithms and protocols, such as sensing-aided channel estimation [42], predictive beamforming served by sensing [43], [44], fast beam alignment and tracking [45], and link blockage mitigation [46]. On the other hand, mobile communications networks also provide significant opportunities and benefits for network sensing or sensing as a service [47]. Nodes share sensing results through the mobile network, where multiple network nodes (base stations, user equipment, etc.) can act as a collaborative sensing system [48]. This collaboration, achieved through sensing data fusion, reduces measurement uncertainty and provides a larger coverage area, as well as higher sensing accuracy and resolution.

B. Motivations and Contributions

Recently, the wireless community has published a lot of research articles and surveys on the topic. The current survey papers tend to focus on specific aspects of THz communications, such as antenna fabrication [55], propagation characterization [58], measurement [63], channel modeling [64], beamforming [57], and hardware [53]. These surveys are more beneficial for researchers who are focusing on a particular aspect of THz communications and need an exhaustive collection of the existing research outcomes. On the other hand, some magazine articles such as [51], [66] offer overviews which cover relatively wide ranges of aspects but are rather concise on many topics. Moreover, prior literature primarily concentrated on the THz communications from the perspective of the conventional wireless community, while the THz sensing has received much less attention. Last but not least, most of the literature does not take into account the particular applications, requirements, and scenarios of 6G.

Responding to the discussion above, our article presents a comprehensive treatment and technology survey about THz

TABLE I
A COMPARISON OF THIS SURVEY WITH THE EXISTING WORKS.

Reference	Year	Content Coverage							
		6G	Sensing	ISAC	THz Channel	THz Ant. & Beamforming	THz Device& Transceiver	Synergy w. 6G Key Tech.	THz Trial& Experiment
Mukherjee and Gupta [49]	2008					✓	✓		
Ostmann and Nagatsuma [50]	2011				✓	✓	✓		✓
Nagatsuma *et al.* [24]	2016						✓		
K. M. S. Huq *et al.* [51]	2019	✓			○		○	○	
K. Tekbiyik *et al.* [52]	2019				✓	✓	✓		✓
Z. Chen *et al.* [53]	2019					✓	✓		
M. Naftaly *et al.* [54]	2019		✓						
Y. He *et al.* [55]	2020					✓			
S. Ghafoor *et al.* [56]	2020	○			✓	○			
B. Ning *et al.* [57]	2021					✓			
F. Lemic *et al.* [58]	2021	○			✓	✓			
H. Sarieddeen *et al.* [59]	2021	○	✓			✓		✓	
E. Castro-Camus1 *et al.* [60]	2021		✓						
C.-X. Wang *et al.* [61]	2021	✓			✓	✓	○		
D. Moltchanov *et al.* [62]	2022	✓			✓	○			
C. Chaccour *et al.* [34]	2022	✓	✓	✓				✓	
C. Han *et al.* [63]	2022				✓				○
D. Serghiou *et al.* [64]	2022	✓			✓				
I. F. Akyildiz *et al.* [65]	2022	✓			✓		✓		✓
A. Shafie *et al.* [66]	2022	○				○	○	✓	
This survey paper	2023	✓	✓	✓	✓	✓	✓	✓	✓

Note:
For each column, the ✓symbol means that this aspect is discussed in detail in the reference, the ○ symbol stands for that this aspect is only mentioned briefly, and the blank indicates that this aspect is missing at all.

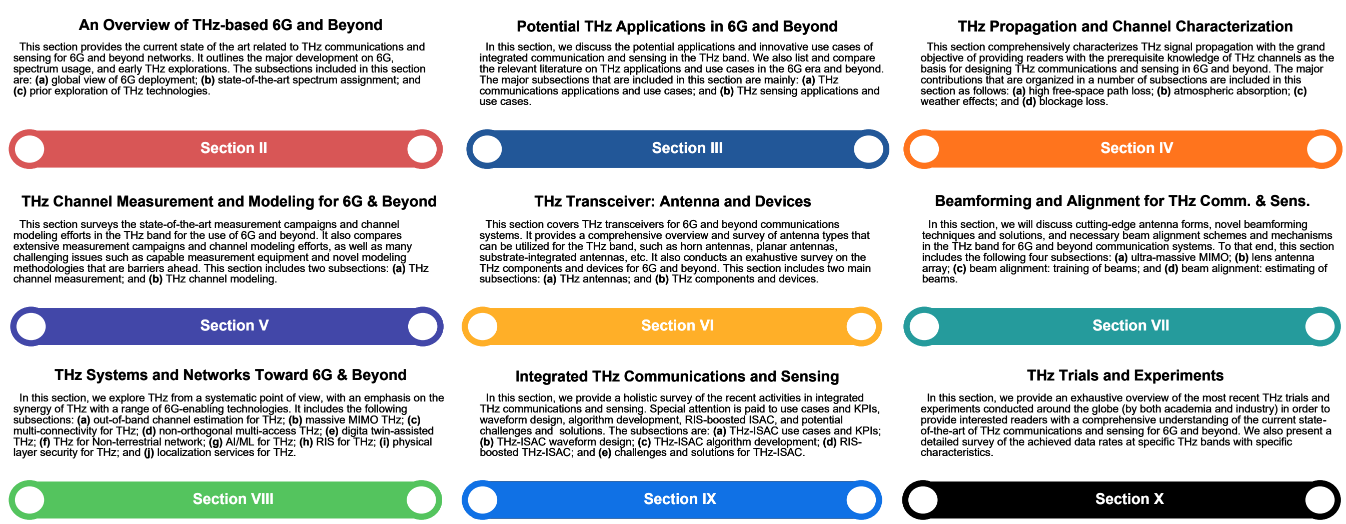

Fig. 3. Outline of the structure of this survey.

communications and sensing to clarify the advantages of THz over other bands for 6G and beyond, potential THz-based 6G applications, THz signal propagation characterization, THz channel modeling, THz measurement, THz antennas, photonic-electronic devices for THz transceiver, beam forming, beam alignment, THz networking, the synergy with other potential 6G technologies, THz-based integrated sensing and communications, and THz experimental test-beds. Table I compares this work with the existing ones in terms of the covered topics, aiming at justifying the novelty and contributions of this survey. From an application and implementation perspectives, we hope that this work can provide researchers in THz communication, THz sensing, and 6G with a holistic view of the current state of the art and highlight the issues and challenges that are open for further research.

The major contributions of this survey include:

- First, this work aims to answer a fundamental question: *Why do 6G and beyond need to exploit the THz band*?

It clarifies the comparative advantages of THz over other frequency bands in both communications and sensing in the scenarios of 6G and beyond.

- We provide a state-of-the-art overview of related fields by summarizing the global 6G development, latest spectrum assignment for IMT, and early exploration efforts in THz technologies.
- This article envisions potential THz-based communications and sensing applications for 6G and beyond.
- This survey comprehensively characterizes THz signal propagation, covering the phenomenon of *path loss, atmospheric absorption, weather effects, and blockage*.
- Up-to-date THz measurement campaigns by means of three measurement methods, i.e., *frequency-domain vector network analyzer (VNA), time-domain sliding, and time-domain spectroscopy (TDS)*, are outlined.
- THz channel modeling, both deterministic and statistical, are surveyed.
- This survey provides readers with the necessary knowledge required to design and build transceivers for THz communications and sensing, including the recent advances in THz antennas, THz electronic devices, and THz photonic devices.
- We elaborate on how to compensate for the large propagation loss through beamforming over large-scale antenna arrays. The fundamentals of ultra-massive multi-input multi-output (UMMIMO), lens antenna array, beam tracking, beam estimation, and beam alignment are introduced.
- From a systematic perspective, we explore the paradigms for THz networking, with an emphasis on the synergy of THz communications and sensing with other 6G-enabling technologies, covering MMIMO, UMMIMO, NOMA, reconfigurable intelligent surfaces (RIS), non-terrestrial networks, digital twins, AI and machine learning (ML). Moreover, we discuss security, localization, integrated communications and sensing, multi-connectivity, and channel awareness for THz networks.
- This article discusses the building blocks, opportunities, and challenges for ISAC over the THz band, elaborating its unique advantages, use cases, key performance indicators (KPIs), joint waveform design, efficient algorithm design, and potential solutions.
- Last but not least, we list the latest advances in THz trials and experiments to give readers an insightful view of the practicality of THz communications and sensing.

C. The Structure of this Survey

Overall, this survey aims to provide researchers with a holistic view of the current state of the art about all issues required to design and build THz-based wireless communications and sensing systems for 6G and beyond. Also, we hope this work can highlight the issues and challenges that are open for further research to speed up the research endeavors. To improve the readability, an outline of the survey is illustrated in Fig.3.

II. An Overview of THz-based 6G Systems

With the objective of facilitating an insightful view, this section summarizes the current state of the art in the related fields. First, Sec. II-A offers a global view of 6G development, followed by the status of spectrum usage for the IMT services worldwide in Sec. II-B. Then, the early THz exploration efforts are listed in Sec. II-C.

A. Global View of 6G Development

At the beginning of 2019, South Korea's three network operators and U.S. Verizon were in a dispute with each other, vying for the title of being the world's first provider of the 5G communications services. This event marked the arrival of the 5G era [1]. In the past few years, the term '5G' has remained one of the most prominent buzzwords in the media, drawing unprecedented attention from the whole society. Apart from continuously enhancing network capacity and improving system performance as previous generations had done, 5G expands mobile communications services from human-centric to human-and-things, and meanwhile from the consumer market to vertical industries [67]. This has substantially increased the potential scale of mobile subscriptions from billions (i.e. equivalent to the world's population) to almost countless interconnectivity among humans, machines, and things.

In 2020, the outbreak of the COVID-19 pandemic led to a significant loss of human life worldwide and imposed unprecedented challenges on societal and economic activities. However, this public health crisis has underscored the unique role of telecommunications networks and digital infrastructure in keeping society operational and families connected. This is particularly relevant for the values of 5G applications, such as remote health care, online education, mobile working, autonomous vehicles, unmanned delivery, and smart manufacturing [68]. In July 2018, the International Telecommunication Union - Telecommunication (ITU-T) standardization sector established a focus group called *Technologies for Network 2030* with the aim of studying the capabilities of networks for 2030 and beyond [69].

In 2020, the European Commission (EC) initiated the beyond 5G program, under its Horizon 2020 calls — *ICT-20 5G Long Term Evolution* and *ICT-52 Smart Connectivity beyond 5G* — where a batch of pioneer research projects was sponsored. At the beginning of 2021, the EC launched its 6G flagship research project *Hexa-X* [70], followed by the second phase of European level 6G research *Hexa-X-II* in early 2023 [71]. The EC has also announced its strategy to accelerate investment in '*Gigabit Connectivity*' including 5G and 6G to shape Europe's digital future [72]. In October 2020, the Next Generation Mobile Networks (NGMN) alliance announced its new '*6G Vision and Drivers*' project, intending to provide early and timely guidelines for global 6G activities. The first report for this project was published in April 2021 [73]. At its meeting in February 2020, the ITU-R sector decided to start studying future technology trends for the future evolution of International Mobile Telecommunications (IMT-2030) [74].

Motivated by the revolutionary force of 5G, the governments of many countries recognized the significance of mobile communications technologies for driving economic prosperity and sustainable growth. In the past years, many countries have set up research initiatives officially or announced ambitious plans for the development of 6G. The world's first 6G effort, '*6G-Enabled Wireless Smart Society and Ecosystem (6Genesis) Flagship Program*', was carried out by the University of Oulu in April 2018, as part of the Academy of Finland's flagship program [75]. This project focuses on groundbreaking 6G research, with four interrelated strategic areas including wireless connectivity, distributed computing, devices and circuit technology, and services and applications. In September 2019, the world's first 6G white paper '*key drivers and research challenges for 6G ubiquitous wireless intelligence*' was published as an outcome of the first 6G Wireless Summit [76]. Subsequently, a series of white papers have been published, covering twelve specific areas of interest, such as ML, edge intelligence, localization, sensing, and security.

In October 2020, the Alliance for Telecommunications Industry Solutions (ATIS) established the '*Next G Alliance*', an industry-led initiative aimed at advancing North American mobile technology leadership in 6G over the next decade [77]. Founding members of the initiative include leading companies such as AT&T, T-Mobile, Verizon, Qualcomm, Ericsson, Nokia, Apple, Google, Facebook, and Microsoft. Next G Alliance places a strong emphasis on technology commercialization and seeks to encompass the full lifecycle of 6G research, development, manufacturing, standardization, and market readiness. In addition to this, SpaceX, a U.S. company known for its revolutionary reusable rockets, announced the Starlink project in 2015 [78]. This project aims to deploy a very large-scale low Earth orbit (LEO) communications satellite constellation to offer ubiquitous internet access services across the whole planet. The Federal Communications Commission (FCC) approved its initial plan of launching 12,000 satellites, and an application for 30,000 additional satellites is currently under consideration. The Starlink service is currently available to the public in a few countries and regions. Although it is an exaggeration to claim that Starlink will replace 5G or be considered 6G, the impact of such a very large-scale LEO satellite constellation on 6G and beyond should be taken into account seriously in the mobile industry.

In November 2019, the Chinese Ministry of Science and Technology kicked off the research and development efforts for 6G technology, in collaboration with five other ministries or national institutions. The event also marked the establishment of a working group, named *IMT-2030(6G) Promotion Group*, responsible for managing and coordinating the program, and an expert group comprising 37 top researchers from academia, research institutes, and industry. In June 2021, IMT-2030(6G) Promotion Group released its white paper '*6G Vision and Candidate Technologies*', outlining the state-of-the-art research findings of the group [79]. It covers the 6G vision, the driving forces behind its development, potential use cases, ten candidate technologies, and additional insights.

In late 2017, the Japanese Ministry of Internal Affairs and Communications formed a working group to investigate next-generation wireless technologies. Their research findings indicated that 6G should offer transmission rates at least ten times faster than 5G, near-instant connectivity, and massive connection of up to ten million devices per square kilometer. In December 2020, Japan established the *Beyond 5G Promotion Consortium (B5GPC)* with the objective of expediting the development of 6G while enhancing the country's international competitiveness through industry-academia-government collaboration. B5GPC published its inaugural white paper '*Beyond 5G white paper: Message to the 2030s*' in March 2022 [80], summarizing the requirements and expectations of each industry for 6G, the necessary capabilities, and technological trends. South Korea announced its ambition to set up the world's first 6G trial in 2026. In addition, they have unveiled the *K-Network 2030* initiative, which aims to sponsor the development of key 6G technologies, e.g., developing cloud-native networks on South Korean-made AI chips, launching a low-orbit communications satellite by 2027, and creating an open radio access network (RAN) ecosystem for domestic firms.

Last but not least, the German Federal Ministry of Education and Research (BMBF) announced in February 2021 a new funding program called '6G Vision' as part of Germany's broader initiative to establish the country as a leader in 6G technology. In August 2021, under the umbrella organization and networking of a leading project named *the 6G platform*, four 6G research hubs, i.e., 6G-life, 6GEM, 6G RIC, and Open6GHub, were built [81]. A total budget of approximately 250 million euros was assigned, covering 160 research groups at overall 21 universities and 15 research institutes, as well as more than 40 small and medium enterprises. In the subsequent year, eighteen 6G industry projects, such as 6G-ANNA, 6G-TakeOff, 6G-Terafactory, and 6G-Next, and seven projects on resilience, e.g., HealthNet, AKITA, and ConnRAD, were established [82].

In France, the National Agency for Research (ANR) launched in 2021 a national acceleration strategy (the France 2030 plan [https://www.gouvernement.fr/france-2030]) on future communication technologies with a focus on digital transition, telecommunication, and global innovation. On May 1st, 2023, under the France 2023 plan, the project called PEPR 5G and Future Networks started whose objective is to develop advanced technologies for 5G and future networks, by integrating their environmental and societal impacts and the security of the transmitted data. The ANR PEPR 5G project is comprised of 10 interlinked projects, among which the project titled NF-SYSTERA (Devices and SYStems for high-speed links in the sub-TERAhertz range), whose objective is to explore frequency bands beyond 90 GHz for future wireless communication systems in the sub-THz and THz range.

B. Up-to-date Spectrum Usage for IMT

Over the past few decades, the evolution of mobile communications has followed certain key criteria:

- *the signal bandwidth becomes increasingly wide*;
- *the operating frequency band is increasingly high*; and
- *the spectral demand is increasingly large*.

We witnessed that each new-generation cellular system demanded more spectral resources and utilized a larger channel

TABLE II
EVOLUTION OF CELLULAR SYSTEMS.

	Mobile Generation				
	1G	2G	3G	4G	5G
Main Standard	AMPS	GSM	WCDMA	LTE-Advanced	NR
First Deployment Year	1979	1991	2000	2009	2019
Peak Data Rate	10 kbps (signalling)	384 kbps	2 Mbps	1 Gbps	20 Gbps
Signal Bandwidth	30 kHz	200 kHz	5 MHz	100 MHz	1 GHz
Frequency Bands	800 MHz	900 MHz & 1800 MHz	Below 2.1 GHz	Sub-6 GHz	Sub-6 GHz/ millimeter wave (mmWave)

bandwidth to support more system capacity and realize a higher data rate than its predecessor.

Let us have a brief review of the history of cellular systems. Initially, the signal bandwidth of a channel in the first generation (1G) system is 20 kHz to 30 kHz that is already sufficient to carry the analog voice signal of a mobile user. The low-frequency band under 1 GHz with favorable propagation characteristics was a preferred choice for system designers at that time. For example, the most dominating 1G standard - Advanced Mobile Phone System (AMPS) [83] - utilizes a pair of 25 MHz (for downlink and uplink, respectively) to carry maximally 832 analog voice users at each cell cluster. Global System for Mobile Communications (GSM) [84] first launched in 1991 supports 1,000 subscribers within a spectrum of $2\times 25\,\mathrm{MHz}$, where eight digital-voice users are multiplexed over each 200 kHz channel using time division multiple access (TDMA).

For the third generation (3G) system, Wideband Code-Division Multiple Access (WCDMA) employs a much wider bandwidth of 5 MHz to carry tens of users per channel simultaneously by means of spread-spectrum modulation techniques [85]. Meanwhile, the applied frequency band migrated gradually from low frequencies to higher frequencies, crossing over 2 GHz for the first time due to the demand for more spectral resources. Further, Long-Term Evolution Advanced (LTE-Advanced), as the unified fourth generation (4G) standard [86], supports a maximal bandwidth of 100 MHz using carrier aggregation so as to realize the peak rate of 1 Gbps in the downlink. Accordingly, its frequency band spans over a wider range, from 450 MHz to 6 GHz, since hundreds of megahertz spectral resources are needed to satisfy the explosive traffic growth of mobile Internet. Until 4G, the cellular systems operated in low-frequency bands below 6 GHz, which are referred to as *the sub-6 GHz band* when high-frequency bands are considered in 5G new radio (NR) [1]. A summary of previous mobile generations with an emphasis on bandwidth and operating frequency bands is given in Table II.

During the ITU-R WRC held in 2015, also known as WRC-15, an item on the agenda was designated to identifying high-frequency bands above 24 GHz that could be used for IMT-2020 mobile services. After conducting follow-up studies after WRC-15, the ITU-R found that ultra-low latency and high data-rate applications would require larger, contiguous spectrum blocks. As a result, WRC held in 2019, a.k.a. WRC-19, assigned a total of 13.5 GHz of the spectrum, consisting of a group of high-frequency bands, for the deployment of 5G mmWave communications. That is

- 24.25-27.5 GHz
- 37-43.5 GHz
- 45.5-47 GHz
- 47.2-48.2 GHz
- 66-71 GHz

Meanwhile, the Third Generation Partnership Project (3GPP) specified the relevant spectrum for 5G NR, which was divided into two frequency ranges:

- FR1 - the First Frequency Range, including the sub-6 GHz frequency band from 450 MHz to 6 GHz
- FR2 - the Second Frequency Range, covering 24.25 GHz to 52.6 GHz.

Initial mmWave deployments are expected to operate in 28 GHz (3GPP NR band n257 and n261) and 39 GHz (3GPP n260) with time-division multiplexing (TDD) mode, followed by 26 GHz (3GPP n258), as specified in Table III.

TABLE III
OPERATING FREQUENCY BANDS SPECIFIED BY 3GPP FOR NR IN FR2. SOURCE: [1]

NR Band	Freq. Range [GHz]	Duplex Mode	Regions
n257	26.5-29.5	TDD	Asia, Americas
n258	24.25-27.5	TDD	Asia, Europe
n259	39.5-43.5	TDD	Global
n260	37.0-40.0	TDD	Americas
n261	27.5-28.35	TDD	Americas

C. Prior Exploration of THz

The term *terahertz* was initially used in the 1970s to describe the spectral line frequency coverage of a Michelson interferometer or the frequency coverage of point contact diode detectors [87]. Before that, spectroscopists had coined this term for emission frequencies below the far IR range, which is the lowest frequency part of IR radiation with a frequency range of about 300 GHz to 20 THz. Millimeter wave refers to the frequency band from 30 GHz to 300 GHz. Hence, the border between the far IR and THz, and the border between mmWave and THz, are still rather blurry. Typically, the THz band refers to EM waves with a frequency band from 0.1 THz to 10 THz. However, other definitions, e.g., 300 GHz to 3 THz, are used parallelly. The difference in using frequency (THz) and wavelength (mmWave) for naming leaves an ambiguity of the range from 100 GHz to 300 GHz, which is also referred to as *upper-mmWave* or *sub-THz* by some researchers. It is envisaged that 5G mainly focuses on the frequency bands below 100 GHz while 6G and beyond will cross over this frequency point. The current trend seems to give more emphasis on using cm and low mmWaves for enhancing communications in 6G, but the THz band is still very critical for sensing.

In order to avoid harmful interference to Earth Exploration Satellite Service (EESS) and radio astronomy operating in the spectrum between 275 GHz and 1 THz, the ITU-R WRC-15 has initiated the activity called '*Studies towards an identification for use by administrations for land-mobile and fixed services applications operating in the frequency range 275–450 GHz*'. At the WRC-19 conference, a new footnote was added to the radio regulations, allowing for the open of the spectrum between 275 GHz and 450 GHz to land mobile and fixed services. Together with the already assigned spectrum below 275 GHz, a total of 160 GHz spectrum, containing two big contiguous spectrum bands with 44 GHz (i.e., from 252 GHz to 296 GHz) and 94 GHz bandwidth, respectively, is available for THz communications without specific conditions necessary to protect EESS [88].

The *mmWave Coalition*, a group of innovative companies and universities united in the objective of removing regulatory barriers to technologies using frequencies ranging from 95 GHz to 275 GHz, submitted comments in January 2019 to the FCC and the National Telecommunications and Information Administration (NTIA) for developing a sustainable spectrum strategy and urged NTIA to facilitate the access to spectrum above 95 GHz. In March 2019, the FCC announced that it opens up the use of frequencies between 95 GHz and 3 THz in the United States, provided 21.2 GHz of spectrum for unlicensed use and permitted experimental licensing for 6G and beyond. In the year 2016, the Defense Advanced Research Projects Agency (DARPA), in collaboration with prominent entities from the semiconductor and defense industries such as Intel, Micron, and Analog Devices, established the Joint University Microelectronics Program (JUMP), comprising six research centers with the goal of addressing both current and emerging challenges in the realm of microelectronic technologies. One such center, the *Center for Converged TeraHertz Communications and Sensing (ComSecTer)*, is focused on the development of advanced technologies tailored to meet the requirements of a future cellular infrastructure.

The first attempt in building a wireless communications system at THz frequencies started in 2008 with the foundation of a Terahertz Interest Group (IGTHz) under the IEEE 802.15 umbrella. In May 2014, Task Group 3d was formed to standardize a switched point-to-point communications system operating in the frequencies from 60 GHz to the lower THz bands. During the meeting in March 2016, the supporting documents for IEEE 802.15.3d were approved, and the call for proposals was issued. Based on the proposal reviews and two sponsor recirculation ballots, IEEE 802.15.3d-2017 was ratified by the IEEE Standards Association (SA) Standards Board in September 2017 [89]. IEEE 802.15.3d-2017 specifies an alternative Physical (PHY) layer at the lower THz frequency band from 252 GHz to 325 GHz for switched point-to-point connections. This standard aims for a maximum speed of over 100 Gbps with eight bandwidths configurations from 2.16 GHz to 69.12 GHz and effective coverage from tens of centimeters to a few hundred meters [90].

III. Potential Applications of THz in 6G and Beyond

The massive amount of spectrum at THz frequencies offers opportunities for ultra-fast wireless applications [51]. It also introduces a new level of flexibility in mobile system design, as THz links can be utilized for wireless backhaul among base stations, which enables ultra-dense architecture, accelerates network deployment, and reduces costs associated with site acquisition, installation, and maintenance. Due to the tiny wavelengths of THz signals, the antenna dimension is very small, opening up possibilities for innovative applications such as nanoscale communications for nanoscale devices or nanomachines, on-chip communications, the Internet of Nano-Things, and intra-body networks [58]. Moreover, THz signals can also be used beyond communication, facilitating high-definition sensing, imaging, and positioning of the surrounding physical environment [91]. This offers the potential to efficiently implement integrated communications and sensing at the THz band. Table IV lists and compares the literature with this survey in terms of potential THz applications and use cases.

A. Terahertz Communications Applications

a) Terabit Cellular Hotspots: The proliferation of mobile and fixed users with high-throughput demand in densely populated urban areas or specific locations, such as industrial sites, necessitates the deployment of ultra-dense networks. The utilization of the THz band can offer an abundance of spectral resources and ultra-wide bandwidth for small cells, which possess a relatively short coverage distance and high likelihood of line-of-sight (LoS) paths, allowing for Terabit communications links. These small cells cater to both static and mobile users in both indoor and outdoor settings, providing specific applications such as ultra-high-definition video delivery, information shower, high-quality virtual reality, and holographic-type communications [9]. By incorporating conventional cellular networks operating in low-frequency bands, a heterogeneous network, consisting of a macro-base-station tier and a small-cell tier, can facilitate seamless connectivity and full transparency across a wide coverage area and global roaming, thus fulfilling the extreme performance requirements of 6G and beyond mobile networks [51].

b) Terabit Campus/Private Networks: THz frequencies provide a means for implementing super-high-rate, ultra-reliable, and hyper-low-latency connectivity within a private or campus network for specific applications such as Industry4.0 and Tactile Internet [10]. This allows for seamless interconnection between ultra-high-speed optical networks and production devices with no discernible speed or delay difference between wireless and wired links. In addition, abundant bandwidths at THz frequencies also make massive connection density a reality [63]. These capabilities facilitate the deployment of industrial networks, linking a vast number of sensors and actuators within a factory, and campus networks providing high data-throughput, low-latency, and high-reliability connections for equipment and machines such as automated guided vehicle (AGV) in a logistic center.

c) Terabit Device-To-Device and Vehicle-to-Everything: THz communications represent a promising tool for providing direct Tbps links between devices in close proximity [92]. Indoor usage scenarios, such as homes or offices, can benefit from the formation of particular device-to-device (D2D) links among a set of personal or commercial devices [93]. Applications such as multimedia kiosks and ultra-high-speed data transfer between personal devices can be supported with Tbps links, enabling the transfer of the equivalent content of a blue-ray disk to a high-definition large-size display in less than one second. THz communications could also have a significant impact on Brain-Computer Interface (BCI) applications, enabling the transfer of vast amounts of collected brain-wave data to the computer that processes the data. In computer vision, THz communications can facilitate the transfer of high-definition video data to platforms running machine learning-based analytical software. Additionally, Tbps D2D links can be applied in outdoor settings for vehicle-to-everything scenarios [94], providing high-throughput, low-latency connectivity between vehicles or between vehicles and surrounding infrastructure [95].

d) Secure Wireless Communication: The use of large-scale antenna arrays can compensate for the path loss and atmospheric attenuation challenges of THz communications. These arrays can provide high gain and narrow beamforming, enabling long-distance communications links while minimizing interference and eavesdropping risks [109]. Additionally, the use of ultra-wide signal bandwidth and spread spectrum techniques can enhance the security of THz communications. Spread spectrum techniques spread the signal over a wide range of frequencies, making it harder for an eavesdropper to intercept the signal. However, it is worth noting that THz communications face unique security challenges that must be addressed. For example, THz waves can penetrate some materials, including clothing and certain types of packaging, which could potentially be exploited by malicious actors [112].

e) Terabit Wireless Backhaul: The installation of fiber optical connections is typically time-consuming and costly, and it may not always be feasible to deploy public optical networks within certain buildings or areas due to property owner objections. However, the next-generation mobile network is expected to be highly heterogeneous, requiring high-throughput backhaul or fronthaul connectivity between network elements such as macro base stations, small cells, relays, and distributed antennas. Highly directive THz links can provide ultra-high-speed wireless backhaul or fronthaul [97], reducing the time and cost of installation and maintenance while enabling greater flexibility in network architecture and communications mechanisms [100]. In addition, mobile or fixed users in rural or remote areas nowadays suffer from worse coverage and low quality of service (QoS). If a cost-efficient and flexible solution cannot be guaranteed, the digital divide between rural areas and major cities will increase. As a wireless backhaul extension of the optical fiber [32], THz wireless links can work well as an essential building block to guarantee a universal telecommunications service with high-quality, ubiquitous connections everywhere.

f) Terahertz Nano-Communications: As we know, the minimal size of an antenna used for the transmission of terahertz signals can be on the magnitude order of micrometers [103]. Intuitively, it will enable wireless connection among nanoscale machines or nanomachines using nanoscale antennas for very tiny specific equipment that performs particular tasks at the nanoscale, such as a biosensor injected into the human blood vessel. Each component of a nanomachine is up to a few hundred cubic nanometers in size, and the size of the entire device is in the order of a few cubic micrometers at most. Several specific use cases of THz nano-communications are provided by [31], i.e.,

- *Health Monitoring:* Sodium, glucose, and other ions in the blood, cholesterol, cancer biomarkers, or the presence of different infectious agents can be detected utilizing nanoscale biosensors injected into the human body or embedded under the skin. A set of biosensors distributed within or around the body, comprising a body sensor network, could collect relevant physical or biochemical data related to a human's health [37].
- *Nuclear, Biological, and Chemical Defense:* Chemical and biological nanosensors are able to detect harmful chemicals and biological threats in a distributed manner. One of the main benefits of using nanosensors rather than classical macroscale or microscale sensors is that a chemical composite can be detected in a concentration as low as one molecule and much more timely than classical sensors [36].
- *Internet-of-Nano-Things:* Using THz nano-communications to interconnect nanoscale machines, devices, and sensors with existing wireless networks [101] and the Internet makes a truly cyber-physical system that can be named as the Internet of Nano-Things (IoNT) [107]. The IoNT enables disruptive applications that will reshape the way humans work or live.
- *On-Chip Communication:* THz communications can provide an efficient and scalable approach to inter-core connections in on-chip wireless networks using planar nano-antenna arrays to create ultra-high-speed links [111]. This novel approach will expectedly fulfill the stringent requirements of the area-constraint and communication-intensive on-chip scenario by its high bandwidth, low latency, and low overhead.

B. Terahertz Sensing Applications

a) Terahertz Sensing: At THz frequencies, the spatial resolution of a signal becomes much finer due to the tiny wavelengths, allowing for high-definition spatial differentiation [19]. THz sensing techniques take advantage of the frequency-selective resonances of various materials in the measured environment, as well as the small wavelengths, typically on the order of micrometers [38]. This enables the extraction of unique information based on the observed

TABLE IV
A SURVEY OF THZ APPLICATIONS AND USE CASES FOR 6G AND BEYOND.

Reference	**THz Communications**							**THz Sensing**		
	Hotspot	**Campus**	**D2D**	**Vehicle**	**Security**	**Backhaul**	**Nanocom.**	**Sensing**	**Imaging**	**Positioning**
H. Sarieddeen *et al.* [33]								✓	✓	✓
K. M.S Huq *et al.* [51]	✓		○	✓		✓	○	○		
K. Tekbiyik *et al.* [52]			○	✓	✓	✓	✓	○	○	○
Z. Chen *et al.* [53]	○						✓	✓	✓	✓
Y. He *et al.* [55]							✓		✓	
B. Ning *et al.* [57]				✓	✓	○	○	✓	○	○
F. Lemic *et al.* [58]							✓			
C. Chaccour *et al.* [34]				✓		✓	○	✓	✓	○
H. Sarieddeen *et al.* [91]								✓	✓	✓
J. M. Jornet *et al.* [96]							✓			
J, Bo Kum *et al.* [97]						✓				
C. Han *et al.* [98]		○		✓		✓	✓	○	○	○
J. M. Eckhardt *et al.* [95]				✓						
S. Ju *et al.* [99]				✓						✓
G. Ke *et al.* [94]			✓	✓						
K. Rikkinen *et al.* [100]						✓				
J. M. Jornet *et al.* [101]							✓			
A. Faisal *et al.* [102]			○	○			✓	✓	✓	✓
J. M. Jornet *et al.* [103]							✓			
K.O. Kenneth *et al.* [104]								✓	✓	
C.-X. Wang *et al.* [61]						✓	✓	○	○	○
S. Helal *et al.* [105]				✓	✓			✓	✓	✓
Q. H. Abbasi *et al.* [37]							✓			
H. Park *et al.* [106]									✓	
Akyildiz and Jornet [107]							✓			
Z. Chen *et al.* [108]					✓	✓		✓		✓
I. B. Djordjevic *et al.* [109]			✓		✓	✓				
Z. Fang *et al.* [110]					✓					
Y. Yang *et al.* [111]							✓			
H. Wymeersch *et al.* [19]					✓			✓	✓	✓
J. Ma *et al.* [112]					✓					
A. A. Mamrashev *et al.* [36]							✓			
A. A. Boulogeorgos *et al.* [32]	✓	✓	✓			✓				
M. Lotti *et al.* [113]									✓	
S. Helal *et al.* [105]								✓		
N. A. Abbasi *et al.* [93]			✓							
C. Zandonella [35]									✓	
O. Li *et al.* [38]	✓	✓					✓		✓	
E. Castro-Camus1 *et al.* [60]									✓	
This survey paper	✓	✓	✓	✓	✓	✓	✓	✓	✓	✓

Note:
For each column, the ✓symbol means that this application is discussed in detail in the reference, the ○ symbol stands for that this application is only mentioned briefly, and the blank indicates that this application is missing at all.

signal signature. THz signals can penetrate non-conducting materials like plastics, fabrics, paper, wood, and ceramics, but they face challenges when penetrating metal materials or when water heavily attenuates their radiation power. The specific strength and phase variations of THz signals caused by different thicknesses, densities, or chemical compositions of materials enable the accurate identification of physical objects [105].

b) Terahertz Imaging: Using THz radiation to form images has many particular technical advantages over microwaves and visible light. THz imaging [106] exhibits high spatial resolution due to smaller wavelengths and ultra-wide bandwidths with moderately sized hardware than imaging using low frequencies. Compared with infrared and visible light, THz waves have better penetration performance, making common materials relatively transparent before THz imaging equipment. There are many security screening applications, such as checking postal packages for concealed objects, allowing THz imaging through envelopes, packages, parcels, and small bags to identify potential hazardous items [35]. Based on the property that THz radiation is non-ionizing and therefore no known health risk to biological cells except for heating has motivated its application in the human body, where ionizing radiation, i.e., ultraviolet, X-Ray, and Gamma Ray, will raise high health risks. Therefore, THz imaging is suitable for the stand-off detection of items such as firearms, bombs, and explosive belts hidden beneath clothing in airports, train stations, and border crossings [60].

c) Terahertz Positioning: It is envisioned that 6G and beyond are required to offer high-accurate positioning and localization in both indoor and outdoor environments, in addition to communications services, which GNSS and conventional multi-cell-based localization techniques using low-frequency bands fail to provide. Devices incorporating THz sensing and THz imaging will likely also provide centimeter-level localization anywhere [114]. On the other hand, leveraging THz imaging for localization has unique benefits compared to other methods. The THz imaging can localize users in the non-line-of-sight (NLoS) areas, even if their travel paths to the base station experience more than one reflection (e.g., multiple bounces). High-frequency localization techniques are based on the concept of SLAM [113], in which the accuracy is improved by collecting high-resolution images of the environment, where the THz imaging mentioned above can provide such high-resolution images. SLAM-based techniques consist of three main steps: imaging the surrounding environment, the estimation of ranges to the user, and the fusion of images with the estimated ranges. Since SLAM deals with relatively slow-moving objects, there is sufficient time to process high-resolution THz measurements. Such measurements can hold sensing information, resulting in complex state models comprising the fine-grained location, size, and orientation of target objects, as well as their electromagnetic properties and material types [91].

IV. THz Propagation and Channel Characterization

Although we have a lot of experience with radio channels over lower frequency bands, we do not have the same with the THz band(s) that exhibit several distinct characteristics of their own [63], [115]. Like microwave and mmWave, THz signals suffer from free-space path loss (FSPL), as inherent attenuation when an electromagnetic wave is radiated from an isotropic antenna. Unfortunately, the receive antenna for the THz band has a weak ability to capture the radiation power due to the tiny wavelength. This leads to a propagation phenomenon that FSPL proportionally grows with the increase of the carrier frequency.

Since the wavelength of a THz wave falls into the same order of magnitude as the dimensions of molecules in the atmosphere and human tissue, strong molecular absorption and particle scattering, which are negligible over low-frequency bands, become significant [64]. To be specific, water vapor and oxygen molecules suspended in the atmosphere impose an incredible loss up to approximately 20 000 dB per kilometer in the worst case. In addition to this gaseous absorption from water molecules, liquid water droplets, in the form of suspended particles into clouds, rain-falling hydrometeors, snowflakes, and fogs, can attenuate the signal strength since their dimensions are comparable to the THz wavelength. Furthermore, surrounding physical objects become sufficiently large in size for scattering, and ordinary surfaces are also too rough to make specular reflections. As a result, a THz wave is susceptible to blockages like buildings, furniture, vehicles, foliage, and even humans.

Full knowledge of signal propagation characteristics and accurate channel modeling is mandatory for designing transmission algorithms, developing network protocols, evaluating system performance, and deploying commercial networks. Therefore, this section comprehensively characterizes THz signal propagation, including path loss, atmospheric absorption, weather effects, and blockage, aiming to provide readers with the prerequisite knowledge of THz channels, as the basis for designing THz communications and sensing in 6G and beyond.

A. High Free-Space Path Loss

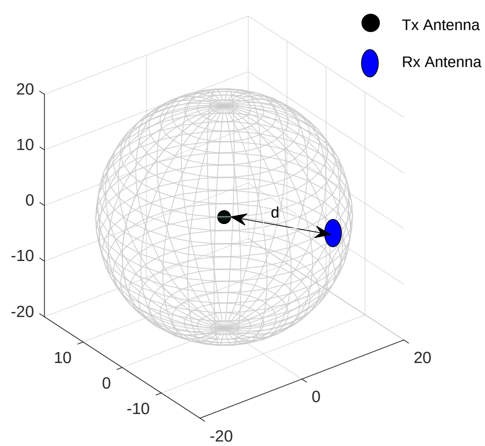

Fig. 4. Illustration of the free-space radiation of an electromagnetic wave, where the energy of a signal radiated from a transmit antenna spreads isotropically. At a propagation distance of d, therefore, the energy evenly distributes over the surface of a sphere with a radius of d.

When an isotropic radiator feeds an EM wave into free space, the energy evenly spreads over the surface of an ever-increasing sphere, as illustrated in Fig. 4. The metric *effective isotropic radiated power (EIRP)* indicates the maximal energy in a particular direction relative to a unity-gain isotropic antenna. Hence, it equals the product of the transmit power P_t and the transmit antenna gain G_t in the direction of a receive antenna. The *law of conservation of energy* states that the total energy contained on the surface of a sphere of any radius d remains constant [116]. Power flux density, namely the power flow per unit area of the incident field at the antenna, is equivalent to the EIRP divided by the surface area of a sphere with radius d, i.e., $\frac{P_tG_t}{4\pi d^2}$. The received power captured by a receive antenna is proportional to its aperture A_r, we have

$$P_r = \left(\frac{P_tG_t}{4\pi d^2}\right) A_r. \tag{1}$$

Meanwhile, the gain of a receive antenna G_r depends on its effective aperture area under the following relationship

$$A_r = G_r \left(\frac{\lambda^2}{4\pi}\right), \tag{2}$$

where λ stands for the wavelength of the transmit signal. Substituting (2) into (1) yields the well-known Friis transmission equation presented by Harald T. Friis in 1946 [117], i.e.,

$$P_r = P_t G_t G_r \left(\frac{\lambda}{4\pi d}\right)^2. \tag{3}$$

Due to the large dynamic range across several orders of magnitude, we usually express the strength of signals and noise in decibels (dB). Free-space path loss is defined as the ratio between the transmit and receive power on a logarithm scale:

$$\mathrm{PL} = 10\lg\frac{P_t}{P_r} = 20\lg\left(\frac{4\pi d}{\lambda}\right) - 10\lg\left(G_t G_r\right), \tag{4}$$

which implies that the FSPL increases 20 dB per decade (ten times) as a function of the carrier frequency. For example, it gets an extra loss of 20 dB from 30 GHz to 300 GHz under the same condition of d, G_t, and G_r. Note that extremely high path loss at THz frequencies only rises from the small aperture area of the receive antenna, which is proportional to the wavelength of its operating frequency.

FSPL does not properly reflect the realistic characteristics of wireless propagation because the physical environment of a terrestrial wireless communications system is distinct from free space. In addition to a LoS path, an electromagnetic wave is reflected, diffracted, and scattered by the surrounding objects in an urban or indoor scenario, forming NLoS paths between a pair of transmit and receive antennas. Due to the differences in energy attenuation, propagation delays, and phase rotations, the additional copies of an electromagnetic wave referred to as multi-path components cause an extra drop in the received signal power. Hence, extensive measurements and accurate modeling of path loss in different frequencies, distances, and propagation environments have to be carried out. The novel uses of the THz band in 6G and beyond such as kiosk downloading, nano-scale networks and wireless backhaul raise many peculiarities, which need to be well investigated.

Plenty of research groups have conducted indoor and outdoor channel measurements to make clear the path-loss effects under the scenarios of THz wireless communications. In 2020, a research team at the University of Southern California employed a channel sounder and a frequency extender for THz channel measurements and built a platform for the exploration of THz communications within a short distance of up to 5.5 m [118]. Later, this team presented the first set of double-directional outdoor measurements over a 100 m distance in urban scenarios based on radio frequency over fiber (RFoF) extensions [119], and the results in an urban environment on a linear moving route for a distance up to 15 m [120]. In addition, their findings unveil that metallic-covered surfaces lead to a considerable enhancement of multi-path, indicating a critical impact of building materials [121] at THz frequencies. Shanghai Jiao Tong University along with Huawei have investigated the LoS and NLoS path loss by carrying out measurements in indoor scenarios at frequencies ranging from 130 GHz to 320 GHz with a frequency-domain VNA-based sounder [122]–[124].

The researchers at New York University (NYU) have also indicated that the factory scenario is a rich-scattering environment due to a massive number of metal structures and objects. In their recent paper [125], path-loss analyses in a factory building based on sub-THz channel measurements with a maximal distance of 40 m using directional horn antennas at 142 GHz were provided. Based on those measurement setups, NYU has also investigated the urban microcell (UMi) large-scale path loss at 28, 38, 73, and 142 GHz [99]. The outcomes indicate that the path-loss exponents are similar across all frequencies, implying that the inter-site separation of base stations does not need to change as frequencies shift towards THz, as antenna gains grow quadratically with frequency if the antenna aperture remains constant [126], [127].

B. Atmospheric Absorption

Although gaseous molecules absorb some energy of an EM wave, atmospheric absorption is negligible over the sub-6G band such that traditional cellular systems do not take it into account when calculating the link budget. However, this effect substantially magnifies for the THz wave, and the absorption loss becomes extremely large at certain frequencies. Such attenuation arises from the interaction of an EM wave and a gaseous molecule [128]. When the THz wavelength approaches the size of molecules in the atmosphere, the incident wave causes rotational and vibrational transitions in polar molecules. These processes have a quantum nature where resonances take place at particular frequencies depending on the internal molecular structure, leading to large absorption peaks at certain frequencies [129].

As a main gaseous component of the atmosphere, oxygen plays a major role in atmospheric absorption under clear air conditions. In addition, water vapor suspended in the air strongly affects the propagation of an electromagnetic wave. The attenuation caused by water vapor dominates the THz band, except only a few specific spectral regions where the effect of oxygen is more evident. A more extensive study of atmospheric absorption is often carried out in radio astronomy and remote sensing. However, from the perspective of wireless communications, the absorption of some additional molecular species, e.g., oxygen isotopic species, oxygen vibrationally excited species, stratospheric ozone, ozone isotopic species, ozone vibrationally excited species, a variety of nitrogen, carbon, and sulfur oxides, is usually negligible compared with that of water vapor and oxygen [130].

Responding to the need to accurately estimate the gaseous absorption at any air pressure, temperature, and humidity, the ITU-R conducted a study item and recommended a mathematical procedure to model these attenuation characteristics. As a combination of the individual spectral lines from oxygen and water vapor, along with small additional factors for the non-resonant Debye spectrum of oxygen below 10 GHz, pressure-induced nitrogen absorption over 100 GHz, and a wet continuum to account for the excess absorption from water vapor, the ITU-R P676 model [131] is built to calculate the value of atmospheric attenuation at any frequency from 1 GHz to 1000 GHz. Alternatively, the high-resolution transmission molecular absorption (HITRAN) database [132], which is a compilation of spectroscopic parameters, can be used to

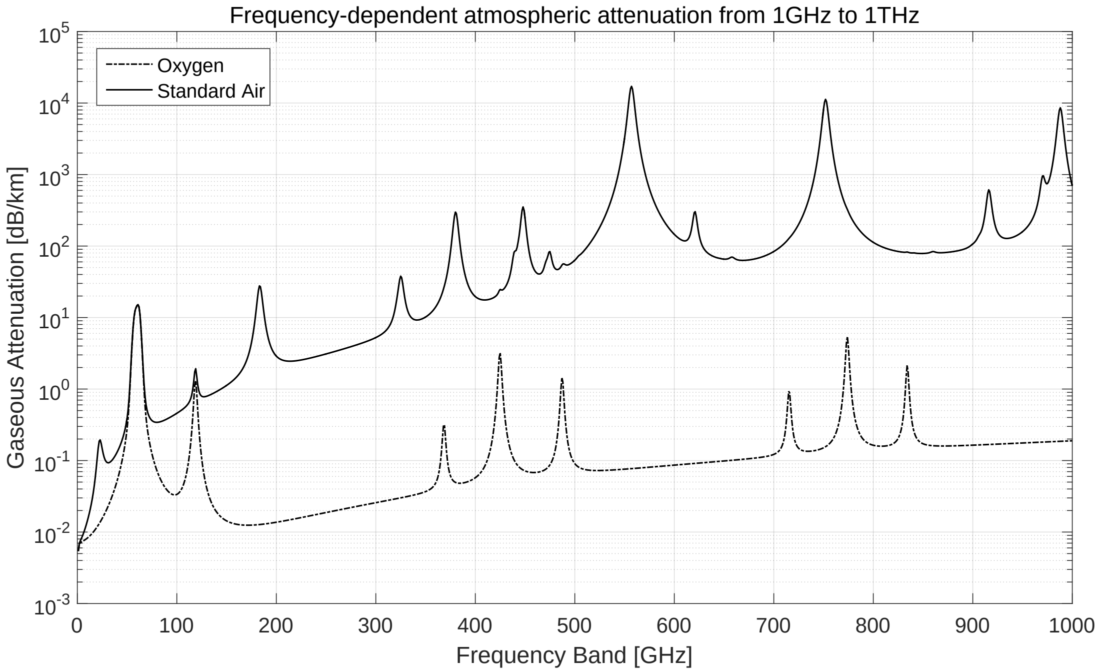

Fig. 5. Illustration of atmospheric absorption from 1 GHz to 1000 GHz, where the legend *Standard Air* stands for a normal atmosphere condition with air pressure 1013.25hPa, temperature 15 °C, and water-vapor density 7.5 g/m^3, according to [131], while *Oxygen* highlights the effect of oxygen absorption by setting water-vapor density to 0 g/m^3. Except for frequencies centered at 60 GHz and 118.7 GHz, the effect of water vapor dominates most of the whole high-frequency band.

predict and analyze the transmission in the atmosphere. To compute the atmospheric absorption at THz, it needs to extract spectroscopic data from the HITRAN database and then apply radiative transfer theory.

The atmospheric attenuation from 1 GHz to 1000 GHz is illustrated in Fig. 5. Assume the air is perfectly dry with a water vapor density of 0 g/m^3, only the effect of oxygen molecules exists, as indicated by *Oxygen* in the figure. Meanwhile, the *Standard Air* shows the usual atmospheric condition at the seal level (with an air pressure of 1013.25 hPa, the temperature of 15 °C, and a water-vapor density of 7.5 g/m^3). Except for two frequency windows centered on 60 GHz and 118.7 GHz, where many oxygen absorption lines merged, the atmospheric attenuation due to water vapor dominates the THz band. As we can see, this absorption loss accounts for a peak of approximately 20 000 dB/km at 560 GHz. In other words, only a short distance of 1 m brings a loss of approximately 20 dB, which is prohibitive for efficient wireless communications. In contrast, the atmospheric attenuation at the sub-6 GHz band is on the order of magnitude around 0.01 dB/km, which is negligible.

To be noticed, for some existing studies of channel characterization in the THz band, which focus on very short-range indoor coverage or nano-communications [133], the atmospheric effect is typically not a major factor. However, for macro-scale THz communications, especially outdoor environments, atmospheric absorption should be taken into consideration. Early in the 1980s, some researchers represented their studies for various atmospheric conditions and elevation angles. For instance, Ernest K. Smith calculated the absorption values due to atmospheric oxygen and water vapor with frequencies spanning from 1 GHz to 340 GHz [134]. Hans J. Liebe and Donald H. Layton [135] performed laboratory measurements of water vapor attenuation at 138 GHz and formed an empirical propagation model that utilizes a local line base to address frequencies up to 1 THz. Molecular absorption and power emission have also been speculated to cause molecular noise, but the phenomenon has not been confirmed by measurements. In [136], Kokkoniemi *et al.* studied the molecular absorption noise from different perspectives and gave their derivations and the general ideas behind the noise modeling.

Some work [96], [137], [138] revealed that oxygen molecules are the main cause of atmospheric absorption over the mmWave band, i.e. 60 GHz and 118.7 GHz predicted by [131], while THz signals primarily suffer from water vapor. In [139], it is highlighted that propagation losses at THz frequencies are more heavily affected by atmospheric absorption compared to that of the mmWave band. Recently, a joint EU-Japan research project under the framework of Horizon 2020, i.e. *ThoR: TeraHertz end-to-end wireless systems supporting ultra-high data Rate applications*, developed an automatic planning algorithm for backhaul links operating at 300 GHz. This algorithm has been tested and evaluated in a realistic scenario of an ultra-dense network in Hannover [140], [141], which includes both wireless and fiber backhaul, taking into account various atmospheric effects. Recent standardization efforts in IEEE 802.15.3d [142] also show that high atmospheric absorption can be alleviated by proper choice of the carrier frequency, e.g., the band from 275 GHz to 325 GHz while having drastically more bandwidth than 5G.

C. Weather Effects

Besides the gaseous absorption, an additional atmospheric impact in an outdoor environment is the weather [143]. Extensive studies of satellite communications channels since the 1970s provided many insights into the propagation characteristics of mmWave and THz signals under various weather conditions [144]. Like water vapor in the atmosphere, the outcomes revealed that liquid water droplets, in the form of suspended particles in clouds, fogs, snowflakes, or rain falling hydrometeors, absorb or scatter the incident signals since their physical dimensions are in the same order as the THz wavelength. Such attenuation is not as strong as the path loss and atmospheric absorption but still needs to be taken into account for proper channel characterization [145].

A cloud is an aggregate of tiny water particles (with a dimension as small as 1 μm) or ice crystals (from 0.1 mm to 1 mm). Water droplets, in the form of raindrops, fogs, hailstones, and snowflakes, are oblate spheroids with radii up to a few tens of millimeters or generally perfect spheres with radii below 1 1 mm. The size of water droplets is comparable to the THz wavelength (0.1 mm to 1 mm). As a result, water droplets attenuate the power of THz waves through absorption and scattering. The ITR-R provided a power-low equation to model the rain attenuation as a function of distance, rainfall rate in millimeters per hour (mm/h), and the mean dimension of raindrops [146]. Fig.6 shows the rain attenuation described by this ITU-R P838 model from 1 GHz to 1000 GHz and rain rate from light rain (1 mm/h) to heavy rain (200 mm/h).

Such attenuation can be treated as an additional loss that is simply added on top of the path loss and gaseous absorption. Besides the ITU-R model, there are other models such as a simplified one given in [147] to describe the rain attenuation. The measurement at 28 GHz demonstrated that heavy rainfall with a rain rate of more than 25 mm/h brings attenuation of about 7 dB/km. Extreme attenuation of up to 50 dB/km occurs at a particular frequency of 120 GHz and an extreme rain rate of 100 mm/h to 150 mm/h. As a rule of thumb, rain provides an excess attenuation of approximately 10 dB to 20 dB over a distance of 1 km at the THz band. Furthermore, the attenuation of cloud and fog can be calculated by the ITU-R P840 model [148] under the assumption that the signals go through a uniform fog or cloud environment. Until now, an equivalent ITU-R model to calculate the snow attenuation does not exist and the snow particles are merely considered as rain drops.

In addition to prior studies of weather effects on the propagation of mmWave signals [143], [145], [149], many recent efforts of investigating THz wave propagation in the presence of rains and fogs have been undertaken through theoretical analysis and experiments such as [150]–[155]. Eom-Bae Moon *et al.* [150] measured THz pulse propagation through a 186 m distance under different weather conditions such as rain falling at 3.5 mm/h and snow falling at 2 cm/h, demonstrating the potential of LoS THz communications, THz sensing, and THz imaging through fog and smoke. J. Ma *et al.* [151] measured the effects of rain attenuation on 0.1 THz to 1 THz frequencies through THz time-domain spectroscopy and a rain chamber, which was designed to generate controllable and reproducible rain conditions. The measurements agreed with theoretical values calculated using Mie scattering theory. In [152], the authors studied rain attenuation with different rainfall rates at mmWave (77 GHz) and low-THz (300 GHz) frequencies. It revealed that the measured results at 77 GHz best agree with the ITU-R P838 model [146] whereas the calculation based on Mie scattering and the Weibull distribution are best fit to the measured data at 300 GHz. Interestingly, the characteristics of rain attenuation have been investigated using raindrop size distribution collected in Indonesia [153]. It reported that attenuation is smaller than the ITU-R model for lower frequencies below 10 GHz but larger than the ITU-R model for higher frequencies over 100 GHz, indicating that the regional variation of rain attenuation should be considered. In [156], Juttula *et al.* analyzed the possible co-channel interference due to rain droplets, showing that the typical interference levels remain modest.

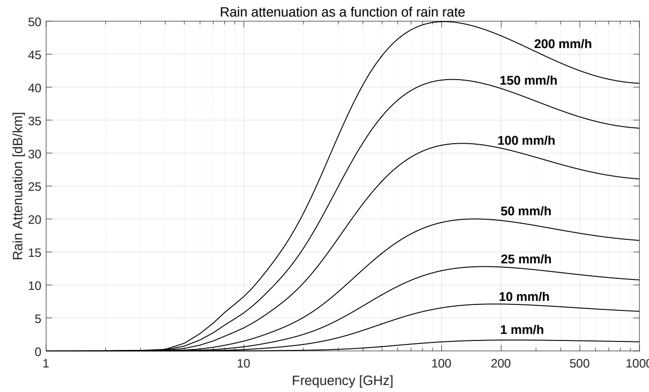

Fig. 6. Rain attenuation measured in dB/km for terrestrial communications links as a function of rain rate and frequency, covering the range from 1 GHz to 1000 GHz. The rain rate is measured in millimeters per hour (mm/h), averaging over a period of time such as one hour. The values from light rain (1 mm/h) to heavy rain (200 mm/h) are illustrated. The peak of attenuation occurs on the frequency band from 100 GHz to 300 GHz since the wavelength in this band matches the size of raindrops.

In addition to rain attenuation, some research efforts have been carried out to make clear the effects of foggy conditions on THz signal propagation. Y. Golovachev *et al.* theoretically and experimentally studied the effects of water droplets suspended in the atmosphere on the propagation of mmWave and THz waves, using a frequency-modulated continuous-wave high-resolution radar operating at 330 GHz [154]. Y. Yang *et al.* experimentally demonstrated the propagation of THz signals through 137 m of dense fog with approximate visibility of 7 m, and reported the observed THz attenuation in [155]. Besides, propagation loss during snowfall has also been studied through measurement campaigns. With the aim of investigating the effect of adverse weather conditions on THz waves and assessing their feasibility for outdoor applications, F. Norouzian *et al.* assessed the attenuation through various intensities of snowfall experimentally at 300 GHz in their work [157], as well as low-THz frequencies (100 GHz to 300 GHz) in [158]. Unlike other weather conditions, there is no theoretical basis for snow because of the challenging nature of defining snowflake shape and size distributions. Nevertheless, results from the measurements indicate that snow attenuation at 300 GHz is less than 20 dB/km for snowfall rates below 20 mm/h [158]. Last but not least, there is work has been done to investigate one of the most common types of contaminant in outdoor environments, i.e., dust or sand in the atmosphere. The authors of [159] quantified the attenuation of 150 GHz and 300 GHz THz waves in the sand for the outdoor scenario of low-THz sensing.

D. Blockage Loss

Due to the tiny wavelength in THz, the dimensions of surrounding physical objects are sufficiently large for scattering, while specular reflections on ordinary surfaces become difficult. On the other hand, THz systems rely heavily on pencil beams to extend the effective propagation distance. As a result, a direct path between the transmitter and receiver is desired. However, the LoS THz link is highly susceptible to being blocked by macro objects, such as buildings, furniture, vehicles, and foliage, and micro-objects, e.g., humans, in comparison with the traditional sub-6G band [160].

A single blockage might cause a signal loss of a few tens of dB. The extent of foliage loss is related to the depth of vegetation [147], where 17 dB, 22 dB, and 25 dB are observed at 28 GHz, 60 GHz, and 90 GHz, respectively. Blockage loss due to vehicles [161] is determined by the vehicle type and geometry, from 20 dB at the front-shield glass to 50 dB at the engine area. The human body blockage imposes a more profound influence because of the dynamic movement of humans and the close interaction of THz devices with humans. The loss attributed to the self-body blockage [162] is expected to reach approximately 40 dB at the THz band. Such blockage losses can dramatically decay the signal power and may even lead to a thorough outage. Hence, it is necessary to clarify the traits of blockage and find effective solutions to avoid being blocked or quickly recover the connection when a link gets blocked.

Statistical models can be applied to estimate the value of blockage loss. For instance, self-body blockage loss is approximated as a Boolean model where a human is treated as a three-dimensional cylinder with centers forming a two-dimensional (2D) Poisson point process (PPP). A LoS blockage probability model assumes that a link of distance d will be LoS with probability $p_L(d)$ and NLoS otherwise. The expressions of $p_L(d)$ are usually obtained empirically for different settings. The blockage probability for a LoS link with a self-body blockage can be estimated by the method given in [163]. In [164], 3GPP specified an urban macro-cell scenario, where a calculation method for a LoS blockage probability is given. The same model applies to the urban micro-cell scenario, with a smaller distance range. There are some variations in the LoS probability expressions across different channel measurement campaigns and environments, e.g., the model developed by NYU [160].

Some prior works also revealed quantitative results to estimate the blockage loss at THz frequencies. For instance, a dynamic blockage causes an extra loss of around 15 dB to 40 dB [165], while the blockage duration is dependent on the density and speed of dynamic blockers that can last longer than 100 ms [162]. Some researchers noted that in the absence of an LoS path, relying on reflected signal paths may not provide adequate signal power. Reflection from rough surfaces like concrete or brick walls attenuates THz signals with a power drop ranging from 40 dB to 80 dB [153]. Another research work [95] shows that the blockage caused by vehicles leads to a loss of 25 dB to 60 dB over the frequency band of 300 GHz. Moreover, some works studied the impact of micro-mobility such as shakes and rotations of user equipment even when the user is in a stationary position [161]. Compared to blockages caused by human bodies, the study of micro-mobility blockages is still in its early stages. Some studies suggest that micro-mobility follows a Markov pattern where user behavior is not controlled [166], while others assume that the user behavior is more regulated [167].

V. THz Channel Measurement and Modeling for 6G and Beyond

Novel 6G usage scenarios such as kiosk downloading, nano-communications, wireless backhauling, and integrated communications and sensing pose many peculiarities in transmission distances, hardware capabilities, and propagation environments [63]. The unique propagation characteristics and particular requirements motivate the research community to rebuild their knowledge and experiences on wireless channels. Extensive measurement campaigns and channel modeling efforts are expected for the success of deploying 6G and beyond. On the other hand, many challenging issues such as capable measurement equipment and novel modeling methodologies are barriers ahead [101]. This section surveys the state-of-the-art measurement campaigns and channel modeling efforts for the THz band in the use of 6G and beyond.

A. THz Channel Measurement

Profound knowledge of propagation characteristics and proper channel models are prerequisites for designing transmission algorithms, developing network protocols, and evaluating performance for THz communications and sensing. Channel measurement is the most critical method for a full understanding of THz signal propagation and subsequently accurate THz channel models. Due to unique characteristics, THz channel measurement requires cutting-edge sounding equipment. There are two major kinds of measurement devices for THz channels, i.e. vector network analyzer (VNA) [168] and channel sounder (CS) [169].

Both devices acquire channel information by transmitting a reference signal and processing the corresponding received signal at the receiver. But their measurements are implemented in distinct ways. The VNA operates in the *frequency domain* [168], which measures the channel transfer function (CTF) for a specific narrowband channel at each time and sequentially scans all frequency points within the band of interest. The CTF of each narrowband channel is modeled by a scalar, and the wideband CTF is obtained by aggregating a large number of narrowband CTFs. Channel impulse response (CIR) is the inverse discrete Fourier transform (IDFT) of the wideband

CTF. This method inherits the advantages of narrowband channel measurements, such as high precision due to individual calibration for each frequency point, and low measurement noise. But it takes a long time and cannot capture dynamic channel effects.

A channel-sounding [169] approach operates in the *time domain*, taking advantage of the classical technique called direct-sequence spread spectrum (DSSS). The transmitter of a CS sends a maximal-length sequence (m-sequence) as a stimulus signal so as to achieve a Dirac-impulse-shaped auto-correlation function. Since a received signal is the convolution of a transmitted signal and a time-varying channel, cross-correlating the received signal with a delayed version of the m-sequence yields the CIR of a measured wideband channel. Time-domain CS works much faster than VNA with frequency scanning and can capture channel dynamic variations. However, its precision is disturbed by strong thermal noise, which is proportional to signal bandwidth. According to the channel measurement methods, there are correspondent state-of-the-art measurement campaigns, which are summarized below.

When deciding on a measurement technique for THz channels, several factors such as signal bandwidth, speed, distance, power consumption, cost, and complexity of the measurement system need to be taken into consideration. In practice, three methodologies are employed for measuring THz channels [63], i.e., *frequency-domain channel measurement using VNA, time-domain channel measurement using sliding correlation, and time-domain channel measurement using TDS*. Based on these three measurement approaches, we provide an overview of the state-of-the-art measurement campaigns as follows.

1) Frequency-Domain VNA Measurement: As introduced, the VNA is a measuring device utilized to assess the response of a component or network at one port in response to an incoming wave at another port. The frequency-domain channel measurements performed using VNA are founded on the principles of linear signal systems. It is important to note that commercial VNAs typically have a limitation on the frequency range that is less than 67 GHz, requiring the use of up-conversing modules for measurements in the THz band. Most of the VNA-based measurement campaigns were focused on frequencies ranging from 140 GHz to 750 GHz and utilized directional horn antennas with antenna gain values between 15 to 26 dBi. The separation between the transmitter and receiver (i.e. the Tx-Rx distance) varied from a minimum of 0.1 m to a maximum of 14 m, and in some cases, was extended to a distance of 100 m with the use of RFoF technique [119].

University of Surrey collaborated with the National Physical Laboratory of the United Kingdom to establish a channel measurement system covering the frequency range of 500-750 GHz [170]. This system utilized the Keysight PNA-X VNA, which was configured with VDI extender heads. The measurement was conducted for LoS scenarios within a distance range of 0.23 m. A research team from Koc University in Turkey also measured THz LoS scenarios with the Tx-Rx distance ranging from 0.01 m to 0.95 m over the frequency band of 260-400 GHz [171]. The measurement was conducted using a VNA in conjunction with a sub-harmonic mixer. The effect of linear and angular displacement between the transmitter and receiver was also investigated. Some researchers from the University of Southern California made advancements to their existing 140 GHz VNA-based measurement equipment, enabling it to support frequencies ranging from 140 GHz to 220 GHz. Indoor LoS measurement in an office setting was conducted, with the measurement distance ranging from 0.5 m to 5.5 m [118].

In addition to LoS, measurement campaigns for NLoS scenarios were also performed with the presence of a reflective surface [172]. Georgia Institute of Technology developed a measurement system for the frequency band of 280-320 GHz using an N5224A PNA VNA and VDI transceivers (Tx210/Rx148). The system was utilized to measure short-range scenarios, such as a desktop environment up to 0.7 m [173] and computer motherboards [174] at frequencies of 300-312 GHz, as well as a data center with a propagation distance of 0.4-2.1 m at 300-320 GHz [175]. They also evaluated the THz wave propagation in a realistic data-center environment. The measurements were taken at a Tx-Rx distance of 1.75 m and 2.28 m, within the frequency range of 300-312 GHz [176].

The previously mentioned studies looked at how THz waves travel and are affected by obstacles when the antennas are in a fixed position. But for some uses, THz signals may come from multiple directions and need to be investigated as well. A joint team from Shanghai Jiao Tong University (SJTU) and Huawei built VNA-based measurement equipment for 140 GHz. Indoor measurements were conducted in a typical meeting room and an office room at distances ranging from 1.8 m to 7.3 m and from 3.75 m to 20 m, respectively. This team analyzed the behaviors of multi-path THz signals components over time and direction, and studied the relationships among different channel parameters, as reported in [123], [177], [178]. Later, the equipment was enhanced to measure 220 GHz THz signals in the same scenario, with distances ranging from 1.8 m to 7.3 m for the meeting room and 2 m to 30 m for the office room, respectively [122]. The receiver was mounted on a rotation unit driven by step motors. Moreover, Y. Wang *et al.* from SJTU [179] built a VNA-based measurement system covering the THz band from 260 GHz to 400 GHz. Indoor channel measurements in the frequency range of 306-321 GHz were performed in an L-shaped hallway and a long corridor at the campus, with distances ranging from 7.7-25 m and 5-31 m, respectively.

2) Time-Domain Sliding Correlation Measurement: Some studies have been done to measure the characteristics of THz waves using the sliding correlation (SC) method over the frequency range up to 300 GHz. A team from NYU developed a measurement system that can switch between two modes: sliding correlation and real-time spread spectrum [180]. Using the SC mode, they focused on the study of how the THz waves at 140 GHz reflect and scatter [181]. They measured THz channels in indoor scenarios including offices, conference rooms, classrooms, long hallways, open-plan cubicles, elevators, and factory buildings, some results are reported in the literature such as [125], [182]–[184]. Besides, this team also conducted the directionally resolved outdoor wideband measurement campaigns in an urban microcell environment [99], [126], [185].

A research team at Technische Universität Braunschweig in Germany has been dedicated to channel measurement, simulation, and antenna design for THz frequencies up to 300 GHz since 2007 [186], [187]. They built a channel sounder at 300 GHz that uses the sliding correlation method with m-sequences of order 12. The clock frequency is selected as 9.22 GHz and the bandwidth reaches 8 GHz, meaning most of the sequence power is focused within 8 GHz in the frequency domain [188]. A joint team from Technische Universität Braunschweig and Beijing Jiao Tong University utilized this equipment to observe the propagation of mmWave and THz waves in railway scenarios [189]. They conducted channel measurements and modeling for a variety of specific scenarios such as train-to-train (T2T) [94], infrastructure-to-infrastructure (I2I) [94], train-to-infrastructure (T2I) [190], and intra-wagon [191], [192], covering the frequency range from 60 GHz to 300 GHz. These measurement activities were conducted in stationary environments, and the measurement of dynamic environments remains a challenge that has to be addressed later [193].

In cooperation with Technische Universität Braunschweig, some researchers at the University of Tampere in Finland investigated reflection and penetration losses of THz frequencies in vehicular communications [95], [194]. Petrov *et al.* measured the signal transmission in automotive settings at 300 GHz, and Eckhardt *et al.* performed a thorough examination of signal transmission at 300 GHz in both single-lane and multi-lane automotive scenarios, respectively. Eckhardt *et al.* also carried out measurements in an actual data center at 300 GHz with a channel sounder, dividing the environment into inter-rack and intra-rack components [195]. The study evaluated the path loss, power delay profile (PDP), and power angular spectrum (PAS), demonstrating the viability of wireless communications at 300 GHz in a data-center scenario.

3) Time-Domain Spectroscopy Measurement: Time-domain spectroscopy is the most straightforward method for measuring impulse responses. It involves transmitting a train of extremely narrow pulses, where the period of the pulse train is greater than the maximum excess delay of the channel. The amplitude of a sampling instance can be considered as the amplitude of the channel impulse response at the time of the exciting pulse, at a delay that is equal to the difference between excitation pulse transmission and the sampling time of the observation [63]. By sampling the received signal at a high speed in the time domain, the impulse response can be directly calculated. THz-TDS makes use of an extensive and scalable bandwidth in the THz frequency band. However, the large setup size and low power output limit its application scenarios [143]. To mitigate the power limitation, lenses are often used at both the transmitter and receiver to enhance the intensity of the pulse signal. The lens beam is highly concentrated, making it well-suited for measuring material properties such as reflection, scattering, and diffraction in the THz frequency range. Despite these, THz-TDS is primarily utilized for channel measurements over short distances, typically less than a few meters.

Many THz-TDS measurements utilized the equipment of Picometrix T-Ray 2000 THz-TDS, which has the capability to emit terahertz pulses with a bandwidth ranging from 0.1 THz to 3 THz [143], [196], [197]. Hossain *et al.* used the THz-TDS to assess the interference between THz devices in the 300 GHz frequency band and applied stochastic geometric techniques to model and analyze the interference [196]. For outdoor scenarios, Federici *et al.* measured the attenuation of THz signals due to weather conditions with the THz-TDS equipment, conducted theoretical analysis, and summarized the impact of various weather factors on THz communications links [143], [197]. Working in conjunction with Brown University, the team at Technische Universität Braunschweig employed a THz-TDS to study the reflection coefficients [198], [199] and the scattering coefficients [200] of different indoor materials across the frequency band from 60 GHz to 1 THz.

THz-TDS is not well-suited for directional scanning due to its large size and narrow beam width. Moreover, the standardization of measurement, calibration, and data analysis using the TDS technology in the THz band needs to be established [201]. Real-time spread spectrum is faster than correlation mode, but it sacrifices dynamic range. To address the diversity of communications scenarios and their varying requirements for speed, dynamic range, Tx-Rx distance, and others in THz channel measurement, it is worth exploring new channel measurement systems that combine both temporal and frequency domain methods.

B. THz Channel Modeling

Developing a wireless communications system requires an accurate channel model that fully captures the major propagation characteristics for the operating carrier frequency. It allows wireless researchers and engineers to assess the performance of different transmission algorithms and medium-control protocols without having to conduct expensive and time-consuming real-world field measurements on their own. A large number of channel models, focusing on the sub-6 GHz frequency band for traditional cellular systems [164], have been built through curve fitting or analytical analysis based on field measurement data. These models reflect all propagation effects, both known and unknown, and therefore work well. Given the peculiarities of THz signal propagation, it is necessary to develop particular THz channel models for research, development, performance evaluation, and standardization [202] of THz communications and sensing in 6G and beyond.

Two widely used techniques for developing appropriate channel models are deterministic [203] and stochastic modeling [204]. The former utilizes the electromagnetic laws of wave propagation to determine the received signal strength at a particular location. The most popular deterministic modeling approach is known as ray tracing [205]. The parameters of each ray, such as attenuation, angle of departure, angle of arrival, propagation delay, and Doppler shift, can be computed taking into account the geometric optic rules of propagation including the computation of path losses via the Friis transmission equation, the Fresnel equation for reflections, the Khirchoff scattering theory, and the universal theory of diffraction. Ray tracing is highly applicable for various static 6G applications at the THz band, e.g., indoor hot spots, wireless backhaul, and nano-networks.

However, the ray-tracing approach suffers from high computational complexity and long simulation time, where accurate information about the geometric environment, the exact knowledge of the boundary conditions, and the properties of different objects are required [205]. To further alleviate the complexity, stochastic modeling is applied to provide a statistical description of the propagation channel. These models are derived from empirical data and need much less computational complexity in comparison with the deterministic ones [206]. In this way, channel data can be generated easily without profound channel knowledge, allowing researchers and engineers to focus on their design and simulation works.

The state-of-the-art channel models in terms of different methodologies are surveyed in this part, as listed in Table V, where we divide these channel models into three categories: *deterministic, statistical, and hybrid*.

1) Deterministic Channel Modelling: Generally, there exist mainly three representative methods for deterministic channel modeling, including ray tracing [205], finite-difference time-domain (FDTD) [213], and channel measurement-based method.

Let us first look at the most popular method namely ray tracing. Visibility tree [207] and ray launching [231] are two alternatives to achieve ray tracing. To date, ray tracing has been calibrated through filed measurements, e.g., the work [190] reports indoor and T2I inside-station scenarios at 300 GHz THz frequencies. In [208], some researchers presented a ray-tracing algorithm based on the Beckmann-Kirchhoff model to simulate the diffuse scattering from rough surfaces at THz frequencies. The authors of [211] modeled the THz channel for a $7\,\mathrm{m} \times 7\,\mathrm{m} \times 3\,\mathrm{m}$ office room, including both LoS and NLoS scenarios and three types of plaster with varying degrees of roughness. In another study [232], a comprehensive multipath channel model based on the ray tracing method was developed for the entire THz band, while assessing capacity and analyzing key parameters in the low THz band (0.1-1 THz). Furthermore, a 3D end-to-end channel model for the THz spectrum was developed, incorporating the elevation plane [233].

The calibration and validation for frequencies between 1.0-10 THz remain challenging due to the lack of material parameters. For single-antenna systems, conventional ray tracing models can analyze communications on a point-to-point basis between the transceiver. In contrast, when dealing with multiple-antenna systems, performing ray tracing for each Tx-Rx link can be prohibitively complex [234]. To reduce the computational complexity associated with multiple antennas, it is possible to perform a single ray tracing simulation that extracts not only the amplitudes and delays but also the directions of the paths. This information can be combined with the array characteristics to generate the transfer function between each transmit and receive antenna pair, which is independent of the antenna array size [235]. Another approach to alleviating the computational burden is to use simplified ray tracing models, such as map-based models. It is based on ray-tracing and uses a simplified 3D geometrical description of the environment [236], which can be much more accurate if Laser is employed for scanning the environment [209], [210], [237].

FDTD is a kind of numerical analysis technique that relies on solving Maxwell's equations directly. This technique is particularly suited for scenarios involving small and complex scatterers, where surface materials exhibit a higher degree of roughness at THz frequencies [213]. However, it demands many memory resources to track solutions at all locations, as well as substantial time and computational power to update the solution at successive time instants [212]. When applied to objects with large dimensions relative to the tiny wavelength of THz signals, FDTD suffers from high computational complexity. In order to apply it effectively, a database of the target environment with sufficiently high resolution is required. This database may be generated from Laser scanning for a point cloud, as mentioned above [237]. In a small intra-device channel, a comparison between ray tracing and FDTD was presented in the literature [214].

Last but not least, another modeling approach called the channel measurement-based method relies on real-world field measurement of the target environment and large-volume data analysis [215]. In recent years, the trend of open-source data has motivated many researchers to make their measurement results available online. Some standardization groups, such as the NextG Channel Model Alliance [238] under the National Institute of Standards and Technology (NIST), aim to make data exchange easier. The European ARIADNE project has provided the initial measurement results and created channel models for D band links in LoS and NLoS office environments [239]. In the context of THz channels, there are some challenges due to the volume of measured data, which is affected by both the large bandwidth and large-scale antenna arrays.

2) Statistical Channel Modelling: Statistical approaches are used to capture the statistical behaviors of wireless channels in various scenarios [219]. One of its main strengths is low computational complexity, which enables fast construction of channel models based on key channel statistics and facilitates simulations of wireless communications. It is broadly classified into two categories, i.e. physical models and analytical models [240]–[242]. The former describes the statistics of the double-directional channel characteristics, such as power delay profile, arrival time, and angle distribution, which are independent of antenna properties. In contrast, the latter mathematically characterizes the impulse response of a channel and antenna characteristics.

a) Physical Models: Early research work on statistical channel modeling for the mmWave or THz band focused on enhancing and adapting the well-known Saleh-Valenzuela (S-V) model through calibration [220], which is based on the observation that multipath components arrive in the form of clusters [216]. Some other research work maintained this concept of clustering while utilizing different distributions, instead of the Poisson process, to describe the time of arrival (ToA) in order to achieve greater conformity with measurement outcomes [218], [219], [221]. Another example referred to as the Zwick model [243] exploits multipath components rather than clusters and does not account for amplitude fading. In [217], the original Zwick model was enhanced to incorporate its applicability to multi-input multi-output (MIMO) systems.

TABLE V
SUMMARY OF THZ CHANNEL MODELLING FOR 6G AND BEYOND

	Methods	Year	References	Contributions
Deterministic	Ray Tracing	2012	Saadane *et al.* [207]	Presents and validates a ray-tracing method for ultra wideband (UWB) indoor propagation channels.
		2018	Sheikh *et al.* [208]	Presents a novel three-dimensional (3D) ray-tracing algorithm based on the Beckmann-Kirchhoff model to model diffuse scattering mechanisms in non-specular directions at terahertz frequencies
		2018	Virk *et al.* [209]	Presents a new method of on-site permittivity estimation for accurate site-specific radio propagation simulations, which is important for cellular coverage analysis.
		2019	Guan *et al.* [190]	The measurement, simulation, and characterization of the train-to-infrastructure inside-station channel at the Terahertz band for the first time.
		2019	Gougeon *et al.* [210]	Describes the BRAVE project, which aims to explore the use of higher frequencies in the sub-THz domain for future wireless communications systems. Discusses the challenges of channel modeling at these frequencies and presents extensions made to a ray-based deterministic tool to address these challenges.
		2020	Sheikh *et al.* [211]	Explores the use of massive MIMO systems at terahertz frequencies. Develops a 3D ray-tracing modeling approach to investigate the impact of surface roughness on THz channel capacity, and calculate channel capacities for both line-of-sight and non-line-of-sight scenarios with different surface roughnesses.
	FDTD	2000	Wang *et al.* [212]	The development of a technique that combines ray tracing and FDTD methods for site-specific modeling of indoor radio wave propagation.
		2007	Zhao *et al.* [213]	Describes a method for modeling the radio channel in a UWB indoor environment using the FDTD method.
		2014	Fricke *et al.* [214]	A conceptual analysis of propagation effects in electromagnetic wave propagation modeling for intra-device communications. Presents a new approach based on FDTD calculations.
	Channel Measurement	2022	Rappaport *et al.* [215]	Offers comprehensive, practical guidance on RF propagation channel characterization at mmWave and sub-terahertz frequencies, with an overview of both measurement systems and current and future channel models.
Statistical	Physical	1999	Kunisch *et al.* [216]	Describes a study where radio waves at 60 GHz carrier frequency with a bandwidth of 960 MHz were measured in an indoor environment. Using the data collected, the authors determine parameters for a multipath model based on a well-known statistical indoor channel model by Saleh *et al.* (1987).
		2002	Zwick *et al.* [217]	Introduces a new stochastic channel model for indoor propagation that is designed specifically for future communications systems with multiple antennas such as spatial-division multiple access, spatial filtering for interference reduction, or MIMO. The model is designed to provide an accurate representation of the indoor propagation channel, taking into account various factors that affect communications performance in such systems.
		2010	Azzaoui *et al.* [218]	Introduce a statistical model of the UWB channel impulse response at 60 GHz. Considers the transfer function as an α-stable random process.
		2013	Priebe *et al.* [219]	Introduces a new stochastic 300 GHz indoor channel model to facilitate fast system simulations and adequate design of upcoming terahertz communications systems. A complete scenario-specific parameter set is provided for the considered environment.
		2014	Gustafson *et al.* [220]	Presents clustering results for a double-directional 60 GHz MIMO channel model and derives a model that is validated with measured data. Suggests that when creating these models, it's important to consider small details in the environment.
		2015	Samimi *et al.* [221]	Presents an omnidirectional spatial and temporal 3-dimensional statistical channel model for 28 GHz dense urban non-line of sight environments.
	Analytical	2003	Svantesson *et al.* [222]	Reports on a study that uses measurements taken at Brigham Young University to investigate the statistical properties of indoor MIMO channels. Investigates whether the covariance matrix can be modeled as a Kronecker product of correlations at the transmitter and receiver, using a likelihood ratio test.
		2015	Sun *et al.* [223]	Investigate MU-MIMO systems with a large number of antennas at the base station. Proposes a beam division multiple access (BDMA) transmission scheme that serves multiple users via different beams, which performs near-optimally, and that the proposed pilot sequences have advantages over other sequences.
		2017	You *et al.* [206]	Proposes a new method for wideband massive MIMO transmission over mmWave/Terahertz bands called BDMA with per-beam synchronization (PBS) in time and frequency. Investigates beam scheduling to maximize the ergodic achievable rates for both uplink and downlink BDMA and develop a greedy beam scheduling algorithm.
Hybrid	Deterministic Hybrid	2000	Wang *et al.* [212]	Presents a hybrid technique based on combining ray tracing and FDTD methods for site-specific modeling of indoor radio wave propagation.
		2006	Reynaud *et al.* [224]	Present an original approach, combining the advantages of UTD and FDTD methods.
		2008	Thiel *et al.* [225]	A novel method of analyzing wave propagation in a building consisting of a heterogeneous mixture of homogeneous and periodic walls is presented. Walls are discretized into finite-size building blocks. FDTD approach is used to compute their electromagnetic response in a periodic arrangement as well as in corner and terminal locations.
		2020	Lecci *et al.* [226]	Introduces a detailed mathematical formulation for quasi-deterministic models/Q-D at mmWave frequencies, that can be used as a reference for their implementation and development. Moreover, it compares channel instances obtained with an open-source National Institute of Standards and Technology Q-D model implementation against real measurements at 60 GHz, substantiating the accuracy of the model.
		2021	Zhu *et al.* [227]	Reviews the main existing channel models suitable for mmWave frequency band as well as the typical channel modeling methods, illustrates the generation procedure of stochastic channel model in the 3GPP standard, he map-based hybrid channel model is demonstrated and analyzed.
	Deterministic-Statistical Hybrid	2014	Maltsev *et al.* [228]	A new Q-D approach is introduced for modeling mmWave channels. The proposed channel model allows the natural description of scenario-specific geometric properties, reflection attenuation and scattering, ray blockage, and mobility effects.
		2014	Samimi *et al.* [229]	Presents UWB statistical spatial and omnidirectional channel models for 28 GHz mmWave cellular dense urban NLoS environments, developed from wideband measurements in New York City that used synthesized timing from 3D ray-tracing.
		2021	Bian *et al.* [230]	A novel 3D non-stationary GBSM for 5G and beyond 5G systems is proposed.

b) Analytical Models: Analytical models take into account the channel and antenna characteristics as a whole, thereby characterizing the impulse response from the transmitter (Tx) antenna element's connector to the receiver (Rx) antenna element's connector. These individual impulse responses are organized into a matrix and the statistical properties of these matrix elements, including correlations, are encompassed. The Kronecker-based model [222] assumes that the correlation between the transmit and receive arrays is separable. However, as the number of antennas increases and single-reflection propagation dominates in the THz band, this assumption becomes less accurate. To respond to this, some other models account for either MIMO or MMIMO channels from the perspective of beams or eigenspaces. For instance, an approach called the virtual channel representation (VCR) [206] characterizes physical propagation by sampling rays in a beam space. These aforementioned models can be also named correlation-based stochastic models (CBSMs). Despite their limited spatial determinism capability, CBSMs are well-suited for evaluating the performance of MMIMO systems due to their low complexity. Unfortunately, it is challenging to properly describe MMIMO channels, especially UMMIMO channels over the THz band, due to the lack of consideration for the near-field effect and non-stationarity. To address this issue, an enhanced method referred to as beam-domain channel model (BDCM) was proposed [223] through rethinking the far-field assumption. As a result, the BDCM is applicable to UMMIMO scenarios for the THz band.

3) Hybrid Channel Modelling: Since different methods have particular pros and cons, hybrid methods are developed to exploit the feasibility of combining the benefits of two or several individuals for a particular scenario [7]. As the deterministic method shows high accuracy with the price of high time and resource consumption but the statistical method has low computational complexity, most existing approaches focus on the hybrid deterministic-statistical way, see [224]–[227]. Moreover, there are other methods that combine two deterministic approaches, like ray tracing and FDTD, called the hybrid deterministic approach. In this paradigm, FDTD works for studying regions close to complex discontinuities, while ray tracing is used to trace the rays outside the FDTD regions. The single interaction between ray tracing and FDTD was presented in [212], where the location of the receiver is restricted in the FDTD region. Later, some works such as [224], [225] extended it for time efficiency and multiple interactions between ray tracing and FDTD.

Although statistical channel models are highly efficient, they struggle to accurately capture spatial consistency and the temporal evolution of cluster correlations. It motivated the development of some hybrid models that incorporate both statistical and geometrical approaches. This hybrid approach enables the inclusion of some channel features that are impossible to characterize through a stochastic model. In 2002, a quasi-deterministic (Q-D) channel model [244] was initially proposed for mmWave channels, which was adopted by the IEEE 801.11ad standardization group for indoor scenarios at 60 GHz [245]. Moreover, the Q-D channel model has been successfully applied for other wireless standards, such as the mmWave Evolution for Backhaul and Access (MiWEBA) [228] and the IEEE 802.11ay [246], which is an evolution of the IEEE 802.11ad standard.

Another hybrid method called geometry-based stochastic channel model (GSCM) incorporates a geometrical component during the stochastic modeling process [219], [241], [242]. Although the placement of scatterers is stochastic, a simplified ray-tracing method that is employed in GSCM is deterministic. A new non-stationary GSCM, called the beyond 5G channel model (B5GCM), was recently introduced in [230], where the researchers derived the correlation functions based on a general 3D space-time-frequency model. It can be categorized into two types: regular-shaped GSCM, which is primarily used for theoretical analysis, such as correlation functions, and irregular-shaped GSCM that can better replicate measured results. Notably, the COST259, COST273, and COST2100 models [247] take advantage of this hybrid benefit, where the clusters of scatterers are placed to form the clusters of multi-path components with similar delays and directions. The well-known 3GPP Spatial Channel Model (SCM) [248] and WINNER II model [249] also followed this approach. Furthermore, Samimi et al. [229] utilized temporal clusters and spatial lobes to handle the temporal and spatial components, respectively.

VI. THz Transceiver: Antennas and Devices

This section aims to provide readers with the necessary knowledge required to design and build THz transceivers. We discuss the cutting-edge antenna technologies that are appropriate for transmitting and receiving THz signals, along with the fundamental and innovative aspects of photonic-electronic devices and components used in constructing THz transceivers.

A. THz Antennas

The conventional concepts of electromagnetic antennas can also be applied in the THz regime, as mentioned in the references [55], [250]. However, due to the very high frequency involved, there are certain limitations and disruptive effects that need to be taken into consideration. The tiny wavelength associated with THz frequencies results in the need for extremely small structures, which raises concerns regarding manufacturing processes. on the other hand, this downsizing of structures enables the feasibility of employing novel manufacturing techniques like low-temperature co-fired ceramic (LTCC), antenna-on-chip design, substrate-integrated waveguide (SIW), and others.

Another significant issue that arises with increasing frequency is the skin effect of conductive materials. Since the skin depth, which refers to the depth of the current in a conductive material, decreases dramatically, the conductivity of metallic materials drops, leading to increased losses in the antenna system. To overcome this issue, researchers have explored the use of new materials like graphene. Graphene, with its exceptional electrical and thermal properties, holds promise for mitigating the skin effect and improving the performance of THz antennas. Its high electron mobility and low resistivity make it an attractive material for overcoming the limitations posed by traditional conductive materials.

In the following, we provide a summary of the main antenna techniques and current research advances in this field.

1) Horn Antennas: Horn antennas are widely used in wireless applications due to their favorable characteristics. Those belong to high directivity antennas, with an achievable gain of up to 25 dBi. Similar to hollow waveguides, these antennas feature low power loss, making them appropriate for low-noise as well as high-power applications. Furthermore, they can be operated within a wide frequency range, which is advantageous for broadband signals. Due to the small wavelength of THz waves, the manufacturing of horn antennas is challenging. Nevertheless, various technologies could be utilized here. Among others, the authors of [251] introduced elective laser melting 3D printing technology to produce several conical horn antennas, covering the frequency bands E (60 GHz to 90 GHz), D (110 GHz to 170 GHz), and H (220 GHz to 325 GHz). Another appropriate technology is LTCC, as a 300 GHz LTCC horn antenna reported in [252].

2) Planar Antennas: Planar transmission line technology, commonly used for THz frequencies, offers various antenna designs. Among these designs, patch antennas based on microstrip line technology are particularly well-known. However, planar antennas generally exhibit inferior performance compared to horn antennas. This is primarily due to the EM wave partially propagating within a dielectric substrate, resulting in increased overall loss. Additionally, the short wavelength relative to the substrate thickness in THz planar structures can lead to substrate mode issues, as mentioned in [253]. In such cases, a portion of the wave energy becomes trapped in the substrate and cannot be effectively utilized. Therefore, it is necessary to implement appropriate measures to mitigate this problem.

Despite the drawbacks discussed above, planar antennas are very popular. The major reason is the production flexibility of the planar structures. The planar shapes can be easily designed and realized using various technologies [254]–[257]. Due to their size, patch antennas can be efficiently combined to build an antenna array, which allows higher control on the antenna pattern [258]–[260]. Due to the short wavelength of THz waves, the distances between the transceiver components might become critical. Thus, the antenna placement on the chip becomes advantageous. In this case, the planar antennas also play an important role, since they are compatible with on-chip design [261]–[263].

3) Substrate-Integrated Antennas: Very short wavelength causes some issues for planar antenna design. However, it can be turned into an advantage by bringing the low-cost manufacturing capability and flexibility of planar structures to the high-performance world of waveguide technology. Authors in [264] give a comprehensive overview on the substrate-integrated circuit technology. In particular, the concept of SIW shows promising results. The idea of SIW is to connect the upper and the lower conductive layers of a substrate by means of via walls. In this way, a rectangular waveguide inside a substrate is formed, whereas the distance between vias defines the upper cutoff frequency. Also, this technology can be extended to on-chip usage. There is a variety of antennas and antenna array designs reported in the literature, such as horn antennas [265], [266], slot antennas [267], [268], patch antennas [269], [270] and some others [271]–[273]. Furthermore, a comprehensive review on SIW antenna technology can be found in [274].

4) Carbon-Based Antennas: Graphene and carbon nanotubes, which are rolled sheets of graphene, are two promising materials to be used within THz range. As mentioned before, due to the strong skin effect, metallic materials, especially copper, suffer reduced conductivity. Thus, the performance of antennas using metallic components is reduced. In contrast, graphene features high conductivity due to the propagation of plasmon mode in this frequency range. Furthermore, the conductivity can be tuned by chemical doping, but also by applying electric and magnetic fields, which allows to the production of tunable antennas [275]. This and some other advantageous properties make graphene interesting for THz applications in general and in particular for antenna design. The most reported efforts are to exchange the metallic conductors by graphene or carbon nanotubes in e. g. planar antenna structures [276], [277]. Besides, the approach of building a dipole antenna based on carbon nanotubes was reported [278], [279].

B. THz Components and Devices

The THz band is generally defined as a frequency band between 0.1 THz and 10 THz, which is far higher than the sub-6GHz band while is much lower than the optical bands. For a long time, it used to be addressed as a terahertz gap [52]. On the one hand, *photonic* devices are not capable of producing such low frequencies. On the other hand, *electronic* oscillators are struggling to reach those high frequencies. In this regard, the THz band used to be unreachable for either *photonic* or *electronic* technologies. For this reason, the attempts to generate the THz radiation were made from both sides of the spectrum.

Initially, due to the limited capability of the components, prior THz research was concentrated on applications such as imaging or spectrometry [35]. This fact attributes to two major reasons:

- These applications require comparably high output power of the signal but are not demanding on the receiver side, since the amplitude rather than the phase of a signal acts as the information carrier.
- The size of the system or the specific operational conditions are not the limiting factor. In this case, some technologies, especially photonic generation and detection are advantageous.

In contrast, THz communications and sensing require the capability of accurate phase recovery, especially the case for digital modulation when both in-phase and quadrature (IQ) branches are exploited. Furthermore, compactness and low energy consumption play critical roles. Thus, the utilization of semiconductor-based integrated circuits is advantageous for THz communications and sensing applications in 6G and beyond systems. In the remaining part of this section, we discuss the fundamentals and state-of-the-art advances of both

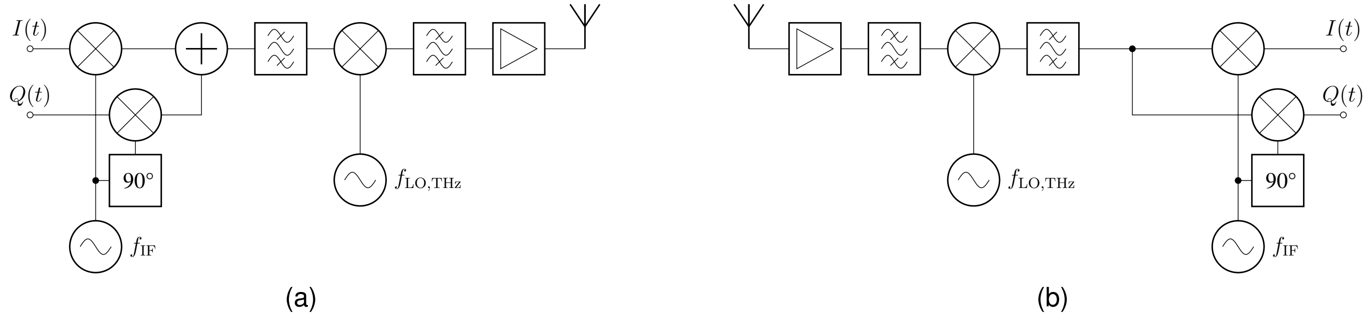

Fig. 7. Architecture of superheterodine (a) transmitter and (b) receiver design including IQ-modulator

photonic and electronic components for implementing THz signal transmission and reception.

1) Electronic Devices: There exist two classes of electronic devices capable of generating THz radiation. On one hand, there are high-power devices, the mostly based principle of an electron tube. These can generate signal power from 10 W to 1 MW. Usually, high transmission power is required for special-purpose applications such as satellite communications. On the other hand, there are semiconductor devices, based on various types of semiconductor materials. Even though these devices show some limitations such as low transmission power, their compactness and cost make them most suitable for conventional communications and sensing devices [280]. Common materials utilized are III-V-semiconductors such as Gallium Arsenide (GaAs), Gallium Nitride (GaN), and Indium Phosphide (InP). Also, Silicon Germanium (SiGe) based devices show promising performance. Compared to the aforementioned technologies, a well-know semiconductor technology known as complementary metal-oxide-semiconductor (CMOS) features some limitations in terms of the transmit power, noise figure, and other parameters. However, recent research results argue that the CMOS technology may also be suitable for THz communications and sensing applicaitons [104].

Most semiconductor THz transmitters and receivers follow the established transceiver design for lower frequencies, such as the heterodyne transceiver approach, as shown in Figure 7. That means a modulated baseband signal is passed to a front-end circuitry. There, it is upconverted to the THz carrier frequency by mixing with the local oscillator (LO) signal. Finally, the signal is amplified and sent over an antenna. At the receiver, the same steps are applied in reverse order, and the downconverted signal is passed to the baseband circuitry for further processing.

The most critical part of the described transceivers is the LO generation since a THz signal needs to be synthesized. In order to do so, a multiplexer cascade is used to multiply, or upconvert, a high-frequency signal to the THz range. On the other hand, every multiplexer stage increases the power of inter-modulation products. A higher number of multiplexer stages also lead to increased noise figure and distortion of the generated signal. Therefore, the number of multiplexers is one of the limiting factors for THz signal generation. For this reason, higher-order modulation products may be utilized as a trade-off. Table VI gives an exemplary literature overview on the available transmitter and receiver front-end performance for different semiconductor technologies. Also, the results on some transceiver chains are discussed below.

Among III-V compound semiconductor materials, InP components show the best results in terms of output power and noise figure. Furthermore, InP transistors feature the maximum oscillating frequency $f_{\max}$ of up to 1.5 THz [294], which is the highest number as compared to other semiconductors. In the literature, a transceiver desgin based on a high-electron-mobility transistor (HEMT) was reported. HEMT supports THz frequencies up to 850 GHz, but particular attention was given to the frequency band around 300 GHz [281], [295], [296]. In addition, most recent results show that a transceiver system achieved a maximum throughput of 120 Gbps [282].

SiGe and CMOS are both silicon-based technologies suitable for the THz frequency band. Due to the intrinsic characteristics of silicon, the maximum oscillation frequency is limited below 1 THz. There are studies that show hetero-junction bipolar transistors (HBTs) based on 130 nm SiGe process reaching $f_{\max}$ of 620 GHz [297] as well as 720 GHz [298]. The components fabricated by SiGe HBTs exhibit some advantages such as good linearity, high gain, and low noise. However, the power gain is limited, which prevents the operation above 500 GHz. Among the recent research work, one of the particular interests focused on the components and devices for D-band communications and sensing. As a result, several transceiver concepts were presented such as [285], [286], [299], [300]. The authors of [301] demonstrated a complete communications link that realizes a high throughput of 200 Gbps. Furthermore, some researchers presents their transceiver design operating around 300 GHz [289], [291], [302]–[304]. Here, a communications link of 100 Gbps was realised [305]. In addition, a detailed survey on SiGe transceiver for different purposes is provided in [306].

Last but not least, the performance of THz devices built by the CMOS technology is lower as compared to other semiconductor technologies. CMOS field-effect transistors (FETs) are able to reach $f_{\max}$ of around 450 GHz, also the power gain is limited. Nevertheless, this technology is known for low production costs, which is its major advantage. Transceiver systems operating at 240 GHz [289], [307], [308] or 300 GHz [309]–[312] were realized. A system, consisting of 105 Gbps transmitter and corresponding 32 Gbps was shown by authors

TABLE VI
OVERVIEW OF SEMICONDUCTOR TRANSMITTER AND RECEIVER TECHNOLOGIES

Semiconductor Techno.	Freq. [GHz]	Transmit Power [dBm]	Noise Figure [dB]	Throughput[Gbps]	Reference	Pub. Year
70 nm InP	300	10	9.8	20	[281]	2016
80 nm InP	300	−3	N/A	120	[282]	2020
130 nm InP	590	−2	—	—	[283]	2016
25 nm InP	850	−0.3	12.7	—	[284]	2017
130 nm SiGe	D-band	9	9	48	[285]	2016
130 nm SiGe	D-band	10	10	—	[286]	2020
130 nm SiGe	240	8.5	—	50	[287]	2017
130 nm SiGe	300	−4.1	—	—	[288]	2021
130 nm SiGe	400	−20	—	—	[267]	2012
28 nm CMOS	240	0.7	—	—	[289]	2022
40 nm CMOS	300	−5.5	—	105	[290], [291]	2017
40 nm CMOS	300	—	27	32	[291], [292]	2017
28 nm CMOS	390	−5.4	—	28	[293]	2020

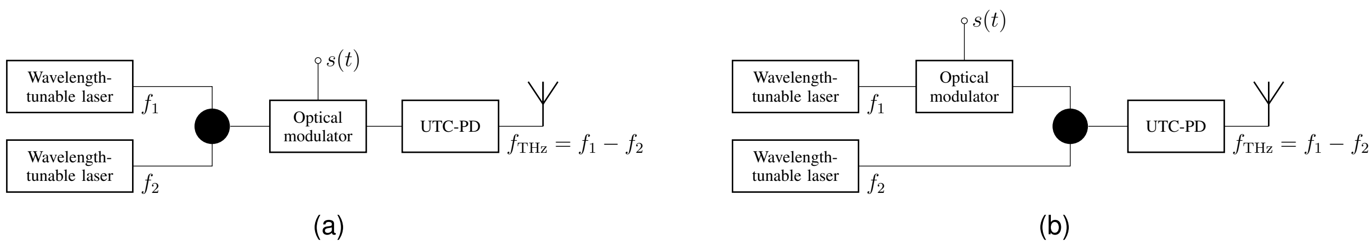

Fig. 8. Configuration of photomixing transmitters with (a) Double sub-carrier modulation. (b) Single sub-carrier modulation [315]

in [290]–[292]. The highest operating frequency reported is 390 GHz, which realized a data throughput of 28 Gbps. Further achievements of CMOS transceiver are summarised in [104], [313], [314].

2) Photonic Devices: In order to get from very high-frequency photonic radiation to a lower THz frequency, an optical frequency downconverter needs to be implemented. Here, the most common technology is known as photomixing. As shown in Figure 8, two laser signals with frequencies f_1 and f_2 are forwarded to a photomixing diode such as uni-traveling-carrier photodiode (UTC-PD) [316]. The photodiode, similar to conventional high-frequency mixing, generates then the modulation products. In this way, a THz signal $f_{\mathrm{THz}} = f_1 - f_2$ is generated. Photomixing provides high tunability and modulation bandwidth. Also, a variety of complex modulation schemes may be implemented with moderate effort, as compared to electronic solutions. Figure 8 exemplary shows two modulation approaches, modulation of both laser signals as well as the single laser signal only [315]. A further advantage is the ability to deliver an optical signal over a large distance by means of an optical fiber. Thus, optical signal generation and modulation may be performed separated from the THz signal generation, which may yield flexibility to the transmitter system [24].

Another way of photonic THz signal generation is called quantum cascade laser (QCL). Conventional lasers emit photons through the recombination of electron-hole pairs across the band gap. Thus, the lower bound for the frequency of the emitted photons is defined by the band gap, which limits the ability of the lasers to work below the infrared band. In contrast, QCL are unipolar [317]. The photons are emitted by quantum jumps of electrons between two different energy levels. These energy levels are defined by the structure of the quantum wells. This provides the possibility to tune the frequency of the laser. Due to the low energy gap between the energy levels, QCLs are well suited for mid-infrared applications. In recent decades, there was also a big progress on QCL development for far-infrared, or THz, range [318]. QCL are able to cover the frequency band of 1 THz to 5 THz with a peak radiation power of 1 W [319]–[321]. However, the operations frequency of QCL is in the cryogenic range, which limits their application area.

VII. BEAM-FORMING AND ALIGNMENT FOR THZ COMMUNICATIONS AND SENSING

The use of the THz band can alleviate the problem of spectrum scarcity and facilitate novel applications, such as nano-scale networks and in-device communications. However, its practical use is challenged by large propagation losses, which generally lead to very short distances of signal transmission [322]. The main causes of this problem include the high spreading loss that grows quadratically with carrier frequency, the gaseous absorption due to oxygen molecules and water vapor in the atmosphere, and the adverse effects of weather conditions, as discussed in the previous section. Such a propagation loss can reach hundreds of decibels per kilometer or even higher. Additionally, this problem is further aggravated by the following two factors [168]:

- *Strong thermal noise*: Noise power is proportional to signal bandwidth with the constant power density. Therefore, the unique advantage of massive bandwidth at the THz band imposes a side effect of strong thermal noise.
- *Hardware constraint*: The transmit power at the THz band is quite constrained since the output power decreases with frequency and is at the level of decibel-milli-Watts in the foreseeable future. Hence, raising power to extend the communications distance is not feasible [100].

To extend the signal transmission distance beyond a few meters, high-gain directional antennas are necessary to compensate for such a high propagation loss in THz communications and sensing. Thanks to tiny wavelengths, massive numbers of elements can be tightly packed in a small area to generate high beamforming gains [323]–[325]. In this section, we will discuss the cutting-edge antenna forms, novel beamforming techniques, and necessary beam alignment schemes at the THz band [57].

A. Ultra-Massive MIMO

Since the length of a resonant antenna is typically in the order of the wavelength at the resonance frequency, the dimension of an array with tens of elements is a few square meters and a few square centimeters at the sub-6G and mmWave bands [102], respectively. Moving to the THz band, the antenna length further reduces. Hundreds of elements can be compacted in an array within a few centimeters using conventional metallic materials. However, this number is not sufficient to overcome the huge propagation loss suffered by THz signals [322].

Taking advantage of surface plasmon polariton (SPP) waves [326], the inter-element separation of an array can be further reduced to the SPP wavelength, which is much smaller than the EM wavelength. Consequently, nanomaterials that support the propagation of SPP waves, such as graphene and metamaterials, are employed to further improve the hardware compactness. Graphene, a one-atom-thick carbon nanomaterial with unprecedented mechanical, electrical, and optical properties, is employed to fabricate plasmonic nano-antennas with a smaller size of almost two orders of magnitude compared to metallic THz antennas [103]. In particular, thousands of graphene-based nano-antennas can be embedded in a few square millimeters at 1 THz. The emergence of nano-antennas paves the way for building very large-scale arrays for THz communications. In 2016, Akyildiz and Jornet [327] presented the concept of UMMIMO communications, and demonstrated a 1024×1024 system where both the transmitter and receiver are equipped with an array of 1024 nano-antennas.

A massive number of elements impose challenges such as prohibitive power consumption and high hardware complexity. It is worth rethinking the array architecture and beamforming schemes in UMMIMO systems at the THz band. Fully digital beamforming can generate a desired beam but it leads to unaffordable energy consumption and hardware cost since each antenna in a large-scale array needs its dedicated radio frequency (RF) chain. This motivates the study of analog beamforming with low complexity. By employing analog phase shifters, only a single RF chain is needed, substantially lowering hardware and power costs. Nevertheless, the analog architecture supports only a single stream, limiting data rates and the number of users. As a compromise of these two forms, hybrid digital-analog architecture is the best choice for THz from the perspective of performance and complexity trade-off. Combining an analog-shifter network with a few RF chains, hybrid beamforming can significantly reduce hardware cost and low energy consumption, while achieving comparable performance as digital beamforming.

Although hybrid beamforming has been extensively studied for the sub-6GHz and mmWave bands [328]–[330], the peculiarities of the THz band, such as channel sparsity [331] and beam squint [332], impose many difficulties for designing an UMMIMO system. Currently, many new forms of hybrid beamforming are discussed in the literature, including array of subarrays (AoSA) to balance the power consumption and data rate, widely-spaced multi-subarray to overcome the low spatial multiplexing gain due to channel sparsity, and true-time-delay-based hybrid beamforming to address the problem of beam squint [333].

1) Array of Subarrays: In a hybrid architecture, the connection between elements and RF chains has two basic forms: fully-connected (FC) and AoSA [334]. In the FC hybrid beamforming, each element is fully connected to all RF chains via a signal combiner, and the signal of an RF chain radiates over all antenna elements via an individual group of phase shifters. Any RF chain should have the capability to drive the entire large-scale antenna array, which is power-aggressive. Particularly, the use of a large number of phase shifters and combiners will exacerbate the problems of high hardware cost and power consumption. In contrast, all elements in AoSA are divided into disjoint subsets called subarrays, and a subarray is only accessible to one specific RF chain [335]. AoSA conducts signal processing at a subarray level with fewer phase shifters, such that hardware cost, power consumption, and signal power loss can be dramatically reduced. In addition, beamforming and spatial multiplexing can be jointly optimized by cooperating with precoding in the baseband.

Recent literature shows the strong interest of researchers to exploit an array of subarrays. For instance, Lin and Li published a series of works on this topic. In [336], they analyzed the ergodic capacity of an indoor single-user THz communications system and obtained an upper bound, providing guidance on the design of antenna subarray size and numbers for certain long-term data rate requirements with different distances. In [337], an adaptive beamforming scheme was proposed for multi-user THz communications that considers the impact of transmission distance. They [338] examined the array-of-subarray structure for multi-user sub-THz communications and analyzed its spectral and energy efficiency. They then showcased a THz-based multi-user system for indoor usage that uses an array-of-subarrays architecture to handle hardware restrictions and channel characteristics in the THz band, which has shown a great advantage by comparing with the FC structure in both spectral and energy efficiency [334]. In [339], Tarboush *et al.* proposed an accurate stochastic simulator of statistical THz channels, named TeraMIMO, aiming at catalyzing the research of UMMIMO antenna configurations. TeraMIMO adopted the AoSA antenna structure for hybrid beamforming and accounted for spatial sparsity.

To further reduce the complexity, various alternating optimization algorithms have been proposed for the AoSA architectures [335]. In contrast to the FC architecture, the AoSA architecture has a restricted number of phase shifters that equals the number of antennas. However, since the RF chains and antennas are connected exhaustively, the FC architecture can achieve data rates comparable to those of the optimal fully-digital beamforming architecture. Conversely, the data rate of the AoSA architecture is significantly lower compared to that of the FC architecture. This is attributed to the partial interconnection between antennas and RF chains. Hence, we need to balance the power consumption and data rate of the THz hybrid beamforming, inspired by the challenge of designing large-scale antenna arrays in THz UMMIMO systems. To address this issue, some researchers introduced a new form of hybrid beamforming called dynamic array-of-subarrays (DAoSA) [340]–[342], which features a flexible hardware connection. DAoSA achieves a good balance between power consumption and data rates by intelligently determining the connection between sub-arrays and RF chains.

2) Widely-Spaced Multi-Subarray: Due to the tiny wavelength, the THz channel is usually sparse, consisting of a LoS path and a few reflection paths. The transmit power concentrates on the LoS path, and the overall angular spread of THz signals is small. For instance, a maximal angular spread of 40° has been observed for indoor environments in the THz band, compared to 120° for indoor scenarios at 60 GHz mmWave frequencies [343]. Since the number of spatial degrees of freedom is upper-bounded by the number of multipath components, the number of data streams or the potential spatial multiplexing gain is much small, limiting the achievable data rate at the THz band. A widely-spaced multi-subarray hybrid beamforming architecture is proposed [344] to overcome the low spatial multiplexing gain due to channel sparsity. Instead of critical spacing, the inter-subarray separation is over hundreds of wavelengths, reducing the correlation between the subarrays.

The widely-spaced multi-subarray (WSMS) hybrid beamforming architecture is promising by exploiting intra-path multiplexing for THz UMMIMO systems [345]. It was discovered in [346] that when the distance between antennas is expanded, the planar-wave assumption becomes invalid, and it is necessary to consider the propagation of spherical waves between antennas. Previous research has examined the use of intra-path multiplexing in LoS MIMO architecture operating at microwave and mmWave frequencies, which enables multiplexing gain to be achieved using just a single LoS path [347]. Given that the intra-path multiplexing gain is not restricted by the number of multipath, it is a highly viable and promising solution for THz communications, which are known to exhibit significant channel sparsity [348]. In [349], the authors demonstrated that the WSMS architecture can substantially improve the spectral efficiency of THz systems through the use of additional intra-path multiplexing gain, which sets it apart from existing hybrid beamforming that solely relies on inter-path multiplexing. As the follow-up, the authors designed an alternating optimization algorithm to maximize the sum rate [350] under the WSMS architecture.

3) True-Time-Delay-Based Hybrid Beamforming: Most of the current hybrid beamforming architectures rely on phase shifters, which are frequency-independent, inducing the same phase rotation at different frequency components of a signal. Under the ultra-wide bandwidth at the THz, these shifters only provide correct phase shifting for a certain frequency point, whereas other frequency points suffer from phase misalignment. As a result, the formed beam is squinted with a substantial power loss, e.g., 5 dB claimed in [333]. To solve the problem of beam squint at the THz band, true-time-delay (TTD) can be applied to substitute phase shifters [332]. The TTD is frequency-dependent, and the phase rotation adjusted by TTD is proportional to the carrier frequency and perfectly matches the ultra-wideband THz beamforming.

According to [351], the TTD-based phase shifting is aligned with the requirements of wideband THz hybrid beamforming, given its proportional relationship with the carrier frequency. While ideal TTDs with infinite or high resolution are capable of precise phase adjustments, they are often associated with high power consumption and hardware complexity [352]. For the perspective of practical THz systems, low-resolution TTDs that strike a balance between energy efficiency and performance are more suitable, as reported in the literature such as [352]–[354]. In [355], a novel hybrid precoding architecture named delay-phase precoding (DPP) was introduced to mitigate the issue of beam squint in THz communications systems. By incorporating a time delay network between digital and analog precoding, DPP generates frequency-dependent beamforming vectors. Similarly, Gao *et al.* [356] proposed a TTD-based hybrid beamforming that aims to address beam squint through virtual subarrays, as first presented in [357]. The proposed algorithm achieves near-optimal performance as that of full-digital precoding.

In order to address the limitation of TTD, Nguyen and Kim [358] proposed a hybrid beamforming scheme that takes into account the relationship between the number of antennas and the required delay for TTD. They also carried out joint optimization under limited delay to create an optimal compensation scheme for beam squint. It is noted that most research work, as mentioned above, focused on 2D hybrid beamforming, which is primarily designed for uniform linear array (ULA). However, ULAs may not be suitable for UMMIMO systems due to limited antenna aperture. In contrast, uniform planar arrays (UPAs) that can accommodate a large number of elements compactly, are more potential for deploying UMMIMO systems. There is a lack of research on beam squint compensation in 3D hybrid beamforming using ULAs for THz broadband UMMIMO systems. Responding to this, the authors of [332] proposed a 3D beamforming architecture by leveraging two-tier TTD, which is able to combat the beam squint effect from both the horizontal and vertical directions. The impact of the array structure on the beam squint has been analyzed in [359].

B. Lens Antenna Array

Despite its high potential at the THz band, hybrid beamforming is still confined by high hardware and power costs due to the use of many analog phase shifters. Some studies [360] demonstrate that the power consumed by phase shifters becomes critical. In this context, a disruptive antenna technology called *lens antenna* [361] draws the focus of academia and industry.

James Clerk Maxwell predicted the existence of EM waves in 1873 and inferred that visible light is a kind of EM waves. To verify Maxwell's theory, early scientists who believed a radio wave is a form of invisible light concentrated on duplicating classic optics experiments into radio. Heinrich Hertz proved the existence of EM waves and also first demonstrated the refraction phenomena of radio waves at 450 MHz using a prism. These experiments revealed the possibility of focusing radio waves on a narrow beam as visible lights through an optical lens. In 1894, Oliver Lodge [362] successfully used an optical lens to concentrate 4 GHz radio waves. In the same year, Indian physicist Jagadish Chandra Bose [363] built a cylindrical sulfur lens to generate a beam in his microwave experiments over 6 GHz to 60 GHz. In 1894, Augusto Righi at the University of Bologna focused radio waves at 12 GHz with 32 cm lenses. In World War II, the race of developing radar technology fostered the emergence of modern lens antennas. Used as a radar reflector, the famous Luneberg lens [364] was invented in 1946, which is also attached to stealth fighters nowadays to make it detectable during training or to conceal their true EM signature.

As refracting visible light by an optical lens, a lens antenna uses a shaped piece of radio-transparent material to bend and concentrate EM waves [365]. It usually comprises an emitter radiating radio waves and a piece of dielectric or composite material in front of the emitter as a converging lens to force the radio waves into a narrow beam. Conversely, the lens directs the incoming radio waves into the feeder in a receive antenna, converting the induced electromagnetic waves into electric currents. To generate narrow beams, the lens needs to be much larger than the wavelength of the EM wave [366]. Hence, a lens antenna is more suitable for mmWave and THz communications, with tiny wavelengths. Like an optical lens, radio waves have a different speed within the lens material than in free space so the varying lens thickness delays the waves passing through it by different amounts, changing the shape of the wavefront and the direction of the waves.

On top of lens antennas, an advanced antenna structure referred to as a lens antenna array has been developed [367]. A lens antenna array usually consists of two major components: an EM lens and an array with antenna elements positioned in the focal region of the lens. EM lenses can be implemented in different ways, e.g., dielectric materials, transmission lines with variable lengths, and periodic inductive and capacitive structures. Despite its various implementation, the function of EM lenses is to provide variable phase shifting for electromagnetic waves at different angles [368]. In other words, a lens antenna array can direct the signals emitted from different transmit antennas to different beams with sufficiently separated angles of departure. Conversely, a lens antenna array at the receiver can concentrate the incident signals from sufficiently separated directions to different receive antennas [369].

Recent research work reported a few high-gain THz lens antennas, such as dielectric or metallic lens antennas [370]–[372]. Dielectric lens antennas have been demonstrated with high gain and wide operating bandwidth by integrating the dielectric lens with a standard rectangular waveguide feed [370] or a leaky-wave feed [371]. But their radiation efficiency needs to be improved. On the other hand, metallic lens antennas have no dielectric loss, making them suitable for THz communications and sensing. In [372], a high-gain THz antenna using a metallic lens composed of metallic waveguide delay lines was reported. For wideband signal transmission, recently, the authors of [373] presented a fully metallic lens antenna with a wide impedance bandwidth and high gain at the D band from 110 GHz to 170 GHz. A flared H-plane horn is used to achieve a large H-plane radiation aperture to further increase the radiation gain.

The deployment of MMIMO systems entails the challenges associated with a huge amount of antenna elements [374]. EM lens arrays with a reasonable number of elements can lower the required number of antennas and corresponding RF chains while maintaining high beamforming gain. However, dielectric EM lenses are difficult to integrate with multiple antenna techniques due to their bulky size, high insertion loss, and long focal lengths to control the beam gain. The metallic lens antennas are defined as artificial composites that obtain electrical properties from their structure rather than their constituent materials. Some studies on metallic lens antennae have been done to achieve beam gain from a single antenna, like [375]. Jaehyun Lee *et al.* proposed a large-aperture metallic lens antenna designed for multi-layer MIMO transmission for 6G, demonstrating that a single large-aperture metallic lens antenna can achieve a beam gain of up to 14 dB compared to the case without a lens. By adopting the proposed large-aperture metallic lens antenna, system-level simulations show that the data throughput of the user equipment is effectively increased [376].

C. Beam Alignment: Training of Beams

The utilization of the promising THz spectrum range is hindered by significant propagation losses imposed on its frequencies. To counteract the losses, large antenna arrays, such as UMMIMO and lens antenna array discussed above, can be employed, but this leads to highly directional and narrow beams [377]. To ensure a satisfactory signal-to-noise ratio (SNR) at the receiver and prevent connection loss, it is critical to maintaining degree-level alignment between the transmitter and receiver beams. Therefore, beam alignment is a critical issue that must be addressed for establishing a reliable connection. This is accomplished by aligning the beams at the transmitter and receiver to the direction of the channel paths, where channel state information (CSI) is critical for implementing the fine alignment [378]. However, traditional channel sensing methods used at lower frequencies are not feasible at THz frequencies due to the significant path

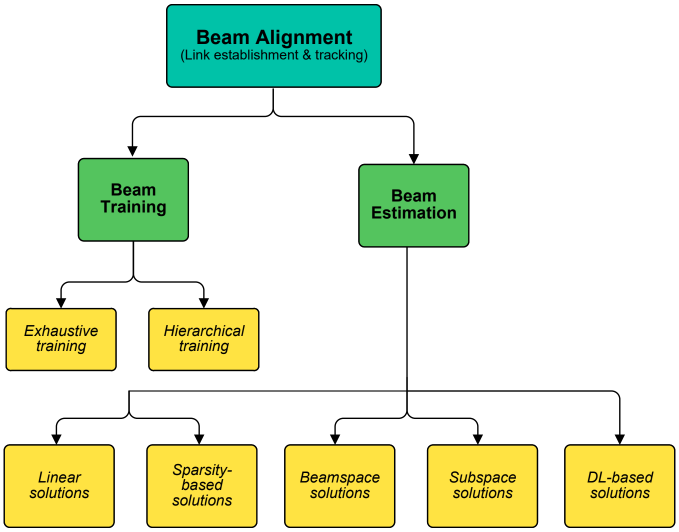

Fig. 9. Illustration of beam alignment techniques.

losses that render pilot signals undetectable during the link establishment stage.

As a result, significant research efforts have been made in recent years to understand the unique characteristics of the THz channel and to develop appropriate beam alignment algorithms. These efforts aim to establish beam alignment during the link establishment stage [379], [380] and to maintain alignment while the beams are in motion (beam tracking). Two categories of beam alignment techniques have been identified: *beam training* [381] and *beam estimation* [382], as shown in Fig. 9. The former involves transmitting known signals and adjusting beamforming parameters to align the beams. The latter involves estimating CSI from received signals and using it to refine the beamforming parameters. This part surveys the state-of-the-art advances in beam tracking techniques, while beam estimation is discussed in the subsequent part.

Beam training involves scanning the channel with directional beams from a codebook to determine the beam pair at the transmitter and receiver that results in the highest SNR of the received signal [383]. Beam training can be broadly classified into two categories: exhaustive and hierarchical training, which are discussed as follows:

1) Exhaustive Training: Many studies have adopted exhaustive training, which involves sequentially probing all the predefined directions in the codebook to find the optimal beam pair that maximizes the SNR at the receiver [384]. This approach is used in the IEEE 802.15.3c standard [385]. However, this method is time-consuming and not practical at THz frequencies, where beams from a large-scale antenna array tend to be very narrow, making it difficult to scan the entire space in a reasonable amount of time. Additionally, the accuracy of the training is limited by the codebook's resolution.

Responding to these limitations, Tan and Dai [386] have improved the exhaustive search by exploiting the beam split effect. They used delay-phase-precoding architecture to control the beam split effect and accelerate the tracking process [387]. By doing so, the split beams have wider angular coverage and can scan many directions in a single shot. Another approach from the RF domain used leaky-wave antennas (LWA) at the transmitter and receiver of a THz link to estimate the angle-of-departure (AoD) and angle-of-arrival (AoA) [388]. The angular radiation of an LWA is frequency-dependent, and the received spectral peak determines the AoD. The bandwidth of the received signal is proportional to the rotation angle over the AoA of the LWA receiver, which speeds up the channel scanning process but requires additional hardware at both the transmitter and receiver.

2) Hierarchical Training: From a practical point of view, many studies have adopted hierarchical training to reduce training overhead [381], [384], [389]–[391]. Hierarchical algorithms are based on multi-resolution codebooks, which contain wide beams at lower levels and narrow beams at higher levels. The search begins at the lowest level and gradually moves to higher levels to find the optimal narrow beam. In [390], the authors proposed a subarray-based multi-resolution codebook, where beams at each level are generated by the contribution of all subarrays. In [391], the authors proposed an accelerated hierarchical training that concurrently scans angular space with different RF chains. The authors of [392] proposed a multi-modal beam pattern-based training that simultaneously radiates beams targeting different directions using a single RF chain. The equally spaced activation approach has been proposed to generate the steering vector for multiple beam radiation. However, the loss at THz frequencies may render the training algorithm ineffective. The authors in [378] and [393] adopted hierarchical training that utilizes the power-angular spectral correlation between sub-6GHz and THz frequencies.

In [394], Stratidakis *et al.* proposed a localization-aided hierarchical beam tracking algorithm that uses location information to reduce pilot overhead. This algorithm assumes the linear motion of a user, which may not be accurate in a realistic scenario. In [395], the authors proposed a unified 3D training and tracking framework based on a 3D hierarchical codebook built upon the quadruple-uniform-planar-array architecture. This proposal offers two advantages: a unified framework for training and tracking and 3D space coverage compared to 2D space coverage in most existing works. The training overhead of hierarchical algorithms is much lower compared to exhaustive ones. However, hierarchical algorithms suffer from a high overhead of feedback messages required for coordination between the transmitter and receiver. The number of levels in multi-resolution codebooks also leads to higher training overhead, which may not enhance performance, especially in multi-hop THz links [396]. A new approach is proposed in [397], where it is based on a multi-armed bandit algorithm and utilizes prior knowledge of channel frequency-selective fading. This algorithm is designed with a hierarchical structure to accelerate the beam alignment process.

D. Beam Alignment: Estimating of Beams

Beam estimation is a method of acquiring channel information with the goal of reducing training overhead when compared to beam scanning techniques. The estimation process begins with initial training, which involves collecting channel measurements. These measurements are then processed to derive the angular information of the target channel. Prior studies have proposed a variety of algorithms, based on linear estimation [398], [399], compressive sensing (ComS)-based sparse estimation [400]–[404], beamspace-based estimation [405], [406], subspace-based estimation [382], [407]–[409], or deep learning-based estimation [382], [410], [411].

1) Linear Estimation: The authors of [398] used an extended Kalman filter, which is a well-known example of linear estimation, to perform beam tracking for a mobile station (MS). The MS sends training symbols over the uplink during each time slot, and the extended Kalman filter-based algorithm at the base station (BS) iteratively estimates the channel parameters (the path gain, AoD, and AoA) from the observed signal. The proposed algorithm achieves millidegree level angle estimation with moderate mobility of the MS and antenna array size. However, the study assumes the BS is equipped with a fully digital beamformer, which is not practical due to the high power consumption imposed by a large number of RF chains. Additionally, the study assumes that the MS is parallel to the BS during tracking, such that AoD equals AoA, which is not realistic because the orientation of the MS can be arbitrary in real-world scenarios. Other linear methods, such as maximum likelihood and least square, can also be applied [399]. However, these estimators require a large number of observations and do not exploit the sparsity feature of THz channels.

2) Compress Sensing-based Sparse Estimation: The sparsity property of THz channels can significantly reduce the computational complexity of beam estimation algorithms by transforming the problem into a sparse recovery problem. A technique referred to as ComS is considered an optimal approach to solving these problems, as discussed by the authors in [403]. They analyzed two ComS-based algorithms, i.e., *greedy compressive sampling matching* and *Dantzig selector-based method*, for solving convex programs. Results show that the ComS-based methods have higher accuracy compared to linear estimation based on least square. The authors in [400] utilized ComS-based techniques to accelerate the training proposed in [378]. In this approach, the estimated angles from wide beams in the first stage are refined using an L1-norm regularized least squares method to obtain accurate estimates of AoD and AoA, reducing the scope of the narrow beam search in the second stage.

Another work in [404] proposed an orthogonal matching pursuit-based fast algorithm to estimate the AoA and AoD of a BS-MS link. This study considered the cost and power consumption of adopting an auxiliary fully-digital array for channel estimation and evaluated the effect of RF imperfections and low-resolution analogue-to-digital converter (ADC) per RF chain. This study adopts the virtual channel model, which assumes that the AoA and AoD are discretely distributed over a spatial grid utilizing the angular sparsity of the THz channel, making it a sparse recovery problem suitable for ComS-based algorithms. However, this discrete grid assumption reduces the estimation accuracy due to the grid resolution. To mitigate this limitation, the authors in [412] proposed an iterative reweight-based super-resolution estimation scheme, which optimizes the on-grid estimation iteratively to converge to neighboring off-grid angles. Simulation results show that the off-grid solution has improved accuracy and spectral efficiency compared to on-grid solutions. Similarly, the authors in [413] proposed a gridless ComS-based algorithm to estimate the AoA for arbitrary 3D antenna arrays, eliminating the quantization error of the grid assumption.

The mentioned ComS-based estimations are generally built on the assumption of angular sparsity of THz channels, which holds in the far field but is not valid in the near field. Therefore, the work in [401] considers ComS-based estimation in the near field where the angular sparsity assumption does not hold. Results show that the channel in the near field exhibits polar sparsity rather than angular sparsity, which was exploited by a ComS-based polar-domain simultaneous orthogonal matching pursuit algorithm.

3) Beamspace-based Estimation: As we know, the MIMO beamspace channel can be realized through the use of a discrete lens array (DLA). This kind of arrays function as passive phase shifters that steer beams towards specific directions based on the incident point to the lens aperture [414]. The number of these directions is limited by the number of antenna elements, resulting in a beam-sparse channel. This artificially created sparsity reduces the pilot overhead required for channel estimation compared to conventional methods. In [405], the authors adopted the DLA-based MIMO system architecture to create the MIMO beamspace channel and utilized its sparsity for fast channel tracking. A *priori* information-aided tracking scheme was proposed for MIMO beamspace systems, where the channel was conventionally estimated in the first three time slots and the physical direction of the MS was then derived based on a temporal variation law. The estimated physical direction was used to determine the support of the beamspace channel, which corresponds to the dominant beam directions. However, the estimation accuracy is greatly dependent on the localization accuracy. In [406], the authors extended the work in [405] and proposed a cooperative localization-aided tracking algorithm with multiple BSs, each equipped with a DLA. These BSs cooperate to accurately localize the MS for improved channel tracking. While beamspace MIMO solutions significantly reduce the overhead in comparison with that of conventional estimation methods, their accuracy may be limited by the discrete directions generated by the DLA and a restricted number of beams.

4) Subspace-based Estimation: When estimating continuously distributed AoA and AoD, another way referred to as subspace-based algorithms can be performed, with the aim of avoiding the estimation error caused by the sparse solutions or beam sparsity in beamspace solutions. In general, these algorithms collect channel measurements and identify the eigenvectors that correspond to the signal subspace. Two widely known algorithms, i.e., MUSIC (MUltiple SIgnal Classification) and ESPRIT (Estimation of Signal Parameters via Rotational Invariance Technique), belong to subspace-based estimation [382], [407].

In [382], the authors adopted the MUSIC algorithm to achieve millidegree-level AoA estimation. This study utilized a hybrid AoSA architecture and collected measurement data by probing random steering vectors. The covariance matrix of the measurement data was then calculated and decomposed into signal and noise subspaces. The AoA was estimated by searching the MUSIC pseudospectrum function for vectors orthogonal to the noise eigenvectors. The estimation was further refined by collecting new measurements based on the coarse estimated angles. In [407], the ESPRIT algorithm was adopted for super-resolution channel estimation, which involved multiple steps such as spatial smoothing, forward-backward averaging techniques [415], singular value decomposition (SVD), and joint diagonalization. While subspace solutions show improved performance compared to sparse solutions, their computational complexity is significantly higher.

5) Deep Learning-based Estimation: Recently, deep learning (DL)-based techniques have emerged as a promising alternative to replace conventional estimators. DL-based solutions are particularly effective for complex multi-user scenarios where the input and output of the channel are not directly related. In [382], a branch of DL referred to as deep convolutional neural network (DCNN) is used to estimate the AoA of a multipath channel. The measurement matrix is collected through random beamforming and combining matrices at the transmitter and receiver, respectively, and fed into the neural network. Three convolutional layers extract the spatial peculiarities of the channel, and two fully-connected layers capture the non-linear relationship between these peculiarities and AoA estimation. Results show higher estimation accuracy than the subspace-based MUSIC algorithm at high SNR.

In [410], a DCNN architecture is used to estimate the near-field channel under the spherical wave propagation model. The proposed DCNN-based approach addresses the spherical wave propagation model by considering the inter-subarray phase error as an output parameter of the network. In [411], deep kernel learning (DKL) combined with Gaussian process regression (GPR) is used to estimate the indoor THz channel in a multi-user scenario. In particular, a deep neural network (DNN) is trained to capture the non-linear relationship between the input and output of the channel. Results show that this DNN-based solution outperformed the minimum-mean square error (MMSE) and least squares-based linear estimators.

Prior studies have demonstrated the superiority of DL-based solutions over conventional solutions in complex scenarios. It also revealed that DL networks need lots of computational and storage resources, intensive offline training, and validation. Moreover, their efficiency in low SNR scenarios requires further investigation. In order to achieve fast initial access in wireless networks, a DNN framework called DeepAI has been proposed, which maps the received signal strength (RSS) to identify the optimal beam direction [416]. The authors have introduced a sequential feature selection (SFS) algorithm that selects efficient and reliable beam pairs for DeepAI's inputs in LoS mmWave channels. However, the SFS algorithm fails to improve the accuracy and performance of DeepAI in NLoS scenarios. Simulation results show that DeepAI outperforms the conventional beam-sweeping method. Another DL-based beam selection algorithm is suitable for 5G NR has been proposed by the authors in [417].

VIII. THz Systems and Networks Toward 6G and Beyond

The ongoing research and development of the 6G system is set to revolutionize the way various domains and layers of a mobile network interact and communicate with each other and with authorized third parties [418], [419]. As we stated numerous times throughout this paper, one of the key enablers of 6G is THz communications and sensing, which promise to deliver ultra-high data rates, ultra-low-latency connectivity, high-resolution sensing, and high-accuracy positioning in the coming decades. Nevertheless, the full potential of THz communications and sensing can only be realized through its integration with other emerging technologies.

In this section, we explore THz networks from a systematic point of view, with an emphasis on the synergy of THz communications and sensing with a range of 6G-enabling technologies, including massive multi-input multi-output, ultra-massive multi-input multi-output, non-orthogonal multiple access, reconfigurable intelligent surfaces, non-terrestrial networks, digital twins, artificial intelligencem machine learning. Moreover, we discuss security, localization, joint communications and sensing, multi-connectivity, and channel awareness for THz systems and networks. By examining these synergies, we hope to shed light on the most significant research challenges and opportunities facing the development and deployment of THz communications and sensing in 6G and beyond networks, as well as the potential benefits for future applications, use cases, and services.

A. THz-MMIMO Systems and Networks

Compared to lower frequencies at sub-6 GHz and mmWave, the THz bands have a much smaller signal wavelength, which leads to a tiny size of antenna (i.e. a larger number of antennas within the same surface area) and narrower beams. Both the factors are beneficial for MMIMO and grant it a greater potential in the THz band than at lower frequencies. For example, Akyildiz and Jornet reported that UMMIMO systems up to the dimension of 1024×1024 can be realized at 1 THz with arrays that occupy just $1\,\mathrm{mm}^2$ [322]. However, the application of MMIMO and/or UMMIMO in practical 6G THz communications and sensing are challenged in various aspects. In addition to the barriers in the fabrication of nano-antenna arrays, the complexity and sparsity of THz channels are also limiting the exploitation of MMIMO in this band. Accurate channel models, physical (PHY) layer enabling technologies, as well as novel link layer design, are needed to release the full potential of THz MMIMO.

A lot of works in modeling THz MMIMO channels have been reported since the late 2010s, overwhelmingly with the ray-tracing methodology. Han *et al.* proposed in [420] a model for UMMIMO channels over a distance to 20 m and in the frequency windows of 0.3 THz to 0.4 THz and 0.9 THz to 1 THz. Busari *et al.* studied the 0.1 THz MMIMO channel in [421] a specific outdoor street-side scenario, investigating the impacts of precoding scheme, carrier frequency, bandwidth, and antenna gain on the system regarding spectral and energy efficiencies. Sheikh *et al.* focused on the critical features of rough surface reflection and diffuse scattering at THz frequencies, and proposed in [422] a 3D indoor model for 0.3 THz and 0.35 THz MMIMO channels with different surface roughness levels, considering both LoS and NLoS scenarios. In the recent work [339], Tarboush *et al.* reported their channel model for wideband UMMIMO THz communications and a simulator based thereon.

Efforts on the physical layer deal with the problem of beamforming and combining from the perspectives of beam training and beam tracking, i.e., finding the best beam pattern and online adjusting it, in order to obtain the best link quality and maintain it against the time variation of the channel. As outlined by Ning *et al.* in their tutorial [57], there are two basic principles of beamforming: the precoding/decoding that is executed in the digital domain, and the beam steering that works in the analog domain. Each of the principles, as well as their hybrid, when applied in the wideband THz systems, must be carefully designed to address two main issues: the spatial-wideband effect that different antennas receive different symbols at the same time, and the frequency-wideband effect that the beam pattern of a phase array codeword changes with the frequency of the signal (a.k.a. the beam squint or beam split). While most existing methods leverage either the digital precoding approach [355], [423], or the precoding/steering hybrid [356], [405], [424], [425], new research interests in the steering approach based on RIS are arising [426], [427]. Whilst higher layer design has not been a major research focus of MMIMO THz systems so far, there is pioneering work on multi-access scheme reported in [206].

B. THz-NOMA Systems and Networks

Another promising RAN technology for enabling THz-MIMO systems and networks is NOMA, which allows allocating of the same radio resources to more than one user simultaneously and invokes the so-called successive interference cancellation (SIC) approach on the receiver side to decode the information for different users successively [428]. Compared to lower frequencies, the low-rank channels in the THz bands can be much more correlated because of the limited-scattering transmission, which reduces the channel orthogonality between different users and makes NOMA a promising technique to improve the spectral efficiency [26]. Serghiou *et al.* [64] believe that in LoS scenarios where spatial processing approaches fail to separate the users from each other, a combination of NOMA with UMMIMO can provide more fair user access in terms of resource allocation, and therewith achieve better spectral efficiency of the overall network. Meanwhile, with proper resource allocation algorithm, NOMA can also enhance the energy efficiency in THz communications and sensing systems [429].

To evaluate the feasibility of MIMO-NOMA systems in THz bands, Sabuj *et al.* proposed in [430] a finite blocklength (FBL) channel model and therewith evaluated the system performance regarding critical machine-type communications (CMTC) scenarios. In contrast to its good performance in LoS scenarios, THz-NOMA performs much poorer when the connected devices are blocked by obstacles [431]. To address this issue, RIS appears as a promising solution. In [432], Xu *et al.* proposed a smart RIS framework for THz-NOMA, which delivers significant enhancements in the system energy efficiency and the reliability of super-fast-experience users. The principle of NOMA requires users to be paired/clustered for sharing radio resources, and relies on an appropriate clustering to achieve satisfactory system performance. Shahjala *et al.* comparatively reviewed the user clustering techniques for MMIMO-NOMA THz systems in [433], and proposed a fuzzy C-means-based clustering approach in [434].

It shall be noted that many popular clustering policies are tending to pair a user with good channel, called cell center user (CCU), to another with poor channel, called cell edge user (CEU). Such policies lead to a gain in the spectral efficiency of the overall system, but a degradation at the CEU due to power splitting. To address this issue, Ding *et al.* proposed in [435] a cooperative non-orthogonal multiple access (CNOMA) scheme where the CCU always forwards the message for CEU that it obtains during the SIC, so that the performance loss at CEU is compensated. However, this design is forcing the CCU to work as a relay which drains its battery. Therefore, simultaneous wireless information and power transfer (SWIPT) is often introduced into CNOMA systems so that the CCU is able to harvest energy from the radio signal to support the relaying [436]. At THz frequencies, due to the high spreading loss and atmospheric absorption, the power propagation loss is more critical than that at lower frequencies, and the SWIPT-assisted CNOMA solution can be more important. Oleiwi and Al-Raweshidy analyzed the performance of SWIPT THz-NOMA in [437], and correspondingly designed a channel-aware pairing mechanism [437].

C. THz-RIS Systems and Networks

The 6G and beyond systems will be revolutionized by the tremendous potential of RIS [438]–[440] and THz [441], the two cutting-edge enablers for the access domain of a futuristic communications and sensing network. The synergy between RIS and THz lies in the fact that RIS can be utilized to improve the performance of THz systems by providing a cost-effective solution to the propagation challenges associated with THz frequencies [442]. By utilizing the reconfigurability and versatility features of RIS, it is possible to address the challenges of THz wave propagation, especially the use of bypassing the blockage of THz beams, thereby improving the overall performance of THz communications and sensing.

By controlling the phase, amplitude, and polarization, RIS can effectively steer, reflect, and amplify electromagnetic waves in THz systems and networks. Consequently, it enables a vast array of applications and use-case scenarios, including beamforming, wireless power transfer, and indoor localization, among others. In addition, by employing RIS-assisted spatial modulation, the THz-RIS systems and networks have the potential to dramatically improve their spectral efficiency. More importantly, RIS can be used to generate virtual channels that compensate for the propagation losses of THz waves in order to increase SNR and the coverage area of THz communications and sensing. By far, the intersection of the

RIS and THz has been intensively studied in the literature. There exist a number of overview and survey papers that provide an insight of such synergies, including [443]–[446]. In addition to the aforementioned survey papers, we discovered during our research that the intersection between these two technologies has been dramatic, including in the context of massive MIMO, millimeter wave, 3D beamforming, satellite networks, and many others. Moreover, a large number and various types of physical layer-related optimization problems have been jointly investigated.

D. THz-Aided Non-Terrestrial Networks

With its ambition of ubiquitous 3D coverage, 6G and beyond are envisioned to include different non-terrestrial infrastructures, such as unmanned aerial vehicle (UAV), high-altitude platform (HAP), LEO satellites, and geostationary Earth orbit (GEO) satellites, as an indispensable part of its architecture. Since the air/space channels and air/space-to-ground channels are less subject to blockages w.r.t. terrestrial channels, the LoS link availability is much higher, implying a vast potential for THz communications and sensing [447]. On the one hand, the tremendous amount of spectral resources offers the feasibility of efficient interconnection among these terrestrial, air, and space platforms through THz communications links. On the other hand, non-terrestrial infrastructures enable the flexible deployment of a variety of THz sensing equipment at favorable altitudes and places.

Nevertheless, the practical deployment of THz-non-terrestrial network (NTN) is still facing various technical challenges, which are including but not limited to: feasibility assessment of THz frequencies for space-to-earth links, transceiver implementation, and accurate NTN platform positioning [448]. Regarding the characterization of THz-NTN channels, the authors of [449] proposed an analytical propagation model for low-altitude NTN platforms such as UAVs in the frequency range 0.275 THz to 3 THz, while the authors of [450] modeled the cross-link interference for LEO satellites. The use of satellites to serve air planes on the THz band and related channel models have been analyzed in [451]. Concerning the THz transceiver implementation, NTN systems pose high antenna design requirements. For example, the antennas are supposed to produce multiple high-gain beams to support dynamic networking and realize long-range communications. There are various approaches towards this aim, which are well summarized in the survey by Guo *et al.* [452]. For THz CubeSat networks, the antennas are required to provide sufficient beamwidth angle to enable faster neighbor discovery, while simultaneously providing a high gain to overcome the path loss. To fulfill these requirements, Alqaraghuli *et al.* designed a two-stage Origami horn antenna [453].

On the PHY layer, digital signal processing techniques are studied to overcome the limitations of the analog front end in THz transceivers. Tamesue *et al.* propose to deploy digital predistortion in RF power amplifiers of THz-NTN systems to compensate the nonlinear distortion [454]. In [455], Kumar and Arnon reported a DNN beamformer to replace the phase shifters in THz-MMIMO antenna arrays for wideband LEO satellite communication. It also creates additional benefits for NTN by deploying THz communications and sensing in conjunction with other novel enabling technologies. For example, RIS can contribute to the deployment of THz in future integrated terrestrial/non-terrestrial networks by means of enhancing the beamforming [456]. By leveraging the ISAC technology, the differential absorption radars (DARs), which are traditionally used for weather sensing, can be granted an extra capability of communicating with LEO satellites [457].

E. Digital Twin-Aided THz Systems and Networks

The digital-twin technology [458] is an emerging novel concept (which is also considered to be as a key enabler of the 6G and beyond systems) in which a virtual replica of a physical system, object, process, network, or link is created employing accurate data collected in real-time [459]. It enables the autonomous control, intelligent monitoring, and accurate self-optimization of physical networks, processes, and systems in a fully virtualized environment. To our knowledge, there exists synergy between the digital-twin technology and THz communications/sensing networks that can produce a combined effect on the 6G and beyond aimed at improving the overall performance in delivering data-driven services. This synergy stems from the fact that both rely on accurate and real-time data that is collected from their corresponding data nodes. On the one hand, THz communications can support the transmission of large amounts of data generated by digital-twin nodes by facilitating high-speed communications links [458], while THz sensing can help the acquisition of high-accuracy environment data for digital twin. On the other hand, a digital twin can improve the overall performance of THz communications and sensing by offering a virtual testing, monitoring, decision-making, and optimization environment for the said THz systems and networks [458].

To be specific, digital twins can be utilized to generate and enable virtual replica (also known as virtual model) for manufacturing processes and systems, such as digital twins for the machines, links, services, materials, networks, and products contained in an industry. By controlling and monitoring the virtual replicas in a real-time manner, it can be feasible to detect and subsequently address any maintenance issues and bottleneck that may arise in the said industry, including device and machine complete failures, unsuccessful service delivery attempts, material shortages, among many others. To enable the digital twinning of manufacturing industry, THz communications/sensing systems and networks can be deployed to acquire, transmit, and receive data (and at some points enrichment information) between the physical objects and virtual replicas of the manufacturing systems, enabling real-time control, accurate decision-making, and autonomous optimization [460].

In the literature, the relationship between digital twin technology and THz systems has received scant attention. During the course of our research, we uncovered three references addressing this intersection of the two technologies. First, the authors in [461] proposed a THz signal guidance system in which a digital twin is utilized aimed at modeling, controlling, and predicting the indoor signal propagation features and characteristics. The authors claim that their methodology achieved the "best" THz signal path from a nearby base station to the targeted user equipment using a number of certain models. Second, in reference [462], the authors proposed a framework that is based on the THz communications system and aimed at implementing the digital-twin prediction for enabling extremely security-sensitive systems and objects. Finally, reference [460] studies the delay minimization optimization problem within the context of THz communications system and visible light communications system. In their study, the authors claim that their approach reduces up to 33.2% transmission delay in comparison to the traditional methods.

F. AI/ML-Aided THz Systems and Networks

THz communication/sensing systems and AI/ML [463]–[465] can benefit from each other synergistically. There are several facets of THz systems that can benefit from the application of AI techniques and ML algorithms in 6G and beyond networks. For example, AI/ML can be employed for (a) signal processing to enhance the quality of THz signals and reduce noise; (b) THz channel estimation to be maintained over long distances and not be affected by atmospheric effects; and (c) the optimization of error correction codes and modulation schemes. On the one hand, the performance, effectiveness, and dependability of THz systems and networks can be improved through the utilization of AI/ML approaches. On the other hand, THz systems can offer high-speed wireless data transfer and high-accuracy sensing capabilities that can be helpful for the deployment of AI/ML services.

In addition, AI/ML algorithms can be utilized to create intelligent and data-driven THz communications and sensing systems capable of adapting to quickly changing environmental conditions. For instance, with advanced AI/ML algorithms, self-healing, self-optimizing, and self-regulating THz communications networks that can modify their parameters autonomously to maintain goal performance and service levels can be created. Moreover, AI/ML can be utilized in THz imaging and sensing application use-case scenarios, including security screening, medical diagnosis, industrial inspection, and many others. THz images can be processed using AI/ML algorithms to extract enrichment and/or useful information, resulting in more accurate and reliable results.

The strong synergistic relationship between AI/ML and THz systems has also been demonstrated by a large number of recent studies published in cutting-edge academic journals and conferences. During our research, we found three papers, [61], [105], [466], that provide a comprehensive overview of various aspects of the AI/ML applicability in THz systems and future research directions in this domain. To be specific, the authors in [61] provide a survey and overview of the current state-of-the-art research in THz communication, including signal processing, front-end chip design, channel modeling, modulation schemes, and resource management. The paper also highlights the challenges and opportunities in 6G THz communications systems and discusses the potential applications of THz communications in various fields. Reference [466] provides a comprehensive review of the recent achievements and future challenges of ML in THz communication. More specifically, the paper summarizes the state-of-the-art research on ML-based THz imaging, sensing, and communications systems, including signal processing, feature extraction, classification, and optimization. The paper also discusses the potential applications of ML in THz technology, such as medical diagnosis, security screening, and wireless communication, and outlines the future research directions and challenges in this field. The authors of [105] cover the fundamentals of THz sensing, including sources of THz radiation, detection techniques, and applications. This paper presents a comprehensive survey of signal processing techniques, including time-domain and frequency-domain methods, feature extraction, and classification. It also reviews recent developments in ML-based THz sensing and highlights the challenges and future directions for signal processing and ML techniques in THz sensing.

Finally, and in addition to the above three overview papers related to THz communications systems, there exist a number of papers that study ML techniques for time-domain spectroscopy and THz imaging [106], the application of AI in THz healthcare technologies [467], two types of low-cost THz tags using ML-assisted algorithms [468], and molecular screening for THz detection using ML-assisted techniques [469].

G. Security in THz Systems and Networks

The security of information and data acquired, transmitted, and received over a THz communications and sensing system can be effectively improved by physical layer security in the access domain, which is the utilization of properties of the physical layer of the THz system. It is a novel methodology that is strongly believed to secure communications and does not rely only on cryptographic approaches. The intersection between physical layer security and the THz system results from the novel physical properties of THz waves, which can be utilized to improve the security of the transmitted information and data. To the best of our knowledge, physical layer security can be deployed in the following aspects of THz communications and sensing: channel authentication, PHY encryption, beamforming, and PHY key generation. These security techniques can improve the security of THz communications and sensing systems and make them suitable for a variety of 6G scenarios, such as hot spots, wireless backhaul, satellite interconnection, positioning, and imaging. Last but not least, the PHY security and the THz systems can be integrated to produce secure and reliable systems for 6G industrial applications.

As of the time of this writing, a number of studies have uncovered numerous facets of the intersection between PHY security and THz systems in 6G and beyond networks. The first studies that we reviewed were conducted in 2017, including [109], [470]. In the previous paper, a hybrid physical and multi-dimensional coded modulation scheme for THz communications systems is proposed. In the latter paper, physical layer authentication in THz systems is presented. Following that, we also found that three studies were conducted (both based on simulation and calculation) on the PHY security related to resiliency against eavesdropping using a directional atmosphere-limited LoS THz link [110], [112], [471]. Regarding eavesdropping probability, the authors of [472] have also investigated decreasing message detection using inherent multi-path THz systems. Finally, a physically secure THz system is studied at 0.31 THz using orbital angular momentum in [473].

H. Localization Services in THz Systems and Networks

Localization services and THz systems are two completely different research areas. Nevertheless, they can be integrated synergistically aimed at improving their capabilities and opening up new avenues for a variety of applications and use cases in the 6G era. The intersection of localization and THz systems results from the unique propagation characteristics of THz frequencies, which can be utilized for localization purposes in the access network domain. THz frequencies are particularly sensitive to rapidly occurring environmental changes, such as the presence of obstacles (a.k.a. problematic objects) or changes in the refractive index of materials in an environment. This extreme sensitivity can be utilized to create THz-based localization services and systems that can operate in a variety of environments, including indoor environments where GPS-based systems may not function optimally.

The integration of localization services into THz systems and network has the potential to enable a variety of novel use cases and applications in the 6G era, such as intelligent factories, manufacturing, healthcare, and many others. THz-based localization services, for instance, could be used to track assets within a factory or warehouse, while THz communications could be used to enable high-speed data transfer between machines and objects in the said factory. THz-based localization services could be deployed to monitor and control patient movement within a hospital, while THz communications could be used to enable wireless video transmission for remote consultations and many other services.

The intersection between localization services and THz communications systems has been studied to some extent in the literature. During our research, we found one tutorial and survey paper that provides a comprehensive overview of THz-band localization techniques for 6G systems. The authors discuss various aspects of THz waves, including propagation characteristics, channel modeling, and antenna design. They also explore different localization methods such as time of arrival, angle of arrival, and hybrid techniques. The paper concludes by highlighting some potential applications of THz-band localization in 6G networks [474]. In addition to the above survey, we discovered in two research articles that researchers have conducted research on various aspects of this intersection. In [475], the authors proposed a deep learning model for 3D THz indoor localization using a structured bidirectional long short-term memory network. The authors claim that their proposed method achieves better localization accuracy than state-of-the-art methods, making it a promising solution for indoor localization in THz-band communications systems. Finally, reference [476] proposes a new deep learning method for THz indoor localization called SIABR, utilizing a structured intra-attention bidirectional recurrent neural network to learn features from the received signal and estimate the location of the target.

I. Multi-Connectivity for THz Systems and Networks

Due to the high atmospheric absorption and low penetration capability, THz signals suffer from such strong propagation loss, fading, shadowing, and blockage, that they are hard to maintain with mobility even when beamforming and combining are ideally performed. To address this issue, THz systems will need multi-connectivity (MC) as an essential feature so that a continuous and stable data connection between the users and the network can be ensured by means of radio link redundancy in case a single radio link fails. The basic principle of MC is to keep multiple radio connections to different BSs simultaneously, but only use one of them at a time for signal transmission. The effectiveness of multi-connectivity in addressing the issue of blockage in THz band has been confirmed by evidence from various studies: a higher density of BSs is proven to enhance the system performance from the perspectives of link probability [477], capacity [477], [478], and session completion rate [479], [480].

Especially, there are two different strategies for selecting the active radio link, namely the closest line of sight multi-connectivity (CMC) where the closest BS with LoS link is always selected for communications and the reactive multi-connectivity (RMC) in which the active radio link is only re-selected when the current LoS link is blocked. While the CMC strategy is significantly outperforming the single-connectivity strategy, the RMC strategy brings only a marginal - sometimes even negative - gain, and is therefore discouraged despite its low signaling overhead [478]. It shall also be noted that the application of MC has an influence on the handover mechanism since it links the status model. In [481], Özkoç *et al.* established an analytical framework to assess the joint impact of the MC degree and the handover constraints on system performance of THz cellular networks.

An alternative and more advanced approach to exploit MC are to allow multiple BSs to simultaneously *serve* multiple mobile stations, i.e., each user may be communicating with multiple BSs rather than one at a time. This is usually known as the network MIMO or distributed MIMO (DMIMO), which exploits the spatial diversity by means of intensifying the BSs instead of antenna units in each array like in classical MMIMO/UMMIMO. To minimize the cross-interference among adjacent BSs and maximize the throughput in DMIMO networks, the coordinated multi-point (CoMP) technologies shall be invoked. CoMP allows different BSs to be clustered into small groups, and to coordinately optimize their user association and beamforming within each group. More specifically, there are two principles of CoMP: the joint transmission (JT) where multiple BSs transmit the same signal simultaneously to the same user equipment (UE), and the coordinated scheduling and beamforming (CSCB) where each BS sends a different signal and the signals are combined at the UE. An example of applying CoMP in the THz band is presented in [482], which combines joint power allocation and quantized co-phasing schemes to maximize the aggregated data rate.

Since the late 2010s, the concepts of DMIMO and CoMP have evolved into the cell-free network (CFN) paradigm, where all UEs in an area are jointly served by numerous single-antenna BSs in a CoMP manner [9]. Having been well studied at mmWave frequencies, the applicability of CFN in the THz band still remains under-studied [102]. Pioneering work was reported in 2022 by Abbasi and Yanikomeroglu [483], considering a NTN scenario. In some research works [484], multi-connectivity also refers to establishing connections in different communications bands, e.g., transmitting control signaling in the sub-6GHz band while delivering data in the THz band (also deliver data when the THz band is in an outage).

J. Channel Awareness for THz Systems and Networks

While modern wireless data transmission technologies generally rely on the knowledge of channel state to achieve satisfactory performance, the acquisition of accurate CSI can be a critical challenge for THz systems and networks. First, the pilot symbols can be easily blocked due to the susceptibility of THz channels, leading to a low efficiency of classical channel estimation methods. Second, THz channels are selective regarding many different parameters, e.g., time, frequency, beam pattern, beam direction, polarization, etc. Therefore, it takes much effort to comprehensively measure the CSI of a THz channel, in addition to a significant overhead to encode the dimensional and sparse CSI. Furthermore, similarly to the pilots, the CSI report from UEs to the network can also be blocked if transmitted in the THz band itself [66].

Regarding these challenges, out-of-band channel estimation occurs as a promising solution. This involves estimating the CSI of THz channels using channel measurements at lower frequencies, e.g. in the sub-6 GHz and/or mmWave bands, lower frequency bands, leveraging the potential spatial correlation among them. To assess the feasibility of this approach, the authors of [485] and [486] studied the spatial similarity among THz, mmWave, and sub-6 GHz bands based on point cloud ray-tracing simulation and field measurements. Their results support the use of out-of-band beam search strategy, not only in LoS scenarios but also even in NLoS ones, when using well-designed antenna patterns in specific frequency bands. Meanwhile, Peng *et al.* demonstrated the feasibility of out-of-band channel estimation beam searching with both ray-tracing simulations [487] and real-world experiments [488].

However, the exploitation of channel similarity for THz communications and sensing is still facing technical challenges. First, the difference in the size of the antenna array within the same aperture leads to a mismatch in the beamwidth between the lower frequencies and the THz signals [66], which is proven to have a stronger impact on channel similarity than the frequency gap itself [486]. Second, the correlation matrix is difficult to estimate, considering its large size and the small dimension of antenna arrays measuring at lower frequencies [66]. Third, despite the feasibility of out-of-band estimation on static THz channels, the dynamics such as user mobility, scatter mobility, and blockages, are lifting the difficulty of this task to the next level [485].

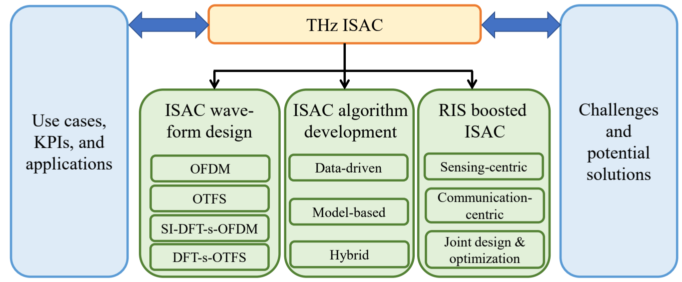

Fig. 10. An architectural overview of THz ISAC.

IX. Integrated THz Communications and Sensing

The novel concepts of "network as a sensor" and "Internet of Senses" become unprecedented essential in the upcoming 6G and beyond cellular networks so as to support a multitude of emerging use cases [19]. The two major functionalities, i.e., sensing (including localization and imaging) and communications, will be merged, synergized, and integrated, beneficial from each other rather than competing for network resources. In other words, future base stations are supposed to provide not only legacy communications services but also localization, sensing, and even electromagnetic imaging capabilities, acting as multi-functional ISAC transceivers [489], [490].

In general physical layer, ISAC broadly contains two widely-adopted terminologies, i.e., radar-communications co-existence (RCC) and dual-functional radar-communications (DFRC) [491]. It aims for enhanced spectral and energy efficiency, reduced hardware cost, and decreased power consumption as well as deployment and computational complexity. In the literature, THz sensing, imaging, localization, and communications were treated separately in [492]–[497]. Different from these, we in this section provide a holistic survey on the recent activities in integrated THz communications and sensing. Special attention is paid to use cases and KPIs, waveform design, algorithm development, RIS-boosted ISAC, and potential challenges and solutions. The architectural overview of THz ISAC is depicted in Fig. 10, and the selected major contributions related to THz ISAC are summarized in Table VII.

A. THz-ISAC Use Cases and KPIs

Localization and sensing, including determining the 2D/3D location and EM properties of objects, alongside multi-scale communications enable a multitude of emerging use cases, which may have different functional and non-functional QoS requirements in terms of accuracy, range, latency, velocity, update rate, reliability, and availability. The use case families consist of various vertical applications, e.g., massive twinning, immersive telepresence, wireless extended reality (XR), cooperative robots, THz internet-of-things (Tera-IoT), local trust zones, vehicular communication and radar sensing [511], and THz integrated access and backhaul (IAB). In general, these fall into the category of data-demanding and delay-sensitive applications. However, the QoS requirements differ from one use case to another. For instance, as two sub-categories of massive twining, manufacturing has more demanding requirements on accuracy, data rate, latency, update rate, reliability,

TABLE VII
SUMMARY OF SELECTED MAJOR CONTRIBUTIONS ON THZ-ISAC

Category	Year	Authors	Contributions
Use cases, KPIs, and application	2020	Wymeersch *et al.* [496]	Listed a series of application examples of RIS-based localization and mapping services.
	2021	Wymeersch *et al.* [19]	Provided an overview of the vision of the European 6G flagship project Hexa-X alongside the envisioned use cases; Discussed the technical enablers and associated research challenges.
	2022	Chen *et al.* [492]	Identified the prospects, challenges, and requirements of THz localization techniques.
	2022	Moltchanov [498]	Evaluated user- and system-centric KPIs of mmWave and THz communications systems.
	2021	Zhang [499]	Set up joint communications and sensing (JCAS) in the mobile network context and envisage its potential applications.
	2022	Akyildiz [500]	Pointed out 6G applications enabled by THz communications and their corresponding performance objectives.
Waveform design	2022	Wu [501]	Proposed SI-DFT-s-OFDM system for THz ISAC.
	2022	Wu [502]	Proposed discrete Fourier transform spread OTFS (DFT-s-OTFS) system to improve the robustness to Doppler effects and reduce peak-to-average power ratio (PAPR) for THz ISAC.
ISAC algorithms	2021	Yang [503]	Leveraged multi-domain cooperation to enhance the performance of the ISAC system through active and passive sensing, multi-user, and multi-frequency band networks.
	2022	Helal [504]	Addressed the effectiveness of deep learning techniques by exploring their promising sensing and localization capabilities at the THz band.
	2022	Mateos-Ramos [505]	Studied model-driven end-to-end learning for joint single target sensing and multiple-input single-output (MISO) communication.
RIS-boosted ISAC	2021	Jiang [506]	Investigated the joint optimization of the intelligent reflecting surfaces (IRS) passive phase-shift matrix (PSM) and precoding matrix of the radar-aided base station for the dual-function radar and communication (DRC) system.
	2021	Wang [507]	Investigated joint constant-modulus waveform and discrete RIS phase shift design, with the aim of minimizing multi-user interference (MUI) under the Cramér-Rao bound (CRB) constraint for direction of arrival (DoA) estimation.
	2021	Wang [508]	Studied the minimization of MUI under the strict beam pattern constraint by jointly optimizing DFRC waveform and RIS phase shift matrix.
	2022	Wang [509]	Minimized the CRB of the 2D DoAs estimation of the sensing target subject to the minimum communications requirement.
Challenges and solutions	2022	Elbir [491]	Studied several design challenges such as beam split, range-dependent bandwidth, near-field beamforming, and distinct channel model for ISAC at THz-band, and provided research opportunities in developing novel methodologies for channel estimation, near-field beam split, waveform design and beam misalignment.
	2022	Han [510]	Elaborated challenges from THz channel and transceiver perspectives, as well as the difficulties of ISAC.

and availability than smart city [19]. A full list of selected use cases and their corresponding performance metrics can be referred to [18], [19], [33], [108], [498]–[500], [512]–[514], closely tied to these of upcoming 6G and beyond systems, for which the ultimate goal would be realizing terabit-per-second links and millimeter-level sensing/localization accuracy [108], [515].

B. THz-ISAC Waveform Design

THz channels usually have short delay spread and THz transceivers suffer from low power amplifier (PA) efficiency (rapid decline on its saturated output power). Besides, frequency selectivity becomes less severe. As a result, coherence bandwidth increases. Therefore, the single-carrier waveform is more preferred compared to the orthogonal frequency-division multiplexing (OFDM) waveform [516]. Sensing integrated DFT-spread-orthogonal frequency-division multiplexing (SI-DFT-s-OFDM) can yield lower PAPR than OFDM while maintaining single-carrier characteristic, as reported in [501], [502], [517]. In addition, it brings a ten-fold improvement in velocity estimation of the moving target and 18% enhancement on data rate. In the ISAC systems, communications and sensing channels may possess different properties. For instance, unlike the THz communications channel, the delay spread of the sensing channel can be quite significant. Thus, different design criteria for communications and sensing waveforms should be considered in terms of cyclic prefix lengths and pilots [517].

Another type of intensively-studied waveform, so-called orthogonal time frequency space (OTFS), can well handle the Doppler effect and accommodate the channel dynamics in the delay-Doppler domain. Nevertheless, it still can not meet the strict requirements of power amplifier efficiency and signal processing complexity. Similar to SI-DFT-s-OFDM, DFT-s-OTFS was proposed to address the high PAPR issue faced in the original OTFS [502]. In contrast to OTFS, DFT-s-OTFS can achieve strong robustness to Doppler spread compared to OFDM and DFT-spread-OFDM (DFT-s-OFDM) and reach lower PAPR compared to its OTFS counterpart [500], [518]. Because of the aforementioned reasons, DFT-s-OTFS is the most promising candidate waveform for ISAC systems.

C. THz-ISAC Algorithm Development

In general, the ISAC algorithms fall into three categories, i.e., data-driven AI-based approaches, model-based approaches, and hybrid approaches (combination of the former two). AI techniques rely on large-volume date sets for training customized neural network (NN) models for sensing, localization, and signal detection, while tackling the mathematically intractable non-linearity issues from, e.g., phase noise and offset, power amplifier, and mutual coupling. On the contrary, for the model-based ISAC algorithms, the majority of them need to harness the well-justified domain knowledge and modeling, such as geometric relationship among the transceivers and the environmental objects, and take full advantage of channel sparsity in the form of rank deficiency of the channel matrix or a limited number of resolvable paths, as to obtain satisfactory performance.

Under the framework of THz ISAC, joint data detection (signal recovery) and sensing parameter estimation are conducted with multi-task NNs in [516]. In a broad sense, the ML roles on ISAC can be classified into three categories:

- joint sensing and communication (JSAC)
- sensing-aided communications [39], [40]
- communication-aided sensing [41].

To be specific, the first category includes the following activities: JSAC waveform design, spatial beam pattern design, inter- and self-interference cancellation, resource allocation, etc. Without any doubt, communications and sensing can be mutually beneficial for each other. In the category of sensing-aided communication, sensing information (treated as prior information), e.g., the location of the transmitter, receiver, and environmental objects, can be leveraged for enhancing the beam prediction/alignment and reducing the overhead of beam training as well as channel sounding [497], [503]. In the dynamic scenario where the user is under mobility, regardless of low or high velocity, such sensing information can be utilized for predicting potential blockages and enabling smooth handovers [23]. Similarly, communications signals can also be exploited to boost the sensing performance during the data transmission phase. The back-scattered data signals can gradually refine/improve the sensing parameter estimation, similar to data-aided channel estimation in the literature [519].

The DL algorithms alongside other counterparts, e.g., deep reinforcement learning and transfer learning, pave the way for the integrated detectors and estimators for both communications and sensing, in terms of e.g., sensing parameters estimation, interference mitigation/cancellation, beam tracking/prediction, and network resource allocation/management [501], [504]. Meanwhile, it can successfully tackle the mathematically intractable non-linearity issues and hardware impairments in the ISAC systems [501]. Furthermore, some latent features related to sensing parameters can be more readily learned and extracted by the adoption of DL algorithms.

In the DFT-s-OTFS system [502], a two-stage sensing parameter estimation approach was proposed, i.e., coarse on-grid search in the first stage followed by refined off-grid search in the second stage for extracting the sensing parameters. Under the framework of ISAC, data detection and sensing parameter estimation can be performed in an iterative manner until a certain preset stopping criterion is reached. Besides, ISAC performance can be further enhanced by multi-domain cooperation through joint active and passive sensing, and multi-user and multi-frequency operations [503]. Tensor decomposition approach is capable of leveraging the channel sparsity and guaranteeing a unique solution for each environmental sensing parameter without any ambiguity [513]. Such sensed information can be then utilized to reconstruct a high-resolution indoor mapping to further boost the prediction of blockages and the availability of LoS path, and reduce the beam tracking frequency. Thus, higher spectrum efficiency in data transmission can be achieved accordingly.

The traditional model-based algorithms adopt compressive sensing techniques, either on-the-grid, off-the-grid, or the combination of the former two (e.g., in [502]), for extracting channel and sensing parameters by taking advantage of channel sparsity [520]–[522]. Model-driven end-to-end learning, belonging to the category of hybrid approaches, for joint single target sensing and MISO communications was studied in [505]. In particular, the authors jointly consider precoder design at the transmitter and target AoA estimation at the receiver while accounting for the hardware impairment.

D. RIS-Boosted THz-ISAC

With the newly-introduced capability of manipulating the radio propagation environment, RIS is able to expand the communications coverage and enhance the sensing performance [491], [523]. The potential roles that can be played by an RIS are multi-fold: scattering, reflecting, refraction, absorption, polarization, and diffraction. With all the preceding degree of freedoms (DoFs), intelligent, programmable wireless propagation environments can be established for carrying out different tasks, e.g., sensing, communications, localization, and imaging. The RIS can enrich the LoS availability by establishing a virtual one when the real one is suffering from temporary blockage, which frequently occurs at THz frequencies.

The various benefits of integrating RIS into ISAC were discussed in [524]. The gains against the RIS-free counterpart heavily rely on the cross-correlation between the sensing and communications channels. The more the mutual coupling, the more gain can be accomplished in terms of ISAC performance. By introducing the RIS, enhanced flexibility and adaptation to channel dynamics is seen in altering the coupling level of these channels [524]. The importance of tight coupling of communications and localization was also emphasized in [525] for the purpose of harnessing the full potential of RISs. That's to say, the brand-new concept of simultaneous localization and communications (SLAC) requires smart RIS control, co-design of communications and localization resources, and the flexible trade-off and reinforcement between the two functionalities.

In the rich RIS-boosted ISAC literature, various optimization problems are formulated with different objectives along with different constraints. These works can be cast into three different classes:

- sensing-centric design [506]
- communication-centric design [507]
- joint design and optimization [20], [508].

For the first category, the objective function is sensing-oriented, while the communications metrics are taken as constraints. For instance, the authors in [506] maximize the SNR at the radar while considering a communications SNR constraint. By addressing this optimization problem, semidefinite relaxation (SDR) along with bisection search is considered for transmit beamforming design while majority-minimization is considered for RIS design. With respect to the second category, the reference [507] takes interference among the communications users as the objective while treating the desired mean square error (MSE) of DoA estimation as a constraint. In terms of the last category, the weighted sum of two objectives, one for communications and the other for sensing, are usually considered [508]. All the categories share some common constraints, e.g., individual transmit power, sum transmit power, hardware (especially for RIS, e.g., phase quantization, constant modulus of amplitude), etc. A holistic comparison among the three classes can be referred to [21], [499].

Recently, a more promising type of RIS, termed as simultaneously transmitting (refracting) and reflecting reconfigurable intelligent surface (STAR-RIS), was introduced, which is able to offer additional benefits thanks to its inherent dual-mode operation and full-dimensional coverage [526], [527]. The STAR-RIS can concurrently reflect and refract the incident signals towards multiple desired MSs. Because of this, the STAR-RIS can further boost the ISAC performance compared to the sole-reflection-type RIS [509], [528], [529]. An outdoor BS is capable of providing both communications and sensing services to the users located indoors and outdoors by installing a STAR-RIS on a transparent glass window [526], [527].

E. Challenges and Solutions for THz-ISAC

The open problems for THz-ISAC are listed and discussed in [19], [516]. For example, waveform design should be customized dependent on the sensing applications. Dynamic beamforming control faces great challenges since the beamwidth is narrow and highly directional [33]. As a consequence, the probability of beam misalignment can be inevitably high. A robust design of candidate beams for communications purpose requires a wider beam width. However, to enhance the sensing resolution and accuracy, narrow beams are preferred. Multiple concurrent beams comprise one fixed sub-beam for point-to-point communications and multiple time-varying sub-beams for sensing purposes can achieve a well-balanced performance between communications and sensing [108]. However, multiple simultaneous beams result in degraded beamforming gains.

Imperfections, resulting from IQ imbalance, PA nonlinear distortions, and phase noise at the local oscillator, need to be compensated for when designing robust THz-ISAC algorithms. The wide-band channel becomes highly selective with high Doppler spread, which may break the orthogonality of OFDM transmission and incur inter-carrier interference [491], [510]. Besides, the near-filed propagation, where channel sparsity vanishes in the angular domain, makes the beamforming design intractable. The beam squint effect makes the designed beam deviate from the exact one, resulting in reduced array gain and performance degradation [510].

The beam squint and split effect will become more obvious as the increase of carrier frequency and bandwidth, causing significant performance degradation on sensing and communication. As examined in [491] for a broadside target, beam split can reach as much as 4° for 0.3 THz with 30 GHz bandwidth while it is only 1.4° for 60 GHz with 2 GHz bandwidth. This effect should be mitigated and compensated for when designing the beamforming patterns, such as DPP [530]. Due to the user mobility and frequent blockage, beam misalignment occurs when LoS path is unavailable between the BS and MS. Provided that the user can be tracked and blockage can be predicted in advance, beam misalignment can be avoided. However, this requires high-precision sensing information. In line with the 5G CSI acquisition signals, the authors in [531] adopt synchronization signal block (SSB) for blockage detection and reference signal (RS) for user tracking.

Until all the above-mentioned challenges are addressed in the forthcoming years, the vision that everything will be sensed, connected, and intelligent can be fulfilled.

X. THz Trials and Experiments

In order to give readers an insightful view of the current status of the practical use of THz communications and sensing towards 6G and beyond, we summarize state-of-the-art THz trials and experiments worldwide in this section, where the achieved data rates at the certain THz bands with specific features are surveyed.

In the past decade, the electronic mixing technology was widely applied to generate high-frequency THz signals by up-converting a low-frequency microwave signal, as the traditional way to realize THz transmission as listed in Table VIII [532], [534], [535]. One of the most remarkable approaches was done by Bell Labs in 2011, where THz radiation at 625 GHz was generated by using an all-solid-state electric mixer. It achieved a data rate of 2.5 Gbps at a distance of 0.2 m under the transmission power of 1 mW [532]. In 2015, the researchers at the University of Stuttgart in Germany successfully transmitted 240 GHz THz signals to the receiver at a distance of 850 m. The trial achieved a peak data rate of 64 Gbps using quadrature phase-shift keying (QPSK) and 8-ary phase-shift keying (8PSK) modulation in a single-channel approach without the use of spatial diversity [534]. In the year 2017, a research team from the China Academy of Engineering Physics achieved ultra-long-distance THz wireless communications over up to 21 km and realized single-channel transmission speed up to 5 Gbps, taking advantage of two Cassegrain antennas with 50 dBi gain each [535].

Because of the inherent properties of electronic devices, the parameters of high-frequency electronic devices gradually approach the theoretical limit, with relatively lower bandwidth and a limited transmission rate. Recently, much attention was shifted to the photonics-assisted heterodyne beating technique

TABLE VIII
SUMMARY OF EXPERIMENTAL AND DEMONSTRATION SYSTEMS FOR THZ COMMUNICATIONS AND SENSING.

Ref.	Year	Freq.[GHz]	BW[GHz]	Rate[Gbps]	Distance [m]	Contributions
[532]	2011	625	narrow N/A	2.5	0.2	A novel approach is reported for 2.5 Gbps signalling at a carrier frequency of 625 GHz. Duobinary baseband modulation on the transmitter side generates a signal with a sufficiently narrow spectral bandwidth to pass an upconverting frequency multiplier chain.
[533]	2013	237.5	35	100	20	Present for the first time, a single-input and single-output wireless communications system at 237.5 GHz for transmitting data over 20 m at a data rate of 100 Gbps from combining terahertz photonics and electronics.
[534]	2015	240	32	64	850	A directive fixed wireless link operating at a center frequency of 240 GHz achieves a data rate of 64 Gbps over a transmission distance of 850 m using QPSK and 8PSK modulation, in a single-channel approach without the use of spatial diversity concepts.
[535]	2017	140	N/A	5	21000	The 16QAM modulation scheme is used in baseband processing, and mixers are used for cascading frequency up and down-converting. Cascading power amplification technique is adopted with a solid-state power amplifier and a vacuum electronic device. A 21 km wireless communications testing is carried out, by means of two Cassegrain antennas with 50 dBi gain each.
[536]	2019	375-500	30	120	1.42	The first experimental demonstration of 2 × 2 MIMO wireless transmission of multi-channel THz-wave signal, which realizes 6 x 20 Gbps six-channel polarization division multiplexing QPSK THz-wave signal delivery over 10 km wireline single-mode fiber-link and 142 cm wireless 2 x 2 MIMO link.
[537]	2020	335-365	30	600	2.8	Demonstration of a hybrid THz photonic-wireless transmission based on a THz orthogonal polarization dual-antenna scheme. Probabilistic shaped 64QAM-OFDM modulation format is used to realize a high transmission rate. A potential total system throughput of 612.65 Gbps is successfully achieved.
[538]	2020	300	40	115	110	A local-oscillator tone is transmitted along with the signal, and the amplitude and phase of the complex signal envelope are digitally reconstructed from the photocurrent by exploiting their Kramers–Kronig-type relation. Using Schottky-barrier diode as a nonlinear receiver element and 16-state QAM, a net data rate of 115 Gbps at a carrier frequency of 0.3 THz over a distance of 110 m is achieved.
[539]	2021	340	30	44.8	104	Demonstrates the capability of over 54/104 meters wireless transmission with a record-breaking net data rate of 128/44.8 Gbps at THz-band by utilizing both suitable dielectric lenses and DSP algorithms, without THz amplifier.
[540]	2021	231	79	240	115	The first transparent Optical-THz-Optical link providing record-high line-rates up to 240 and 190 Gbps over distances from 5 to 115 meters is demonstrated.
[541]	2022	340-510	37.7	103	3	Demonstrates a real-time fiber-THz-fiber 2 × 2 MIMO seamless integration system at 340–510 GHz using commercial DCO modules for baseband signals processing, which realizes a record net rate of 103.125 Gbps DP-QPSK signals delivery over two spans of 20 km wireline single-mode fiber-link and 3 m wireless 2 × 2 MIMO link without using THz power amplifier.
[542]	2023	360-430	37.7	206	1	A novel UWB fiber-THz-fiber seamlessly converged real-time architecture, which utilizes the commercially mature digital coherent optical module to realize ultrahigh-capacity THz real-time wireless communication, is proposed.

for higher data rate and better signal quality, where the rates of THz transmission is able to reach hundreds of Gbps or even Tbps [533], [536]–[540]. It should be pointed out that the THz signal power generated by the photonics-assisted heterodyne beating method is usually limited to the mW level because of the lower responsivity of the uni-traveling carrier photodiode (UTC-PD), resulting in the limited transmission distance. Therefore, some researchers utilized high-gain THz amplifiers or high-gain lens antennas to extend distances to 100 m. In early 2013, the researchers [533] utilized the large frequency range in the THz window between 200 GHz and 300 GHz to implement a single-input single-output (SISO) wireless 100 Gbps link with a carrier frequency of 237.5 GHz over a distance of 20 m. Several years later, a team from Fudan University successfully applied 2 × 2 MIMO and wavelength division multiplexing (WDM) technologies at THz signal transmission, achieving a data rate of 120 Gbps by using QPSK modulation [536]. Meanwhile, some researchers at Zhejiang University in China achieved THz signal transmission of 600 Gbps using 64QAM multi-carrier modulation [537]. However, the distances of THz signal transmission of the above two approaches are only 1.42 m and 2.8 m, respectively.

In the past three years, some research teams have presented prominent improvements in THz communications. The wireless transmission distances were effectively extended to more than 100 m with the assistance of high-gain THz amplifiers or high-gain lens antenna. In 2020, a team at the Karlsruhe Institute of Technology (KIT) took advantage of THz amplifiers and the Kramers-Kronig method for simplifying the design of the receiver and launched an offline multi-carrier THz system. It offers a peak data rate of 115 Gbps at a carrier frequency of 300 GHz over a distance of 110 m [538]. One year later, the Fudan University successfully transmitted a 44.8 Gbps 64QAM-modulated signal over a distance of 104 m without using the THz amplifier but utilizing both suitable dielectric lenses and digital signal processing (DSP) algorithms [539]. In the same year, Yannik Horst *et al.* [540] from Switzerland demonstrated the transparent optical-THz-optical link, providing a transmission rate of 240 Gbps over a distance up to 115 m.

With the objective of achieving full-coverage and low-cost deployment towards future 6G mobile communications, the priority of the hybrid optoelectronic down-conversation solution was presented [541] and [542], where a novel fiber-THz-fiber seamlessly converged real-time architecture was successfully demonstrated. It adopts both dual-polarization photonic up-conversion for THz signal generation and hybrid optoelectronic down-conversion for THz reception, by thoroughly reusing commercial digital coherent optical modules. In the case of hybrid channel transmission with two hops consisting of a 20km-long fiber and 1m-long THz wireless link, a THz signal with a net rate of 206.25 Gbps was successfully transmitted real-timely [542]. It is also pointed out that zhe THz phased array techniques are key to realizing 6G THz mobile communications and sensing, which meets the needs of application scenarios, such as multiple users and beam tracking.

In addtion to the excellent demonstrations and validations that have been achieved by research teams around the world, some equipment suppliers and organizations have also presented great advances in THz commercialization. The NYU WIRELESS is currently focusing on sub-THz bands at 140 GHz, 220 GHz, and higher. The radio-frequency integrated circuit (RFIC) probe stations working up to 220 GHz, and channel sounders for propagation measurements at 140 GHz [92] are provided by the Keysight Technologies. Keysight has also closely corporated with Nokia Bell labs on the sub-THz testbed, which was chosen to verify the performance of transceiver modules, power amplifiers, and antennas under both linear and nonlinear conditions. Recently, Huawei 6G research team has developed and demonstrated THz integrated sensing and communications (THz-ISAC) prototype. Using wireless electromagnetic waves, the prototype can sense and produce images of blocked objects with millimeter-level resolution and communicates at an ultra-high rate of 240 Gbps, opening up new service possibilities for 6G and beyond systems [543].

XI. CONCLUSIONS

In summary, the upcoming 6G and beyond cellular systems are envisioned to exploit the THz band beyond 100 GHz, which not only offers an abundant amount of spectral resources for globally ubiquitous, ultra-high-rate, super-reliable, hyper-low-latency, massive-density telecommunications services but also empowers high-resolution cognition through THz sensing, positioning, and imaging. The use of THz frequencies will bring novel applications such as tera-bits-per-second/Tbps hot spots or links, and, in addition, disruptive uses like nano-scale networks and on-chip communications. Despite its high potential, we do not expect that the THz band is able to totally replace the sub-6GHz and mmWave bands, which have been employed as the basis of previous generations of cellular communications networks. Instead, the THz band is highly probably being used as the complementary resource to aid the success of low-frequency bands in future generations of cellular systems. Meanwhile, there are still tremendous works to be done in terms of characterizing and modeling THz channels, developing affordable, usable THz antennas and devices, designing novel algorithms for long-range THz signal transmission, proposing efficient protocols for flexible THz networking, and elaborately considering its synergy with other 6G-enabling technologies. It is hoped that this survey could be able to provide the researchers with a holistic view of all technical aspects and issues required to design and build THz communications and sensing for 6G and beyond from an application and implementation perspective. Although there is a long journey to go before the success of THz communications and sensing in 6G and beyond cellular systems, this survey might be able to speed up a bit the research endeavors.

APPENDIX A
LIST OF ACRONYMS

+

1024QAM	1024-ary quadrature amplitude modulation
1G	first generation
2D	two-dimensional
2D	two-dimensional
3D	three-dimensional
3G	third generation
3GPP	Third Generation Partnership Project
4G	fourth generation
5G	fifth generation
5GPPP	Fifth Generation Private Public Partnership
6G	sixth generation
8PSK	8-ary phase-shift keying
ADC	analogue-to-digital converter
AGV	automated guided vehicle
AI	artificial intelligence
AMPS	Advanced Mobile Phone System
AoA	angle-of-arrival
AoD	angle-of-departure
AoI	age of information
AoS	age of synchronization
AoSA	array of subarrays
AP	access point

AR	augmented reality
B6G	beyond sixth generation
BDCM	beam-domain channel model
BDMA	beam division multiple access
BS	base station
CCU	cell center user
CEU	cell edge user
CFN	cell-free network
CMC	closest line of sight multi-connectivity
CMOS	complementary metal-oxide-semiconductor
CMTC	critical machine-type communications
CNOMA	cooperative non-orthogonal multiple access
CoMP	coordinated multi-point
ComS	compressive sensing
CRB	Cramér-Rao bound
CS	channel sounder
CSCB	coordinated scheduling and beamforming
CSI	channel state information
CTF	channel transfer function
D2D	device-to-device
DAoSA	dynamic array-of-subarrays
DAR	differential absorption radar
DCNN	deep convolutional neural network
DFRC	dual-functional radar-communications
DFT	discrete Fourier transform
DFT-s-OFDM	DFT-spread-OFDM
DFT-s-OTFS	discrete Fourier transform spread OTFS
DKL	deep kernel learning
DL	deep learning
DLA	discrete lens array
DMIMO	distributed MIMO
DNN	deep neural network
DoA	direction of arrival
DoF	degree of freedom
DPP	delay-phase precoding
DRC	dual-function radar and communication
DSP	digital signal processing
DSSS	direct-sequence spread spectrum
EC	European Commission
EESS	Earth Exploration Satellite Service
EIRP	effective isotropic radiated power
EM	electromagnetic
FBL	finite blocklength
FC	fully-connected
FCC	Federal Communications Commission
FDTD	finite-difference time-domain
FET	field-effect transistor
FSPL	free-space path loss
GaAs	Gallium Arsenide
GaN	Gallium Nitride
GEO	geostationary Earth orbit
GHz	gigahertz
GNSS	Global Navigation Satellite System
GPR	Gaussian process regression
GSM	Global System for Mobile Communications
HAP	high-altitude platform
HBT	heterojunction bipolar transistor
HEMT	high-electron-mobility transistor
IAB	integrated access and backhaul
IMT	International Mobile Telecommunications
InP	Indium Phosphide
IoNT	Internet of Nano-Things
IQ	in-phase and quadrature
IR	infrared
IRS	intelligent reflecting surfaces
ISAC	integrated sensing and communications
ITU-R	International Telecommunication Union - Radiocommunication
ITU-T	International Telecommunication Union - Telecommunication
JCAS	joint communications and sensing
JSAC	joint sensing and communication
JT	joint transmission
KPI	key performance indicator
LEO	low Earth orbit
LO	local oscillator
LoS	line-of-sight
LTCC	low-temperature co-fired ceramic
LTE-Advanced	Long-Term Evolution Advanced
LWA	leaky-wave antennas
MC	multi-connectivity
MIMO	multi-input multi-output
MISO	multiple-input single-output
ML	machine learning
MMIMO	massive multi-input multi-output
MMSE	minimum-mean square error
mmWave	millimeter wave
MS	mobile station
MSE	mean square error
MUI	multi-user interference
NF	near field
NGMN	Next Generation Mobile Networks
NLoS	non-line-of-sight
NN	neural network
NOMA	non-orthogonal multiple access
NR	new radio
NTN	non-terrestrial network
OFDM	orthogonal frequency-division multiplexing
OTFS	orthogonal time frequency space
OWC	optical wireless communications
PA	power amplifier
PAPR	peak-to-average power ratio
PHY	physical
PPP	Poisson point process
PSM	phase-shift matrix
QAM	quadrature amplitude modulation
QCL	quantum cascade laser
QoS	quality of service
QPSK	quadrature phase-shift keying
RAN	radio access network
RCC	radar-communications coexistence
RF	radio frequency
RFoF	radio frequency over fiber
RIS	reconfigurable intelligent surfaces
RMC	reactive multi-connectivity
RS	reference signal

RSS	received signal strength
SC	sliding correlation
SDR	semidefinite relaxation
SIC	successive interference cancellation
SiGe	Silicon Germanium
SISO	single-input single-output
SIW	substrate-integrated waveguide
SLAC	simultaneous localization and communications
SLAM	simultaneous localization and mapping
SNR	signal-to-noise ratio
SPP	surface plasmon polariton
SSB	synchronization signal block
STAR-RIS	simultaneously transmitting (refracting) and reflecting reconfigurable intelligent surface
SWIPT	simultaneous wireless information and power transfer
TDD	time-division multiplexing
TDMA	time division multiple access
TDS	time-domain spectroscopy
Tera-IoT	THz internet-of-things
THz	terahertz
ToA	time of arrival
TTD	true-time-delay
UAV	unmanned aerial vehicle
UE	user equipment
ULA	uniform linear array
ULBC	ultra-reliable low-latency broadband communication
uMBB	ubiquitous mobile broadband
UMi	urban microcell
UMMIMO	ultra-massive multi-input multi-output
UPAs	uniform planar arrays
URLLC	ultra-reliable low-latency communications
UTC-PD	uni-traveling-carrier photodiode
UWB	ultra wideband
VLC	visible light communication
VNA	vector network analyzer
VNF	virtual network function
VR	virtual reality
WCDMA	Wideband Code-Division Multiple Access
WRC	World Radiocommunication Conference
WSMS	widely-spaced multi-subarray
WSN	wireless sensor network
XR	extended reality

REFERENCES

[1] E. Dahlman, S. Parkvall, and J. Sköld, *5G NR - The Next Generation Wireless Access Technology*. London, the United Kindom: Academic Press, Elsevier, 2021.

[2] E. C. Strinati *et al.*, "6G: The next frontier: From holographic messaging to artificial intelligence using subterahertz and visible light communication," *IEEE Veh. Technol. Mag.*, vol. 14, no. 3, pp. 42–50, Sep. 2019.

[3] W. Jiang and H. D. Schotten, "The kick-off of 6G research worldwide: An overview," in *Proc. 2021 Seventh IEEE Int. Conf. on Comput. and Commun. (ICCC)*, Chengdu, China, Dec. 2021.

[4] W. Saad *et al.*, "A vision of 6G wireless systems: Applications, trends, technologies, and open research problems," *IEEE Netw.*, vol. 34, no. 3, pp. 134–142, May 2020.

[5] T. Huang *et al.*, "A survey on green 6G network: Architecture and technologies," *IEEE Access*, vol. 7, pp. 175 758–175 768, Dec. 2019.

[6] "Cloud VR network solution white paper," White Paper, HUAWEI, 2018.

[7] B. Han *et al.*, "Optimal resource dedication in grouped random access for massive machine-type communications," in *2017 IEEE Conference on Standards for Communications and Networking (CSCN)*, 2017, pp. 72–77.

[8] M. Nasimi *et al.*, "Platoon–assisted Vehicular Cloud in VANET: Vision and Challenges," 2019 European Symposium on Computer and Communications (ESCC 2019), Paris, France, 2 – 4 September 2019.

[9] W. Jiang *et al.*, "The road towards 6G: A comprehensive survey," *IEEE Open J. Commun. Society*, vol. 2, pp. 334–366, Feb. 2021.

[10] G. Fettweis, "The tactile internet: Applications and challenges," *IEEE Veh. Technol. Mag.*, vol. 9, no. 1, pp. 64–70, Mar. 2014.

[11] Y. Wu, K. Zhang, and Y. Zhang, "Digital twin networks: A survey," *IEEE Internet Things J.*, vol. 8, no. 18, pp. 13 789 – 13 804, Sep. 2021.

[12] P. Yang *et al.*, "6G wireless communications: Vision and potential techniques," *IEEE Netw.*, vol. 33, no. 4, pp. 70–75, Jul. 2019.

[13] Z. Xiong *et al.*, "When mobile Blockchain meets edge computing," *IEEE Commun. Mag.*, vol. 56, no. 8, pp. 33–39, Aug. 2018.

[14] K. David and H. Berndt, "6G vision and requirements: Is there any need for beyond 5G?" *IEEE Veh. Technol. Mag.*, vol. 13, no. 3, pp. 72–80, Sep. 2018.

[15] B. Zong *et al.*, "6G technologies: Key drivers, core requirements, system architectures, and enabling technologies," *IEEE Veh. Technol. Mag.*, vol. 14, no. 3, pp. 18–27, Sep. 2019.

[16] B. Rong, "6G: The next horizon: From connected people and things to connected intelligence," *IEEE Wireless Commun. Mag.*, vol. 28, no. 5, pp. 8 – 8, Oct. 2021.

[17] W. Tong and P. Zhu, *6G: The Next Horizon - From Connected People and Things to Connected Intelligence*. Cambridge, United Kingdom: Cambridge University Press, 04 2021.

[18] H. Wymeersch *et al.*, "6G radio requirements to support integrated communication, localization, and sensing," in *Proc. Joint Eur. Conf. Netw. Commun. & 6G Summit (EuCNC/6G Summit)*, 2022, pp. 463–469.

[19] ——, "Integration of communication and sensing in 6G: a joint industrial and academic perspective," in *Proc. IEEE 32nd Int. Symp. Pers. Indoor Mobile Radio Commun. (PIMRC)*, 2021, pp. 1–7.

[20] J. A. Zhang *et al.*, "An overview of signal processing techniques for joint communication and radar sensing," *IEEE J. Sel. Topics Signal Process.*, vol. 15, no. 6, pp. 1295–1315, 2021.

[21] J. Wang *et al.*, "Integrated sensing and communication: Enabling techniques, applications, tools and data sets, standardization, and future directions," *IEEE Internet Things J.*, vol. 9, no. 23, pp. 23 416–23 440, 2022.

[22] T. S. Rappaport *et al.*, "Wireless communications and applications above 100 GHz: Opportunities and challenges for 6G and beyond," *IEEE Access*, vol. 7, pp. 78 729 – 78 757, Jun. 2019.

[23] U. Demirhan and A. Alkhateeb, "Radar aided proactive blockage prediction in real-world millimeter wave systems," in *Proc. IEEE Int. Conf. on Commun. (ICC)*, 2022, pp. 4547–4552.

[24] T. Nagatsuma *et al.*, "Advances in terahertz communications accelerated by photonics," *Nature Photonics*, vol. 10, no. 6, pp. 371–379, 2016.

[25] W. Jiang and H. D. Schotten, "Cell-free massive MIMO-OFDM transmission over frequency-selective fading channels," *IEEE Commun. Lett.*, vol. 25, no. 8, pp. 2718 – 2722, Aug. 2021.

[26] Y. Liu *et al.*, "Developing NOMA to next generation multiple access: Future vision and research opportunities," *IEEE Wireless Commun. Mag.*, vol. 29, no. 6, pp. 120–127, 2022.

[27] ITU-R M.2410, "Minimum requirements related to technical performance for IMT-2020 radio interface(s)," ITU-R, Recommendation M.2410-0, Nov. 2017.

[28] J. Kahn and J. Barry, "Wireless infrared communications," *Proc. IEEE*, vol. 85, no. 12, pp. 265 – 298, Feb. 1997.

[29] P. H. Pathak *et al.*, "Visible light communication, networking, and sensing: A survey, potential and challenges," *IEEE Commun. Surv. Tutor.*, vol. 17, no. 4, pp. 2047 – 2077, 2015, Fourth Quarter.

[30] Z. Xu and B. M. Sadler, "Ultraviolet communications: Potential and state-of-the-art," *IEEE Commun. Mag.*, vol. 46, no. 5, pp. 67–73, May 2008.

[31] I. F. Akyildiza, J. M. Jornet, and C. Han, "Terahertz band: Next frontier for wireless communications," *Physical Communication*, vol. 12, pp. 16 – 32, Sep. 2014.

[32] A.-A. A. Boulogeorgos *et al.*, "Terahertz technologies to deliver optical network quality of experience in wireless systems beyond 5G," *IEEE Commun. Mag.*, vol. 56, no. 6, pp. 144 – 151, Jun. 2018.

[33] H. Sarieddeen *et al.*, "Next generation terahertz communications: A rendezvous of sensing, imaging, and localization," *IEEE Commun. Mag.*, vol. 58, no. 5, pp. 69–75, 2020.

[34] C. Chaccour *et al.*, "Seven defining features of terahertz (THz) wireless systems: A fellowship of communication and sensing," *IEEE Commun. Surv. Tutor.*, vol. 24, no. 2, pp. 967 – 993, 2022, second Quarter.

[35] C. Zandonella, "Terahertz imaging: T-ray specs," *Nature*, vol. 424, no. 6950, p. 721, Aug. 2003.

[36] A. A. Mamrashev *et al.*, "Detection of nuclear spin isomers of water molecules by terahertz time-domain spectroscopy," *IEEE Trans. Terahertz Sci. Techno.*, vol. 8, no. 1, pp. 13 – 18, Jan. 2018.

[37] Q. H. Abbasi *et al.*, "Nano-communication for biomedical applications: A review on the state-of-the-art from physical layers to novel networking concepts," *IEEE Access*, vol. 4, pp. 3920 – 3935, Jul. 2016.

[38] O. Li *et al.*, "Integrated sensing and communication in 6G a prototype of high resolution thz sensing on portable device," in *Proc. IEEE Eur. Conf. on Net. and Commun. (EUCNC)& 6G Summit*, Porto, Portugal, Jun. 2021.

[39] A. Hu and J. He, "Position-aided beam learning for initial access in mmwave mimo cellular networks," *IEEE Systems Journal*, vol. 16, no. 1, pp. 1103–1113, 2022.

[40] J. He, H. Wymeersch, and M. Juntti, "Leveraging location information for ris-aided mmwave mimo communications," *IEEE Wireless Commun. Let.*, vol. 10, no. 7, pp. 1380–1384, 2021.

[41] U. Demirhan and A. Alkhateeb, "Integrated sensing and communication for 6G: Ten key machine learning roles," *arXiv preprint arXiv:2208.02157*, 2022.

[42] X. Chen *et al.*, "Sensing-aided uplink channel estimation for joint communication and sensing," *IEEE Wireless Commun. Lett.*, vol. 12, no. 3, pp. 441 – 445, Mar. 2023.

[43] F. Liu *et al.*, "Radar-assisted predictive beamforming for vehicular links: Communication served by sensing," *IEEE Trans. Wireless Commun.*, vol. 19, no. 11, pp. 7704 – 7719, Nov. 2020.

[44] J. Mu *et al.*, "Integrated sensing and communication-enabled predictive beamforming with deep learning in vehicular networks," *IEEE Commun. Lett.*, vol. 25, no. 10, pp. 3301 – 3304, Oct. 2021.

[45] W. Chen *et al.*, "Enhancing THz/mmWave network beam alignment with integrated sensing and communication," *IEEE Commun. Lett.*, vol. 26, no. 7, pp. 1698 – 1702, Jul. 2022.

[46] J. Wang *et al.*, "Internet of vehicles: Sensing-aided transportation information collection and diffusion," *IEEE Trans. Veh. Technol.*, vol. 67, no. 5, pp. 3813 – 3825, May 2018.

[47] W. Wang and Q. W. abd Kazem Sohraby, "Multimedia sensing as a service (MSaaS): Exploring resource saving potentials of at cloud-edge IoT and fogs," *IEEE Internet Things J.*, vol. 4, no. 2, pp. 487 – 495, Apr. 2017.

[48] S. He *et al.*, "Collaborative sensing in internet of things: A comprehensive survey," *IEEE Commun. Surv. Tutor.*, vol. 24, no. 3, pp. 1435 – 1474, 2022, third Quarter.

[49] P. Mukherjee and B. Gupta, "Terahertz (THz) frequency sources and antennas - a brief review," *Int. J. Infrared Millimeter Waves*, vol. 29, p. 1091–1102, Sep. 2008.

[50] T. Kleine-Ostmann and T. Nagatsuma, "A review on terahertz communications research," *J. Infrared, Millimeter, and Terahertz Waves*, vol. 32, p. 143–171, Jan. 2011.

[51] K. M. S. Huq *et al.*, "Terahertz-enabled wireless system for beyond-5G ultra-fast networks: A brief survey," *IEEE Netw.*, vol. 33, no. 4, pp. 89 – 95, Jul. 2019.

[52] K. Tekbıyık *et al.*, "Terahertz band communication systems: Challenges, novelties and standardization efforts," *Physical Commun.*, vol. 35, p. 100700, 2019.

[53] Z. Chen *et al.*, "A survey on terahertz communications," *China Commun.*, vol. 16, no. 2, pp. 1 – 35, Feb. 2019.

[54] M. Naftaly *et al.*, "Industrial applications of terahertz sensing: State of play," *Sensors*, vol. 19, no. 4203, Sep. 2019.

[55] Y. He *et al.*, "An overview of terahertz antennas," *China Commun.*, vol. 17, no. 7, pp. 124 – 165, Jul. 2020.

[56] S. Ghafoor *et al.*, "MAC protocols for terahertz communication: A comprehensive survey," *IEEE Commun. Surv. Tutor.*, vol. 22, no. 4, pp. 2236 – 2282, Aug. 2020, Fourth Quarter.

[57] B. Ning *et al.*, "Beamforming technologies for ultra-massive mimo in terahertz communications," *IEEE Open J. Commun. Society*, vol. 4, pp. 614–658, 2023.

[58] F. Lemic *et al.*, "Survey on terahertz nanocommunication and networking: A top-down perspective," *IEEE J. Sel. Areas Commun.*, vol. 39, no. 6, pp. 1506 – 1543, Jun. 2021.

[59] H. Sarieddeen *et al.*, "An overview of signal processing techniques for terahertz communications," *Proc. IEEE*, vol. 109, no. 10, pp. 1628 – 1665, Oct. 2021.

[60] E. Castro-Camus, M. Koch, and D. M. Mittleman, "Recent advances in terahertz imaging: 1999 to 2021," *Applied Physics*, vol. 128, no. 12, Dec. 2021.

[61] C.-X. Wang *et al.*, "Key technologies in 6g terahertz wireless communication systems: A survey," *IEEE Veh. Techno. Maga.*, vol. 16, no. 4, pp. 27–37, 2021.

[62] D. Moltchanov *et al.*, "A tutorial on mathematical modeling of 5G/6G millimeter wave and terahertz cellular systems," *IEEE Commun. Surv. Tutor.*, vol. 24, no. 2, pp. 1072 – 1116, 2022, second Quarter.

[63] C. Han *et al.*, "Terahertz wireless channels: A holistic survey on measurement, modeling, and analysis," *IEEE Commun. Surv. Tutor.*, vol. 24, no. 3, pp. 1670 – 1707, Jun. 2022, third Quarter.

[64] D. Serghiou *et al.*, "Terahertz channel propagation phenomena, measurement techniques and modeling for 6G wireless communication applications: A survey, open challenges and future research directions," *IEEE Commun. Surv. Tutor.*, vol. 24, no. 4, pp. 1957 – 1996, 2022, fourth Quarter.

[65] I. F. Akyildiz *et al.*, "Terahertz band communication: An old problem revisited and research directions for the next decade," *IEEE Trans. Commun.*, vol. 70, no. 6, pp. 4250 – 4285, Jun. 2022.

[66] A. Shafie *et al.*, "Terahertz communications for 6G and beyond wireless networks: Challenges, key advancements, and opportunities," *IEEE Netw.*, pp. 1 – 8, Dec. 2022, early Access.

[67] J. Navarro-Ortiz *et al.*, "A survey on 5G usage scenarios and traffic models," *IEEE Commun. Surv. Tutor.*, vol. 22, no. 2, pp. 905 – 929, Feb. 2020.

[68] Y. Siriwardhana *et al.*, "The fight against the COVID-19 pandemic with 5G technologies," *IEEE Eng. Manage. Rev.*, vol. 48, no. 3, pp. 72 – 84, Sep. 2020.

[69] "A blueprint of technology, applications and market drivers towards the year 2030 and beyond," White Paper, ITU-T FG-NET-2030, May 2019.

[70] Eu horizon2020 hexa-x preject. [Online]. Available: https://hexa-x.eu/

[71] Horizon europe hexa-x-ii preject. [Online]. Available: https://hexa-x-ii.eu/

[72] "Shaping Europe's digital future," Communication-COM(2020)67, European Commission, Brussels, Belgium, Feb. 2020.

[73] "6G drivers and vision (1st version)," White Paper, NGMN Alliance, Apr. 2021.

[74] "Future technology trends for the evolution of IMT towards 2030 and beyond," Liaison statement, ITU-R Working Party 5D, Oct. 2020.

[75] Finland 6genesis flagship project. [Online]. Available: https://www.6gflagship.com/

[76] "Key drivers and research challenges for 6G ubiquitous wireless intelligence," White Paper, 6G Flagship, University of Oulu, Sep. 2019.

[77] "6G market development: A north american perspective," White Paper, Next G Alliance, 2022.

[78] Spacex Starlink. [Online]. Available: https://www.starlink.com/

[79] "6G vision and candidate technologies," White Paper, IMT-2030 Promotion Group, Jun. 2021.

[80] "Beyond 5G white paper: Message to the 2030s," White Paper, Beyond 5G Promotion Consortium, Mar. 2022.

[81] F. Fitzek *et al.*, "6G activities in germany," *IEEE Future Netw.*, vol. 15, Dec. 2022.

[82] H. D. Schotten, "Overview of German 6G program," Report, ETSI Research Conference 2023, Feb. 2023.

[83] N. Ehrlich, "The advanced mobile phone service," *IEEE Commun. Mag.*, vol. 17, no. 2, pp. 9 – 16, Mar. 1979.

[84] M. Rahnema, "Overview of the GSM system and protocol architecture," *IEEE Commun. Mag.*, vol. 31, no. 4, pp. 92 – 100, Apr. 1993.

[85] H. Holma and A. Toskala, *WCDMA for UMTS-Radio Access for Third Generation Mobile Communications (Third Edition)*. England: John Wiley & Sons Inc., 2004.

[86] D. Astely *et al.*, "LTE: the evolution of mobile broadband," *IEEE Commun. Mag.*, vol. 47, no. 4, pp. 44–51, Apr. 2009.

[87] P. H. Siegel, "Terahertz technology," *IEEE Trans. Microwave Theory and Techniques*, vol. 50, no. 3, pp. 910 – 928, Mar. 2002.

[88] T. Kuerner and A. Hirata, "On the impact of the results of WRC 2019 on THz communications," in *Proc. 3rd Int. Workshop on Mobile Terahertz Sys. (IWMTS)*, Essen, Germany, Jul. 2020, pp. 1–3.

[89] IEEE 802.15.3d-2017, "802.15.3d-2017 - IEEE standard for high data rate wireless multi-media networks–amendment 2: 100 Gb/s wireless switched point-to-point physical layer," IEEE Computer Society, New York, USA, Standard 802.15.3d-2017, 2017.

[90] V. Petrov, T. Kurner, and I. Hosako, "IEEE 802.15.3d: First standardization efforts for sub-terahertz band communications toward 6G," *IEEE Commun. Mag.*, vol. 58, no. 11, pp. 28 – 33, Nov. 2020.

[91] H. Sarieddeen *et al.*, "Next generation Terahertz communications: A rendezvous of sensing, imaging, and localization," *IEEE Commun. Mag.*, vol. 58, no. 5, pp. 69 – 75, May 2020.

[92] S. Ju and T. S. Rappaport, "Sub-terahertz spatial statistical MIMO channel model for urban microcells at 142 GHz," in *Proc. 2021 IEEE Global Commun. Conf. (Globecom)*, Madrid, Spain, Feb. 2021, pp. 1 – 6.

[93] J. G. Ponce *et al.*, "THz band channel measurements and statistical modeling for urban D2D environments," *IEEE Trans. Wireless Commun.*, vol. 22, no. 3, pp. 1466 – 1479, Mar. 2023.

[94] K. Guan *et al.*, "Channel sounding and ray tracing for train-to-train communications at the THz band," in *Proc. Eur. Conf. Antennas Propag. (EuCAP)*, Krakow, Poland, Apr. 2019, pp. 1 – 5.

[95] J. M. Eckhardt *et al.*, "Channel measurements and modeling for low-terahertz band vehicular communications," *IEEE J. Sel. Areas Commun.*, vol. 39, pp. 1590 – 1603, Jun. 2021.

[96] J. M. Jornet and I. F. Akyildiz, "Femtosecond-long pulse-based modulation for terahertz band communication in nanonetworks," *IEEE Trans. Commun.*, vol. 62, pp. 1742 – 1754, May 2014.

[97] B. K. Jung *et al.*, "Simulation and automatic planning of 300 GHz backhaul links," in *Proc. Int. Conf. Infrared Millimeter THz Waves (IRMMW-THz)*, Paris, France, Sep. 2019, pp. 1 – 3.

[98] C. Han *et al.*, "Terahertz wireless channels: A holistic survey on measurement, modeling, and analysis," *IEEE Commun. Surveys Tuts.*, vol. 24, pp. 1670 – 1707, Nov. 2022.

[99] S. Ju and T. S. Rappaport, "Sub-terahertz spatial statistical MIMO channel model for urban microcells at 142 GHz," in *Proc. 2021 IEEE Global Commun. Conf. (Globecom)*, Madrid, Spain, Dec. 2022, pp. 1 – 6.

[100] K. Rikkinen *et al.*, "THz radio communication: Link budget analysis toward 6G," *IEEE Commun. Mag.*, vol. 58, no. 11, pp. 22 – 27, Nov. 2020.

[101] J. M. Jornet and I. F. Akyildiz, "Channel modeling and capacity analysis for electromagnetic wireless nanonetworks in the terahertz band," *IEEE Trans. Wireless Commun.*, vol. 10, no. 10, pp. 3211 – 3221, Oct. 2011.

[102] A. Faisal *et al.*, "Ultramassive MIMO systems at Terahertz bands: Prospects and challenges," *IEEE Veh. Technol. Mag.*, vol. 15, no. 4, pp. 33 – 42, Dec. 2020.

[103] J. M. Jornet and I. F. Akyildiz, "Graphene-based plasmonic nano-antenna for Terahertz band communication in nanonetworks," *IEEE J. Sel. Areas Commun.*, vol. 31, no. 12, pp. 685 – 694, Dec. 2013.

[104] K. K.O. *et al.*, "Opening terahertz for everyday applications," *IEEE Commun. Mag.*, vol. 57, no. 8, pp. 70–76, August 2019.

[105] S. Helal *et al.*, "Signal processing and machine learning techniques for terahertz sensing: An overview," *IEEE Sig. Proces. Maga.*, vol. 39, no. 5, pp. 42–62, 2022.

[106] H. Park and J.-H. Son, "Machine learning techniques for thz imaging and time-domain spectroscopy," *Sensors*, vol. 21, no. 4, 2021.

[107] I. F. Akyildiz and J. M. Jornet, "The Internet of nano-things," *IEEE Wireless Commun. Mag.*, vol. 17, no. 6, pp. 58 – 63, Dec. 2010.

[108] Z. Chen *et al.*, "Terahertz wireless communications for 2030 and beyond: A cutting-edge frontier," *IEEE Commun. Mag.*, vol. 59, no. 11, pp. 66–72, 2021.

[109] I. B. Djordjevic, "Oam-based hybrid free-space optical-terahertz multidimensional coded modulation and physical-layer security," *IEEE Photonics Journal*, vol. 9, no. 4, pp. 1–12, 2017.

[110] Z. Fang *et al.*, "Secure communication channels using atmosphere-limited line-of-sight terahertz links," *IEEE Trans. on THz Scie. and Techn.*, vol. 12, no. 4, pp. 363–369, 2022.

[111] Y. Yang *et al.*, "Terahertz topological photonics for on-chip communication," *Nature Photonics*, vol. 14, p. 446–451, Oct. 2020.

[112] J. Ma *et al.*, "Security and eavesdropping in terahertz wireless links," *Nature*, vol. 563, p. 89–93, Oct. 2018.

[113] M. Lotti *et al.*, "Radio SLAM for 6G systems at THz frequencies: Design and experimental validation," *Preprint*, Dec. 2022, arXiv:2212.12388.

[114] H. Sarieddeen, M.-S. Alouini, and T. Y. Al-Naffouri, "Terahertz-band ultra-massive spatial modulation MIMO," *IEEE J. Sel. Areas Commun.*, vol. 37, no. 9, pp. 2040 – 2052, Sep. 2019.

[115] T.-I. Jeon *et al.*, *Free Space Loss and Atmospheric Effects*. Cham: Springer International Publishing, 2022, pp. 51–64.

[116] D. Tse and P. Viswanath, *Fundamentals of Wireless Communication*. Cambridge, United Kingdom: Cambridge University Press, 07 2005.

[117] H. T. Friis, "A note on a simple transmission formula," *Proc. IRE and Waves and Electrons*, pp. 254–256, May 1946.

[118] N. A. Abbasi *et al.*, "Channel measurements and path loss modeling for indoor THz communication," in *2020 14th Eur. Conf. on Ant. Propag. (EuCAP)*, Copenhagen, Denmark, Mar. 2020, pp. 1 – 5.

[119] ——, "Double directional channel measurements for THz communications in an urban environment," in *Proc. 2020 IEEE Int. Commun. Conf. (ICC)*, Dublin, Ireland, Jun. 2020, pp. 1 – 6.

[120] ——, "Double-directional channel measurements for urban THz communications on a linear route," in *Proc. 2021 IEEE Int. Commun. Conf. Workshops (ICC Workshops)*, Montreal, QC, Canada, Jul. 2021, pp. 1 – 6.

[121] ——, "Ultra-wideband double directional channel measurements for THz communications in urban environments," in *Proc. 2021 IEEE Int. Commun. Conf. (ICC)*, Montreal, QC, Canada, Jun. 2021, pp. 1 – 6.

[122] J. He *et al.*, "Channel measurement and path-loss characterization for low-terahertz indoor scenarios," in *Proc. 2021 IEEE Int. Commun. Conf. Workshops (ICC Workshops)*, Montreal, QC, Canada, Jul. 2021, pp. 1 – 6.

[123] Y. Chen *et al.*, "Channel measurement and ray-tracing-statistical hybrid modeling for low-terahertz indoor communications," *IEEE Trans. Wireless Commun.*, vol. 20, pp. 8163 – 8176, Jun. 2021.

[124] Y. Li *et al.*, "Channel measurement and analysis in an indoor corridor scenario at 300 GHz," in *Proc. 2022 IEEE Int. Commun. Conf. (ICC)*, Seoul, South Korea, May 2022, pp. 2888 – 2893.

[125] S. Ju *et al.*, "Sub-terahertz channel measurements and characterization in a factory building," in *Proc. 2021 IEEE Int. Commun. Conf. (ICC)*, Seoul, South Korea, May 2022, pp. 2882 – 2887.

[126] S. Ju and T. S. Rappaport, "140 GHz urban microcell propagation measurements for spatial consistency modeling," in *Proc. 2021 IEEE Int. Commun. Conf. (ICC)*, Montreal, QC, Canada, Jun. 2021, pp. 1 – 6.

[127] Y. Xing and T. S. Rappaport, "Millimeter wave and terahertz urban microcell propagation measurements and models," *IEEE Commun. Lett.*, vol. 25, pp. 3755 – 3759, Oct. 2021.

[128] D. V. der Weide, J. Murakowski, and F. Keilmann, "Gas-absorption spectroscopy with electronic terahertz techniques," *IEEE Trans. Microwave Theory Tech.*, vol. 48, no. 4, pp. 740 – 743, Apr. 2000.

[129] D. M. Slocum *et al.*, "Atmospheric absorption of terahertz radiation and water vapor continuum effects," *J. Quant. Spectroscopy Radiative Transfer*, vol. 127, pp. 49–63, Sep. 2013.

[130] G. A. Siles, J. M. Riera, and P. G. del Pino, "Atmospheric attenuation in wireless communication systems at millimeter and THz frequencies," *IEEE Antennas Propag. Mag.*, vol. 57, no. 1, pp. 48 – 61, Feb. 2015.

[131] ITU-R P.676, "Attenuation by atmospheric gases and related effects," ITU-R, Recommendation P676-12, 08 2019.

[132] I. Gordon *et al.*, "The HITRAN2020 molecular spectroscopic database," *J. Quantitative Spectrosc. Radiative Transfer*, vol. 277, Jan. 2022, art. no. 107949.

[133] J. Kokkoniemi *et al.*, "Frequency and time domain channel models for Nanonetworks in Terahertz band," *IEEE Trans. Antennas Propag.*, vol. 63, no. 2, pp. 678 – 691, Feb. 2015.

[134] E. K. Smith, "Centimeter and millimeter wave attenuation and brightness temperature due to atmospheric oxygen and water vapor," *Radio Sci.*, vol. 17, pp. 1455 – 1464, Nov. 1982.

[135] H. J. Liebe and D. H. Layton, "Millimeter-wave properties of the atmosphere: Laboratory studies and propagation modeling," in *NASA STI/Recon Technical Report*, Washington, DC, USA, Oct. 1987, p. 21387.

[136] J. Kokkoniemi, J. Lehtomäki, and M. Juntti, "A discussion on molecular absorption noise in the Terahertz band," *Nano Commun. Netw.*, vol. 8, p. 35–45, Jun. 2016.

[137] J. M. Jornet and I. F. Akyildiz, "Channel modeling and capacity analysis for electromagnetic wireless nanonetworks in the terahertz band," *IEEE Trans. Wireless Commun.*, vol. 10, pp. 3211 – 3221, Aug. 2011.

[138] W. Jiang and F.-L. Luo, *6G Key Technologies: A Comprehensive Guide*. New York, USA: IEEE Press & Wiley, 2023.

[139] K. Tekbıyık *et al.*, "Terahertz band communication systems: Challenges, novelties and standardization efforts," *Phys. Commun.*, vol. 35, p. 100700, Aug. 2019.

[140] B. K. Jung *et al.*, "Link-level and system-level simulation of 300 GHz wireless backhaul links," in *Proc. Int. Symp. Antennas Propag. (ISAP)*, Osaka, Japan, Jan. 2021, pp. 619 – 620.

[141] B. K. Jung and T. Kürner, "Automatic planning algorithm of 300 GHz backhaul links using ring topology," in *Proc. Eur. Conf. Antennas Propag. (EuCAP)*, Dusseldorf, Germany, Mar. 2021, pp. 1 – 5.

[142] V. Petrov *et al.*, "IEEE 802.15.3d: First standardization efforts for sub-terahertz band communications toward 6G," *IEEE Commun. Mag.*, vol. 58, pp. 28 – 33, Nov. 2020.

[143] J. F. Federici *et al.*, "Review of weather impact on outdoor terahertz wireless communication links," *Nano Commun. Netw.*, vol. 10, pp. 13 – 26, Dec. 2016.

[144] R. K. Crane, "Prediction of attenuation by rain," *IEEE Trans. Commun.*, vol. 28, no. 9, pp. 1717–1733, Sep. 1980.

[145] Z.-K. Weng *et al.*, "Millimeter-wave and terahertz fixed wireless link budget evaluation for extreme weather conditions," *IEEE Access*, vol. 9, pp. 163 476 – 163 491, Dec. 2021.

[146] ITU-R P.838, "Specific attenuation model for rain for use in prediction methods," ITU-R, Recommendation P838-3, 2005.

[147] P. F. M. Smulders and L. M. Correia, "Characterisation of propagation in 60 GHz radio channels," *Electronics and Commun. Engineering J.*, vol. 9, no. 2, pp. 73 – 80, Apr. 1997.

[148] ITU-R P.840, "Attenuation due to clouds and fog," ITU-R, Recommendation P840-8, 08 2019.

[149] G. M. Brooker *et al.*, "Seeing through dust and water vapor: Millimeter wave radar sensors for mining applications," *J. Field Robot.*, vol. 24, pp. 527 – 577, Jul. 2007.

[150] E.-B. Moon, T.-I. Jeon, and D. R. Grischkowsky, "Long-path THz-TDS atmospheric measurements between buildings," *IEEE Trans. Terahertz Sci. Techno.*, vol. 5, pp. 742 – 750, Jul. 2015.

[151] J. Ma *et al.*, "Comparison of experimental and theoretical determined terahertz attenuation in controlled rain," *J. Infrared Millimeter Terahertz Waves.*, vol. 36, pp. 1195 – 1202, Aug. 2015.

[152] F. Norouzian *et al.*, "Rain attenuation at millimeter wave and low-THz frequencies," *IEEE Trans. Antennas Propag.*, vol. 68, pp. 421 – 431, Jan. 2020.

[153] Marzuki *et al.*, "Characteristics of rain attenuation for microwave-to-terahertz waveband from raindrop size distribution observation in indonesia," in *Proc. Photon. Electromagn. Res. Symp. Spring (PIERS-Spring)*, Rome, Italy, Jun. 2019, pp. 362 – 367.

[154] Y. Golovachev *et al.*, "Propagation properties of sub-millimeter waves in foggy conditions," *J. Appl. Phys.*, vol. 125, p. 151612, Apr. 2019.

[155] Y. Yang *et al.*, "Broadband THz signals propagate through dense fog," *IEEE Photon. Technol. Lett.*, vol. 27, pp. 383 – 386, Feb. 2015.

[156] H. Juttula *et al.*, "Rain induced co-channel interference at 60GHz and 300GHz frequencies," in *Proc. 2019 IEEE Int. Commun. Conf. (ICC)*, Shanghai, China, May 2019.

[157] F. Norouziari *et al.*, "Low-THz wave snow attenuation," in *Proc. Int. Conf. Radar (RADAR)*, Brisbane, QLD, Australia, Aug. 2018, pp. 1 – 4.

[158] ——, "Experimental study on low-THz automotive radar signal attenuation during snowfall," *IET Radar Sonar Navig.*, vol. 13, pp. 1421 – 1427, May 2019.

[159] R. Du *et al.*, "Characterisation of attenuation by sand in low-THz band," in *Proc. IEEE Radar Conf. (RadarConf)*, Seattle, WA, USA, Jun. 2017, pp. 294 – 297.

[160] T. S. Rappaport *et al.*, *Millimeter wave wireless communications*. Englewood Cliffs, NJ, USA: Pearson Education, Sep. 2014.

[161] V. Petrov *et al.*, "The effect of small-scale mobility on terahertz band communications," in *Proc. 5th ACM Int. Conf. Nanoscale Comput. Commun.*, New York, NY, USA, Sep. 2018, pp. 1 – 2.

[162] C. Slezak *et al.*, "Empirical effects of dynamic human-body blockage in 60 GHz communications," *IEEE Commun. Mag.*, vol. 56, pp. 60 – 66, Dec. 2018.

[163] S. Tripathi *et al.*, "Millimeter-wave and terahertz spectrum for 6G wireless," in *6G Mobile Wireless Networks*, Y. Wu *et al.*, Eds. Cham: Springer International Publishing, 2021, pp. 83–121.

[164] 3GPP TR38.900, "Study on channel model for frequency spectrum above 6 GHz," 3GPP, Technical Report TR38.900 v15.0.0, 06 2018.

[165] M. Gapeyenko *et al.*, "Spatially-consistent human body blockage modeling: A state generation procedure," *IEEE Trans. Mobile Comput.*, vol. 19, pp. 2221 – 2233, Sep. 2020.

[166] N. Stepanov *et al.*, "Statistical analysis and modeling of user micromobility for THz cellular communications," *IEEE Trans. Veh. Technol.*, vol. 71, pp. 725 – 738, Jan. 2022.

[167] ——, "Accuracy assessment of user micromobility models for thz cellular systems," in *Proc. 5th ACM Workshop Millimeter-Wave THz Netw. Sens. Syst.*, New York, NY, USA, Oct. 2021, pp. 37 – 42.

[168] B. Peng *et al.*, "Channel modeling and system concepts for future terahertz communications: Getting ready for advances beyond 5G," *IEEE Veh. Technol. Mag.*, vol. 15, no. 2, pp. 136–143, Jun. 2020.

[169] S. Rey *et al.*, "Channel sounding techniques for applications in THz communications: A first correlation based channel sounder for ultra-wideband dynamic channel measurements at 300 GHz," in *Proc. 9th Int. Congress on Ultra Modern Telecommun. and Control Sys. and Workshops (ICUMT)*, Munich, Germany, Nov. 2017, pp. 449–453.

[170] D. Serghiou *et al.*, "Ultra-wideband terahertz channel propagation measurements from 500 to 750 GHz," in *Proc. Int. Conf. U.K.-China Emerg. Technol. (UCET)*, Glasgow, UK, Aug. 2020, pp. 1 – 4.

[171] N. Khalid and O. B. Akan, "Wideband THz communication channel measurements for 5G indoor wireless networks," in *Proc. 2016 IEEE Int. Commun. Conf. (ICC)*, Kuala Lumpur, Malaysia, May 2016, pp. 1 – 6.

[172] N. Khalid *et al.*, "Statistical characterization and analysis of low-THz communication channel for 5G internet of things," *Nano Commun. Netw.*, vol. 22, p. 100258, Dec. 2019.

[173] S. Kim and A. G. Zajić, "Statistical characterization of 300-GHz propagation on a desktop," *IEEE Trans. Veh. Technol.*, vol. 64, pp. 3330 – 3338, Aug. 2015.

[174] ——, "Characterization of 300-GHz wireless channel on a computer motherboard," *IEEE Trans. Antennas Propag.*, vol. 64, pp. 5411 – 5423, Dec. 2016.

[175] C.-L. Cheng and A. G. Zajić, "Characterization of propagation phenomena relevant for 300 GHz wireless data center links," *IEEE Trans. Antennas Propag.*, vol. 68, pp. 1074 – 1087, Feb. 2020.

[176] C.-L. Cheng, S. Sangodoyin, and A. Zajić, "THz cluster-based modeling and propagation characterization in a data center environment," *IEEE Access*, vol. 8, pp. 56 544 – 56 558, Mar. 2020.

[177] Z. Yu *et al.*, "Wideband channel measurements and temporal-spatial analysis for terahertz indoor communications," in *Proc. 2020 IEEE Int. Commun. Conf. Workshops (ICC Workshops)*, Dublin, Ireland, Jun. 2020, pp. 1 – 6.

[178] Y. Chen *et al.*, "140 GHz channel measurement and characterization in an office room," in *Proc. 2021 IEEE Int. Commun. Conf.*, Dublin, Ireland, Jun. 2021, pp. 1 – 6.

[179] Y. Wang *et al.*, "0.3 THz channel measurement and analysis in an L-shaped indoor hallway," in *Proc. 2022 IEEE Int. Commun. Conf. (ICC)*, Seoul, Korea, Republic of, May 2022, pp. 2870 – 2875.

[180] G. R. MacCartney and T. S. Rappaport, "A flexible millimeter-wave channel sounder with absolute timing," *IEEE J. Sel. Areas Commun.*, vol. 35, pp. 1402 – 1418, Mar. 2017.

[181] S. Ju *et al.*, "Scattering mechanisms and modeling for terahertz wireless communications," in *Proc. 2019 IEEE Int. Commun. Conf.*, Shanghai, china, May 2019, pp. 1 – 7.

[182] Y. Xing and T. S. Rappaport, "Propagation measurement system and approach at 140 GHz-moving to 6G and above 100 GHz," in *Proc. 2018 IEEE Global Commun. Conf. (Globecom)*, Abu Dhabi, United Arab Emirates, Dec. 2018, pp. 1 – 6.

[183] Y. Xing *et al.*, "Indoor wireless channel properties at millimeter wave and sub-terahertz frequencies," in *Proc. 2019 IEEE Global Commun. Conf. (Globecom)*, Waikoloa, HI, USA, Dec. 2019, pp. 1 – 6.

[184] S. Ju *et al.*, "Millimeter wave and sub-terahertz spatial statistical channel model for an indoor office building," *IEEE J. Sel. Areas Commun.*, vol. 39, pp. 1561 – 1575, Apr. 2021.

[185] O. Kanhere and T. S. Rappaport, "Outdoor sub-THz position location and tracking using field measurements at 142 GHz," in *Proc. 2021 IEEE Int. Commun. Conf.*, Montreal, QC, Canada, Jun. 2021, pp. 1 – 6.

[186] R. Piesiewicz *et al.*, "Short-range ultra-broadband terahertz communications: Concepts and perspectives," *IEEE Antennas Propag. Mag.*, vol. 49, pp. 24 – 39, Dec. 2007.

[187] K. Thomas *et al.*, "Towards THz communications - status in research, standardization and regulation," *J. Infrared Millimeter Terahertz Waves*, vol. 35, pp. 53 – 62, Aug. 2014.

[188] S. Rey *et al.*, "Channel sounding techniques for applications in THz communications: A first correlation based channel sounder for ultra-wideband dynamic channel measurements at 300 GHz," in *Proc. Int. Congr. Ultra Modern Telecommun. Control Syst. Workshops (ICUMT)*, Munich, Germany, Nov. 2017, pp. 449 – 453.

[189] K. Guan *et al.*, "Channel characterization and capacity analysis for THz communication enabled smart rail mobility," *IEEE Trans. Veh. Technol.*, vol. 70, pp. 4065 – 4080, Apr. 2021.

[190] ——, "Measurement, simulation, and characterization of train-to-infrastructure inside-station channel at the terahertz band," *IEEE Trans. THz Sci. Technol.*, vol. 9, pp. 291 – 306, May 2019.

[191] ——, "Channel sounding and ray tracing for THz channel characterization," in *Proc. U.K.-Europe-China Workshop Millimetre-Waves Terahertz Technol. (UCMMT)*, Tianjin, China, Sep. 2020, pp. 1 – 3.

[192] ——, “Channel characterization for intra-wagon communication at 60 and 300 GHz bands,” *IEEE Trans. Veh. Technol.*, vol. 68, pp. 5193 – 5207, Jun. 2019.

[193] ——, “On millimeter wave and THz mobile radio channel for smart rail mobility,” *IEEE Trans. Veh. Technol.*, vol. 66, pp. 5658 – 5674, Jul. 2017.

[194] V. Petrov *et al.*, “Measurements of reflection and penetration losses in low terahertz band vehicular communications,” in *Proc. Eur. Conf. Antennas Propag. (EuCAP)*, Copenhagen, Denmark, Mar. 2020, pp. 1 – 5.

[195] J. M. Eckhardt *et al.*, “Measurements in a real data centre at 300 GHz and recent results,” in *Proc. Eur. Conf. Antennas Propag. (EuCAP)*, Krakow, Poland, Mar. 2019, pp. 1 – 5.

[196] Z. Hossain *et al.*, “Stochastic interference modeling and experimental validation for pulse-based terahertz communication,” *IEEE Trans. Veh. Technol.*, vol. 18, pp. 4103 – 4115, Aug. 2019.

[197] J. Ma *et al.*, “Comparison of experimental and theoretical determined terahertz attenuation in controlled rain,” *J. Infrared Millimeter Terahertz Waves*, vol. 36, pp. 1195 – 1202, Aug. 2015.

[198] R. Piesiewicz *et al.*, “Scattering analysis for the modeling of THz communication systems,” *IEEE Trans. Antennas Propag.*, vol. 55, pp. 3002 – 3009, Nov. 2007.

[199] C. Jansen *et al.*, “The impact of reflections from stratified building materials on the wave propagation in future indoor terahertz communication systems,” *IEEE Trans. Antennas Propag.*, vol. 56, pp. 1413 – 1419, May 2008.

[200] ——, “Diffuse scattering from rough surfaces in THz communication channels,” *IEEE Trans. THz Sci. Technol.*, vol. 1, pp. 462 – 472, Nov. 2011.

[201] M. Naftaly *et al.*, “Metrology state-of-the-art and challenges in broadband phase-sensitive terahertz measurements,” *Proc. IEEE*, vol. 105, pp. 1151 – 1165, Jun. 2017.

[202] S.-K. Yong, “Channel modeling sub-committee final report,” IEEE P802.15 Working Group for Wireless Personal Area Networks (WPANs) TG3c, Technical Report IEEE 15-07-0584-01-003c, 03 2007.

[203] C. Han and Y. Chen, “Propagation modeling for wireless communications in the terahertz band,” *IEEE Commun. Mag.*, vol. 56, no. 6, pp. 96–101, Jun. 2018.

[204] A. A. M. Saleh and R. Valenzuela, “A statistical model for indoor multipath propagation,” *IEEE J. Sel. Areas Commun.*, vol. 5, no. 2, pp. 128 – 137, Feb. 1987.

[205] A. S. Glassner, *An introduction to ray tracing*. San Francisco, USA: Academic Press, 1989.

[206] L. You *et al.*, “BDMA for millimeter-wave/terahertz massive MIMO transmission with per-beam synchronization,” *IEEE J. Sel. Areas Commun.*, vol. 35, pp. 1550 – 1563, Jul. 2017.

[207] R. Saadane and M. Wahbi, “UWB indoor radio propagation modelling in presence of human body shadowing using ray tracing technique,” *Int. J. Commun. Netw. Inf. Security*, vol. 4, Apr. 2022, art. no. 2.

[208] F. Sheikh *et al.*, “A novel ray-tracing algorithm for non-specular diffuse scattered rays at terahertz frequencies,” in *Proc. Int. Workshop Mobile THz Syst. (IWMTS)*, Duisburg, Germany, Jul. 2018, pp. 1 – 6.

[209] U. T. Virk *et al.*, “On-site permittivity estimation at 60 GHz through reflecting surface identification in the point cloud,” *IEEE Trans. Antennas Propag.*, vol. 66, pp. 3599 – 3609, Jul. 2018.

[210] G. Gougeon *et al.*, “Ray-based deterministic channel modelling for sub-THz band,” in *Proc. IEEE Int. Symp. Pers. Indoor Mobile Radio Commun. (PIMRC Workshops)*, Boston, MA, USA, Jul. 2019, pp. 1 – 6.

[211] F. Sheikh, Y. Gao, and T. Kaiser, “A study of diffuse scattering in massive MIMO channels at terahertz frequencies,” *IEEE Trans. Antennas Propag.*, vol. 68, pp. 997 – 1008, Feb. 2020.

[212] Y. Wang, S. Safavi-Naeini, and S. Chaudhuri, “A hybrid technique based on combining ray tracing and FDTD methods for site-specific modeling of indoor radio wave propagation,” *IEEE Trans. Antennas Propag.*, vol. 48, pp. 743 – 754, May 2000.

[213] Y. Zhao, Y. Hao, and C. Parini, “Fdtd characterisation of UWB indoor radio channel including frequency dependent antenna directivities,” in *Antennas Wireless Propag. Lett.*, Manchester, UK, Apr. 2007, pp. 191 – 194.

[214] A. Fricke *et al.*, “Time-domain propagation investigations for terahertz intra-device communications,” in *Proc. Eur. Conf. Antennas Propag. (EuCAP)*, The Hague, Netherlands, May 2014, pp. 1760 – 1764.

[215] T. S. Rappaport *et al.*, *Radio Propagation Measurements and Channel Modeling*. Cambridge, United Kingdom: Cambridge University Press, 07 2022.

[216] J. Kunisch *et al.*, “MEDIAN 60 GHz wideband indoor radio channel measurements and model,” in *Proc. IEEE Veh. Technol. Conf. (VTC)*, Amsterdam, Netherlands, Sep. 1999, pp. 2393 – 2397.

[217] T. Zwick, C. Fischer, and W. Wiesbeck, “A stochastic multipath channel model including path directions for indoor environments,” *IEEE J. Sel. Areas Commun.*, vol. 20, pp. 1178 – 1192, Aug. 2002.

[218] N. Azzaoui and L. Clavier, “Statistical channel model based on α-stable random processes and application to the 60 GHz ultra wide band channel,” *IEEE Trans. Commun.*, vol. 58, pp. 1457 – 1467, May 2010.

[219] S. Priebe and T. Kurner, “Stochastic modeling of THz indoor radio channels,” *IEEE Trans. Wireless Commun.*, vol. 12, pp. 4445 – 4455, Sep. 2013.

[220] C. Gustafson *et al.*, “On mm-Wave multipath clustering and channel modeling,” *IEEE Trans. Antennas Propag.*, vol. 62, pp. 1445 – 1455, Mar. 2014.

[221] M. K. Samimi and T. S. Rappaport, “3-D statistical channel model for millimeter-wave outdoor mobile broadband communications,” in *Proc. IEEE Int. Conf. Commun. (ICC)*, London, UK, Jun. 2015, pp. 2430 – 2436.

[222] T. Svantesson and J. Wallace, “Tests for assessing multivariate normality and the covariance structure of MIMO data,” in *Proc. IEEE Int. Conf. Acoust. Speech Signal Process. (ICASSP)*, Hong Kong, China, Apr. 2003, pp. 656 – 659.

[223] C. Sun *et al.*, “Beam division multiple access transmission for massive MIMO communications,” *IEEE Trans. Commun.*, vol. 63, pp. 2170 – 2184, Jun. 2015.

[224] S. Reynaud *et al.*, “Hybrid FDTD/UTD indoor channel modeling. application to Wifi transmission systems,” in *Proc. IEEE Veh. Technol. Conf. (VTC)*, Montreal, QC, Canada, Sep. 2006, pp. 1 – 5.

[225] M. Thiel and K. Sarabandi, “A hybrid method for indoor wave propagation modeling,” *IEEE Trans. Antennas Propag.*, vol. 56, pp. 2703 – 2709, Aug. 2008.

[226] M. Lecci *et al.*, “Quasi-deterministic channel model for mmWaves: Mathematical formalization and validation,” in *Proc. IEEE Global Commun. Conf. (GLOBECOM)*, Taipei, Taiwan, Dec. 2020, pp. 1 – 6.

[227] Z. Qiuming *et al.*, “3GPP tr 38.901 channel model,” 3GPP, Technical Report TR38.901 v14.0.0, 01 2021.

[228] A. Maltsev *et al.*, “Quasi-deterministic approach to mmWave channel modeling in a non-stationary environment,” in *Proc. IEEE Global Commun. Conf. (Globecom)*, Austin, TX, USA, Dec. 2014, pp. 966 – 971.

[229] M. K. Samimi and T. S. Rappaport, “Ultra-wideband statistical channel model for non line of sight millimeter-wave urban channels,” in *Proc. IEEE Global Commun. Conf. (GLOBECOM)*, Austin, TX, USA, Dec. 2014, pp. 3483 – 3489.

[230] J. Bian *et al.*, “A general 3D non-stationary wireless channel model for 5G and beyond,” *IEEE Trans. Wireless Commun.*, vol. 20, pp. 3211 – 3224, May 2021.

[231] J. S. Lu *et al.*, “A discrete environment-driven GPU-based ray launching algorithm,” *IEEE Trans. Antennas Propag.*, vol. 67, pp. 1180 – 1192, Feb. 2019.

[232] C. Han, A. O. Bicen, and I. F. Akyildiz, “Multi-ray channel modeling and wideband characterization for wireless communications in the terahertz band,” *IEEE Trans. Wireless Commun.*, vol. 14, pp. 2402 – 2412, May 2015.

[233] C. Han and I. F. Akyildiz, “Three-dimensional end-to-end modeling and analysis for graphene-enabled terahertz band communications,” *IEEE Trans. Veh. Technol.*, vol. 66, pp. 5626 – 5634, Jul. 2017.

[234] K. Ng *et al.*, “Modelling and performance prediction for multiple antenna systems using enhanced ray tracing,” in *Proc. IEEE Wireless Commun. Netw. Conf. (WCNC)*, Orleans, LA, USA, Mar. 2005, pp. 933 – 937.

[235] A. F. Molisch, “Modeling of directional wireless propagation channels,” *URSI Radio Sci. Bull*, vol. 66, pp. 16 – 26, Sep. 2002.

[236] I. Carton *et al.*, “Validation of 5g METIS map-based channel model at mmWave bands in indoor scenarios,” in *Proc. Eur. Conf. Antennas Propag. (EuCAP)*, Davos, Switzerland, Apr. 2016, pp. 1 – 5.

[237] J. Pascual-Garcia *et al.*, “Wireless channel simulation using geometrical models extracted from point clouds,” in *Proc. IEEE Int. Symp. Antennas Propag. USNC/URSI Nat. Radio Sci.*, Boston, MA, USA, Jul. 2018, pp. 83 – 84.

[238] Nextg channel model alliance. [Online]. Available: https://www.nist.gov/ctl/nextg-channel-model-alliance

[239] J. Kokkoniemi *et al.*, "Initial results on D band channel measurements in LOS and NLOS office corridor environment," in *Proc. 2022 16th Eur. Conf. Antennas and Propag. (EUCAP)*, Madrid, Spain, Apr. 2022.

[240] J. Blanz and P. Jung, "A flexibly configurable spatial model for mobile radio channels," *IEEE Trans. Commun.*, vol. 46, pp. 367 – 371, Mar. 1998.

[241] P. Petrus, J. Reed, and T. Rappaport, "Geometrical-based statistical macrocell channel model for mobile environments," *IEEE Trans. Commun.*, vol. 50, pp. 495 – 502, Mar. 2002.

[242] O. Norklit and J. Andersen, "Diffuse channel model and experimental results for array antennas in mobile environments," *IEEE Trans. Antennas Propag.*, vol. 46, pp. 834 – 840, Jun. 1998.

[243] T. Zwick, C. Fischer, D. Didascalou, and W. Wiesbeck, "A stochastic spatial channel model based on wave-propagation modeling," *IEEE J. Sel. Areas Commun.*, vol. 18, pp. 6 – 15, Jan. 2000.

[244] J. Kunisch and J. Pamp, "An ultra-wideband space-variant multipath indoor radio channel model," in *Proc. IEEE Conf. Ultra Wideband Syst. Technol.*, Reston, VA, USA, Nov. 2003, pp. 290 – 294.

[245] A. Maltsev *et al.*, "Statistical channel model for 60 GHz WLAN systems in conference room environment," in *Proc. 4th Eur. Conf. Antennas Propag.*, Barcelona, Spain, Nov. 2010, pp. 1 – 5.

[246] ——, "Channel modeling in the next generation mmWave Wi-Fi: IEEE 802.11ay standard," in *Proc. Eur. Wireless Conf.*, Oulu, Finland, May 2016, pp. 1 – 8.

[247] A. F. Molisch *et al.*, "The COST259 directional channel model-part i: Overview and methodology," *IEEE Trans. Wireless Commun.*, vol. 5, pp. 3421 – 3433, Dec. 2006.

[248] Sophia Antipolis, "Study on 3D channel model for LTE," 3GPP, Technical Report TR36.873 v12.7.0, 01 2018.

[249] M. Döttling *et al.*, *WINNER II Channel Models*. WILEY, 2010, pp. 39–92.

[250] R. Xu *et al.*, "A review of broadband low-cost and high-gain low-terahertz antennas for wireless communications applications," *IEEE Access*, vol. 8, pp. 57 615–57 629, 2020.

[251] B. Zhang *et al.*, "Metallic 3D printed antennas for millimeter- and submillimeter wave applications," *IEEE Trans. Terahertz Sci. Techno.*, vol. 6, no. 4, pp. 592–600, July 2016.

[252] T. Tajima *et al.*, "300-GHz step-profiled corrugated horn antennas integrated in LTCC," *IEEE Trans. Antennas Propa.*, vol. 62, no. 11, pp. 5437–5444, Nov 2014.

[253] G. Rebeiz, "Millimeter-wave and terahertz integrated circuit antennas," *Proc. IEEE*, vol. 80, no. 11, pp. 1748–1770, Nov 1992.

[254] A. Sharma and G. Singh, "Rectangular microstirp patch antenna design at thz frequency for short distance wireless communication systems," *J. Infrared, Millimeter, and Terahertz Waves*, vol. 30, pp. 1–7, 2009.

[255] A. S. Dhillon, D. Mittal, and E. Sidhu, "Thz rectangular microstrip patch antenna employing polyimide substrate for video rate imaging and homeland defence applications," *Optik*, vol. 144, pp. 634–641, 2017. [Online]. Available: https://www.sciencedirect.com/science/article/pii/S0030402617308355

[256] Q. Rubani, S. H. Gupta, and A. Kumar, "Design and analysis of circular patch antenna for wban at terahertz frequency," *Optik*, vol. 185, pp. 529–536, 2019. [Online]. Available: https://www.sciencedirect.com/science/article/pii/S0030402619304437

[257] I. Llatser, C. Kremers, A. Cabellos-Aparicio, J. M. Jornet, E. Alarcón, and D. N. Chigrin, "Graphene-based nano-patch antenna for terahertz radiation," *Photonics and Nanostructures - Fundamentals and Applications*, vol. 10, no. 4, pp. 353–358, 2012, taCoNa-Photonics 2011. [Online]. Available: https://www.sciencedirect.com/science/article/pii/S1569441012000727

[258] U. Nissanov *et al.*, "High gain terahertz microstrip array antenna for future generation cellular communication," in *2020 Int. Conf. Artificial Intelligence, Big Data, Computing and Data Commun. Syst. (icABCD)*, Aug 2020, pp. 1–6.

[259] S. A. Naghdehforushha and G. Moradi, "High directivity plasmonic graphene-based patch array antennas with tunable thz band communications," *Optik*, vol. 168, pp. 440–445, 2018. [Online]. Available: https://www.sciencedirect.com/science/article/pii/S0030402618305977

[260] K. R. Jha and G. Singh, "Microstrip patch array antenna on photonic crystal substrate at terahertz frequency," *Infrared Physics & Technology*, vol. 55, no. 1, pp. 32–39, 2012. [Online]. Available: https://www.sciencedirect.com/science/article/pii/S1350449511001009

[261] M. Alibakhshikenari *et al.*, "High-gain on-chip antenna design on silicon layer with aperture excitation for terahertz applications," *IEEE Antennas and Wireless Propag. Lett.*, vol. 19, no. 9, pp. 1576–1580, Sep. 2020.

[262] ——, "Study on on-chip antenna design based on metamaterial-inspired and substrate-integrated waveguide properties for millimetre-wave and thz integrated-circuit applications," *Journal of Infrared, Millimeter, and Terahertz Waves*, vol. 42, pp. 17–28, 2021.

[263] E. Seok *et al.*, "A 410GHz CMOS push-push oscillator with an on-chip patch antenna," in *2008 IEEE Int. Solid-State Circuits Conf. - Digest of Tech. Papers*, Feb 2008, pp. 472–629.

[264] K. Wu *et al.*, "Substrate-integrated millimeter-wave and terahertz antenna technology," *Proc. IEEE*, vol. 100, no. 7, pp. 2219–2232, July 2012.

[265] Y. Cai *et al.*, "A low-profile wideband surface-mountable substrate-integrated waveguide horn antenna," *IEEE Antennas Wireless Propag. Lett.*, vol. 16, pp. 2730–2733, 2017.

[266] H. Jin *et al.*, "E-Band substrate integrated waveguide orthomode transducer integrated with dual-polarized horn antenna," *IEEE Trans. Antennas and Propag.*, vol. 66, no. 5, pp. 2291–2298, May 2018.

[267] S. Hu *et al.*, "A SiGe BiCMOS transmitter/receiver chipset with on-chip SIW antennas for terahertz applications," *IEEE J. Solid-State Circuits*, vol. 47, no. 11, pp. 2654–2664, Nov 2012.

[268] J. Xu *et al.*, "140-ghz planar siw slot antenna array with a large-via-fence dielectric loading in ltcc," in *2012 6th Eur. Conf. Antennas and Propag. (EUCAP)*, March 2012, pp. 3542–3545.

[269] M. Alibakhshikenari *et al.*, "High-isolation antenna array using siw and realized with a graphene layer for sub-terahertz wireless applications," *Scientific Reports*, vol. 11, no. 1, pp. 1–14, 2021.

[270] K. Fan, Z.-C. Hao, and Q. Yuan, "A low-profile wideband substrate-integrated waveguide cavity-backed e-shaped patch antenna for the Q-LINKPAN applications," *IEEE Trans. Antennas and Propag.*, vol. 65, no. 11, pp. 5667–5676, Nov 2017.

[271] U. Nissanov, G. Singh, and N. Kumar, "High gain microstrip array antenna with siw and fss for beyond 5g at thz band," *Optik*, vol. 236, p. 166568, 2021. [Online]. Available: https://www.sciencedirect.com/science/article/pii/S0030402621002928

[272] A. A. Althuwayb, "On-chip antenna design using the concepts of metamaterial and siw principles applicable to terahertz integrated circuits operating over 0.6–0.622 thz," *Int. J. Antennas and Propag.*, vol. 2020, pp. 1–9, 2020.

[273] R. Camblor-Diaz *et al.*, "Sub-millimeter wave frequency scanning 8×1 antenna array," *Progress In Electromagnetics Research*, vol. 132, pp. 215–232, 2012.

[274] M. Alibakhshikenari *et al.*, "A comprehensive survey on antennas on-chip based on metamaterial, metasurface, and substrate integrated waveguide principles for millimeter-waves and terahertz integrated circuits and systems," *IEEE Access*, vol. 10, pp. 3668–3692, 2022.

[275] R. R. Hartmann, J. Kono, and M. E. Portnoi, "Terahertz science and technology of carbon nanomaterials," *Nanotechnology*, vol. 25, no. 32, p. 322001, jul 2014. [Online]. Available: https://dx.doi.org/10.1088/0957-4484/25/32/322001

[276] G. Lu *et al.*, "Carbon-based THz microstrip antenna design: A review," *IEEE Open J. Nanotechno.*, vol. 3, pp. 15–23, 2022.

[277] D. Correas-Serrano and J. S. Gomez-Diaz, "Graphene-based antennas for terahertz systems: A review," 2017.

[278] J. Hao and G. W. Hanson, "Infrared and optical properties of carbon nanotube dipole antennas," *IEEE Trans. Nanotechno.*, vol. 5, no. 6, pp. 766–775, Nov 2006.

[279] S. F. Mahmoud and A. R. AlAjmi, "Characteristics of a new carbon nanotube antenna structure with enhanced radiation in the sub-terahertz range," *IEEE Trans. Nanotechno.*, vol. 11, no. 3, pp. 640–646, May 2012.

[280] J.-S. Rieh, S. Jeon, and M. Kim, "An overview of integrated THz electronics for communication applications," in *2011 IEEE 54th Int. Midwest Symp. Circ. Syst. (MWSCAS)*, Aug 2011, pp. 1–4.

[281] H.-J. Song *et al.*, "Demonstration of 20Gbps wireless data transmission at 300GHz for kiosk instant data downloading applications with InP MMICs," in *2016 IEEE MTT-S Int. Microwave Symp. (IMS)*, May 2016, pp. 1–4.

[282] H. Hamada *et al.*, "300GHz-band 120-Gb/s wireless front-end based on InP-HEMT PAs and mixers," *IEEE J. Solid-State Circuits*, vol. 55, no. 9, pp. 2316–2335, Sep. 2020.

[283] M. Urteaga *et al.*, "A 130nm InP HBT integrated circuit technology for THz electronics," in *2016 IEEE Int. Electron Devices Meeting (IEDM)*, Dec 2016, pp. 29.2.1–29.2.4.

[284] K. M. K. H. Leong *et al.*, "850GHz receiver and transmitter front-ends using InP HEMT," *IEEE Trans. Terahertz Sci. Techno.*, vol. 7, no. 4, pp. 466–475, July 2017.

[285] S. Carpenter *et al.*, "A D-band 48Gbit/s 64-QAM/QPSK direct-conversion I/Q transceiver chipset," *IEEE Trans. Microwave Theory and Techni.*, vol. 64, no. 4, pp. 1285–1296, April 2016.

[286] M. Elkhouly *et al.*, "D-band phased-array TX and RX front ends utilizing radio-on-glass technology," in *2020 IEEE Radio Freq. Integrated Circuits Symp. (RFIC)*, Aug 2020, pp. 91–94.

[287] J. Grzyb *et al.*, "A 240GHz high-speed transmission link with highly-integrated transmitter and receiver modules in SiGe HBT technology," in *2017 42nd Int. Conf. Infrared, Millimeter, and Terahertz Waves (IRMMW-THz)*, Aug 2017, pp. 1–2.

[288] J. Yu *et al.*, "A 300GHz transmitter front end with -4.1 dbm peak output power for sub-THz communication using 130nm SiGe BiCMOS technology," *IEEE Trans. Microwave Theory Techni.*, vol. 69, no. 11, pp. 4925–4936, Nov 2021.

[289] S. Londhe and E. Socher, "A 232–242GHz coherent transmitter with 1.2mW peak radiated power in 28nm CMOS," in *2022 52nd Eur. Microwave Conf. (EuMC)*, Sep. 2022, pp. 143–146.

[290] K. Takano *et al.*, "A 105Gb/s 300GHz CMOS transmitter," in *2017 IEEE Int. Solid-State Circuits Conf. (ISSCC)*, Feb 2017, pp. 308–309.

[291] M. Fujishima, "300-GHz-band CMOS transceiver," in *2017 IEEE MTT-S Int. Microwave and RF Conf. (IMaRC)*, Dec 2017, pp. 306–309.

[292] S. Hara *et al.*, "A 32Gbit/s 16QAM CMOS receiver in 300GHz band," in *2017 IEEE MTT-S Int. Microwave Symp. (IMS)*, June 2017, pp. 1703–1706.

[293] C. D'heer and P. Reynaert, "A high-speed 390GHz bpook transmitter in 28nm CMOS," in *2020 IEEE Radio Freq. Integrated Circ. Symp. (RFIC)*, Aug 2020, pp. 223–226.

[294] X. Mei *et al.*, "First demonstration of amplification at 1THz using 25-nm InP high electron mobility transistor process," *IEEE Electron Device Lett.*, vol. 36, no. 4, pp. 327–329, April 2015.

[295] S. Kim *et al.*, "300GHz integrated heterodyne receiver and transmitter with on-chip fundamental local oscillator and mixers," *IEEE Trans. Terahertz Sci. Techno.*, vol. 5, no. 1, pp. 92–101, Jan 2015.

[296] H. Hamada *et al.*, "300GHz 100Gb/s InP-HEMT wireless transceiver using a 300GHz fundamental mixer," in *2018 IEEE/MTT-S Int. Microwave Symp. (IMS)*, June 2018, pp. 1480–1483.

[297] H. Rücker and B. Heinemann, "Device architectures for high-speed SiGe HBTs," in *2019 IEEE BiCMOS and Compound Semico. Integrated Circuits and Techno. Symp. (BCICTS)*, Nov 2019, pp. 1–7.

[298] B. Heinemann *et al.*, "SiGe HBT with fx/fmax of 505GHz/720GHz," in *2016 IEEE Int. Electron Devices Meeting (IEDM)*, Dec 2016, pp. 3.1.1–3.1.4.

[299] A. Karakuzulu *et al.*, "Full D-band transmit–receive module for phased array systems in 130-nm SiGe BiCMOS," *IEEE Solid-State Circuits Lett.*, vol. 4, pp. 40–43, 2021.

[300] Y. Zhao *et al.*, "A 160-GHz subharmonic transmitter and receiver chipset in an SiGe HBT technology," *IEEE Trans. Microwave Theory and Techni.*, vol. 60, no. 10, pp. 3286–3299, Oct 2012.

[301] A. Karakuzulu *et al.*, "A four-channel bidirectional d-band phased-array transceiver for 200Gb/s 6G wireless communications in a 130-nm BiCMOS technology," *IEEE J. Solid-State Circuits*, pp. 1–13, 2023.

[302] R. Han *et al.*, "A SiGe terahertz heterodyne imaging transmitter with 3.3 mw radiated power and fully-integrated phase-locked loop," *IEEE J. Solid-State Circuits*, vol. 50, no. 12, pp. 2935–2947, Dec 2015.

[303] M. H. Eissa *et al.*, "Wideband 240-GHz transmitter and receiver in BiCMOS technology with 25-Gbit/s data rate," *IEEE J. Solid-State Circuits*, vol. 53, no. 9, pp. 2532–2542, Sep. 2018.

[304] ——, "Frequency interleaving IF transmitter and receiver for 240-GHz communication in SiGe:C BiCMOS," *IEEE Trans. Microwave Theory and Techniques*, vol. 68, no. 1, pp. 239–251, Jan 2020.

[305] P. Rodríguez-Vázquez *et al.*, "A 16-QAM 100-Gb/s 1-M wireless link with an EVM of 17% at 230 GHz in an SiGe technology," *IEEE Microwave and Wireless Components Lett.*, vol. 29, no. 4, pp. 297–299, April 2019.

[306] D. Kissinger, G. Kahmen, and R. Weigel, "Millimeter-wave and terahertz transceivers in SiGe BiCMOS technologies," *IEEE Trans. Microwave Theory Techni.*, vol. 69, no. 10, pp. 4541–4560, Oct 2021.

[307] S. V. Thyagarajan, S. Kang, and A. M. Niknejad, "A 240GHz fully integrated wideband QPSK receiver in 65nm CMOS," *IEEE J. Solid-State Circuits*, vol. 50, no. 10, pp. 2268–2280, Oct 2015.

[308] S. Kang, S. V. Thyagarajan, and A. M. Niknejad, "A 240 GHz fully integrated wideband QPSK transmitter in 65nm CMOS," *IEEE J. Solid-State Circuits*, vol. 50, no. 10, pp. 2256–2267, Oct 2015.

[309] M. Fujishima, "Ultrahigh-speed terahertz transceiver with CMOS technology," in *2019 Eur. Microwave Conf. in Central Europe (EuMCE)*, May 2019, pp. 199–202.

[310] K. Katayama *et al.*, "A 300 GHz CMOS transmitter with 32-QAM 17.5 Gb/s/ch capability over six channels," *IEEE J. Solid-State Circuits*, vol. 51, no. 12, pp. 3037–3048, Dec 2016.

[311] I. Abdo *et al.*, "A 300GHz wireless transceiver in 65nm CMOS for IEEE802.15.3d using push-push subharmonic mixer," in *2020 IEEE/MTT-S Int. Microwave Symp. (IMS)*, Aug 2020, pp. 623–626.

[312] Q. Zhong *et al.*, "300-GHz CMOS QPSK transmitter for 30-Gbps dielectric waveguide communication," in *2018 IEEE Custom Integrated Circuits Conf. (CICC)*, April 2018, pp. 1–4.

[313] ——, "CMOS terahertz receivers," in *2018 IEEE Custom Integrated Circ. Conf. (CICC)*, April 2018, pp. 1–8.

[314] M. Fujishima, "Overview of sub-terahertz communication and 300GHz CMOS transceivers," *IEICE Electronics Express*, vol. 18, no. 8, pp. 20 212 002–20 212 002, 2021.

[315] T. Nagatsuma *et al.*, "Terahertz wireless communications based on photonics technologies," *Opt. Express*, vol. 21, no. 20, pp. 23 736–23 747, Oct 2013. [Online]. Available: https://opg.optica.org/oe/abstract.cfm?URI=oe-21-20-23736

[316] T. Ishibashi and H. Ito, "Uni-traveling-carrier photodiodes," *Journal of Applied Physics*, vol. 127, no. 3, 01 2020, 031101. [Online]. Available: https://doi.org/10.1063/1.5128444

[317] R. Kazarinov and R. Suris, "Possible amplification of electromagnetic waves in a semiconductor with a superlattice," *Fiz. Tekh. Poluprovodn.*, vol. 5, pp. 797–800, 1971.

[318] M. A. Belkin and F. Capasso, "New frontiers in quantum cascade lasers: high performance room temperature terahertz sources," *Physica Scripta*, vol. 90, no. 11, p. 118002, oct 2015. [Online]. Available: https://dx.doi.org/10.1088/0031-8949/90/11/118002

[319] S. Kumar, "Recent progress in terahertz quantum cascade lasers," *IEEE J. Sel. Topics Quantum Electronics*, vol. 17, no. 1, pp. 38–47, Jan 2011.

[320] M. S. Vitiello and A. Tredicucci, "Physics and technology of terahertz quantum cascade lasers," *Advances in Physics: X*, vol. 6, no. 1, p. 1893809, 2021.

[321] Z. Chen *et al.*, "Wireless communication demonstration at 4.1THz using quantum cascade laser and quantum well photodetector," *Electronics Lett.*, vol. 47, no. 17, p. 1, 2011.

[322] I. F. Akyildiz, C. Han, and S. Nie, "Combating the distance problem in the millimeter wave and Terahertz frequency bands," *IEEE Commun. Mag.*, vol. 56, no. 6, pp. 102 – 108, Jun. 2018.

[323] X. Yang, W. Jiang, and B. Vucetic, "A random beamforming technique for omnidirectional coverage in multiple-antenna systems," *IEEE Trans. Veh. Technol.*, vol. 62, no. 3, pp. 1420 – 1425, 3 2013.

[324] W. Jiang and X. Yang, "An enhanced random beamforming scheme for signal broadcasting in multi-antenna systems," in *Proc. IEEE 23rd Int. Symp. on Pers., Indoor and Mobile Radio Commun. (PIMRC)*, Sydney, Australia, 09 2012, pp. 2055–2060.

[325] X. Yang, W. Jiang, and B. Vucetic, "A random beamforming technique for broadcast channels in multiple antenna systems," in *Proc. 2011 IEEE Veh. Techno. Conf. (VTC Fall)*, San Francisco, USA, 09 2011, pp. 1–6.

[326] M. J. Lockyear, A. P. Hibbins, and J. R. Sambles, "Microwave surface-plasmon-like modes on thin metamaterials," *Phys. Rev. Lett.*, vol. 102, no. 7, p. 073901, Feb. 2009.

[327] I. F. Akyildiz and J. M. Jornet, "Realizing ultra-massive MIMO (1024x1024) communication in the (0.06–10) Terahertz band," *Nano Commun. Networks J.*, vol. 8, pp. 46–54, 2016.

[328] A. F. Molisch *et al.*, "Hybrid beamforming for massive MIMO: A survey," *IEEE Trans. Commun.*, vol. 55, no. 9, pp. 134 – 141, Sep. 2017.

[329] J. Zhang, X. Yu, and K. B. Letaief, "Hybrid beamforming for 5G and beyond millimeter-wave systems: A holistic view," *IEEE Open J. Commun. Society*, vol. 1, pp. 77 – 91, 12 2019.

[330] I. Ahmed *et al.*, "A survey on hybrid beamforming techniques in 5G: Architecture and system model perspectives," *IEEE Commun. Surv. Tutor.*, vol. 20, no. 4, pp. 3060 – 3097, 2018, fourthquarter.

[331] R. He *et al.*, "Wireless channel sparsity: Measurement, analysis, and exploitation in estimation," *IEEE Wireless Commun. Mag.*, vol. 28, no. 4, pp. 113 – 119, Aug. 2021.

[332] Y. Wu *et al.*, "3-D hybrid beamforming for Terahertz broadband communication system with beam squint," *IEEE Trans. Broadcasting*, 2022, early Access.

[333] C. Han, L. Yan, and J. Yuan, "Hybrid beamforming for Terahertz wireless communications: Challenges, architectures, and open problems," *IEEE Wireless Commun. Mag.*, vol. 28, no. 4, pp. 198 – 204, Aug. 2021.

[334] C. Lin and G. Y. Li, "Terahertz communications: An array-of-subarrays solution," *IEEE Commun. Mag.*, vol. 54, no. 12, pp. 124 – 131, Dec. 2016.

[335] X. Yu *et al.*, "Alternating minimization algorithms for hybrid precoding in millimeter wave MIMO systems," *IEEE J. Sel. Topics Signal Process.*, vol. 10, pp. 485 – 500, Apr. 2016.

[336] C. Lin and G. Y. Li, "Indoor terahertz communications: How many antenna arrays are needed?" *IEEE Trans. Wireless Commun.*, vol. 14, pp. 3097 – 3107, Jun. 2015.

[337] ——, "Adaptive beamforming with resource allocation for distance-aware multi-user indoor terahertz communications," *IEEE Trans. Commun.*, vol. 63, pp. 2985 – 2995, Aug. 2015.

[338] ——, "Energy-efficient design of indoor mmWave and Sub-THz systems with antenna arrays," *IEEE Trans. Wireless Commun.*, vol. 15, pp. 4660 – 4672, Jul. 2016.

[339] S. Tarboush *et al.*, "TeraMIMO: A channel simulator for wideband ultra-massive MIMO terahertz communications," *IEEE Trans. Veh. Technol.*, vol. 70, pp. 12 325 – 12 341, Dec. 2021.

[340] L. Yan, C. Han, and J. Yuan, "A dynamic array-of-subarrays architecture and hybrid precoding algorithms for terahertz wireless communications," *IEEE J. Sel. Areas Commun.*, vol. 38, pp. 2041 – 2056, Sep. 2020.

[341] L. Yan *et al.*, "Dynamic-subarray with fixed phase shifters for energy-efficient terahertz hybrid beamforming under partial CSI," *IEEE Trans. Wireless Commun.*, vol. 38, pp. 1 – 1, Nov. 2022.

[342] L. Yan, C. Han, and J. Yuan, "Energy-efficient dynamic-subarray with fixed true-time-delay design for terahertz wideband hybrid beamforming," *IEEE J. Sel. Areas Commun.*, vol. 40, pp. 2840 – 2854, Oct. 2022.

[343] Y. Xing and T. S. Rappaport, "Millimeter wave and Terahertz urban microcell propagation measurements and models," *IEEE Commun. Lett.*, vol. 25, no. 12, pp. 3755 – 3759, Dec. 2021.

[344] L. Yan *et al.*, "Joint inter-path and intra-path multiplexing for terahertz widely-spaced multi-subarray hybrid beamforming systems," *IEEE Trans. Commun.*, vol. 70, no. 2, pp. 1391 – 1406, Feb. 2022.

[345] X. Song *et al.*, "Two-level spatial multiplexing using hybrid beamforming for millimeter-wave backhaul," *IEEE Trans. Wireless Commun.*, vol. 17, pp. 4830 – 4844, Jul. 2018.

[346] J. Chen, S. Wang, and X. Yin, "A spherical-wavefront-based scatterer localization algorithm using large-scale antenna arrays," *IEEE Commun. Lett.*, vol. 20, pp. 1796 – 1799, Sep. 2016.

[347] H. Do, N. Lee, and A. Lozano, "Reconfigurable ulas for line-of-sight MIMO transmission," *IEEE Trans. Wireless Commun.*, vol. 20, pp. 2933 – 2947, Sep. 2021.

[348] H. Do *et al.*, "Terahertz line-of-sight MIMO communication: Theory and practical challenges," *IEEE Commun. Mag.*, vol. 59, pp. 104 – 109, Mar. 2021.

[349] L. Yan *et al.*, "Joint two-level spatial multiplexing and beamforming in terahertz ultra-massive MIMO systems," in *Proc. IEEE Int. Conf. Computer Commun. (INFOCOM) workshops*, Paris, France, May 2019, pp. 873 – 878.

[350] H. Shen *et al.*, "Alternating Optimization Based Hybrid Beamforming in Terahertz Widely-spaced Multi-subarray Systems," in *Proc. IEEE Global Commun. Conf. (Globecom)*, Rio de Janeiro, Brazil, Dec. 2022, pp. 1760 – 1765.

[351] C. Lin *et al.*, "Subarray-Based Coordinated Beamforming Training for mmWave and Sub-THz Communications," *IEEE J. Sel. Areas Commun.*, vol. 35, pp. 2115 – 2126, Mar. 2017.

[352] R. Rotman *et al.*, "True Time Delay in Phased Arrays," *Proc. IEEE*, vol. 104, pp. 504 – 518, Mar. 2016.

[353] V. Boljanovic *et al.*, "Fast Beam Training With True-Time-Delay Arrays in Wideband Millimeter-Wave Systems," *IEEE Trans. Circuits Syst. I*, vol. 68, pp. 1727 – 1739, Apr. 2021.

[354] E. Ghaderi *et al.*, "An integrated discrete-time delay-compensating technique for large-array beamformers," *IEEE Trans. Circuits Syst. I*, vol. 66, pp. 3296 – 3306, Sep. 2019.

[355] L. Dai *et al.*, "Delay-phase precoding for wideband THz massive MIMO," *IEEE Trans. Wireless Commun.*, vol. 21, pp. 7271 – 7286, Sep. 2022.

[356] F. Gao *et al.*, "Wideband beamforming for hybrid massive mimo terahertz communications," *IEEE J. Sel. Areas Commun.*, vol. 39, pp. 1725 – 1740, Jun. 2021.

[357] B. Wang *et al.*, "Wideband beamforming for hybrid phased array terahertz systems," in *Proc. IEEE Int. Conf. Commun. (ICC)*, Montreal, QC, Canada, Jun. 2021, pp. 1 – 6.

[358] D. Q. Nguyen and T. Kim, "Joint delay and phase precoding under true-time delay constraints for THz massive MIMO," in *Proc. IEEE Int. Conf. Commun. (ICC)*, Seoul, Korea, Republic of, May 2022, pp. 3496 – 3501.

[359] N. T. Nguyen *et al.*, "Beam squint effects in THz communications with UPA and ULA: Comparison and hybrid beamforming design," in *Proc. 2013 IEEE Global Commun. Conf. (Globecom)*, Rio de Janeiro, Brazil, Dec. 2022.

[360] S. Payami, M. Ghoraishi, and M. Dianati, "Hybrid beamforming for large antenna arrays with phase shifter selection," *IEEE Trans. Wireless Commun.*, vol. 15, no. 11, pp. 7258 – 7271, Nov. 2016.

[361] O. Quevedo-Teruel, M. Ebrahimpouri, and F. Ghasemifard, "Lens antennas for 5G communications systems," *IEEE Commun. Mag.*, vol. 56, no. 7, pp. 36 – 41, Jul. 2018.

[362] O. Lodge, "The origin or basis of wireless communication," *Nature*, vol. 111, p. 328–332, 1923.

[363] A. A. Mhaske *et al.*, "A bose horn antenna radio telescope (BHARAT) design for 21 cm hydrogen line experiments for radio astronomy teaching," *American J. Phys.*, vol. 90, p. 948, Nov. 2022.

[364] C. Pfeiffer and A. Grbic, "A printed, broadband luneburg lens antenna," *IEEE Trans. Antennas Propag.*, vol. 58, no. 9, pp. 3055 – 3059, Sep. 2010.

[365] M. Bosiljevac *et al.*, "Non-uniform metasurface Luneburg lens antenna design," *IEEE Trans. Antennas Propag.*, vol. 60, no. 9, pp. 4065 – 4073, Sep. 2012.

[366] R. Milne, "Dipole array lens antenna," *IEEE Trans. Antennas Propag.*, vol. 30, no. 4, pp. 704 – 712, Jul. 1982.

[367] Y. Zeng and R. Zhang, "Millimeter wave MIMO with lens antenna array: A new path division multiplexing paradigm," *IEEE Trans. Commun.*, vol. 64, no. 4, pp. 1557 – 1571, Apr. 2016.

[368] J. Yang *et al.*, "Communication and localization with extremely large lens antenna array," *IEEE Trans. Wireless Commun.*, vol. 20, no. 5, pp. 3031 – 3048, May 2021.

[369] Y. Zeng and R. Zhang, "Cost-effective millimeter-wave communications with lens antenna array," *IEEE Wireless Commun. Mag.*, vol. 24, no. 4, pp. 81 – 87, Aug. 2017.

[370] Z.-C. Hao *et al.*, "Development of a low-cost THz metallic lens antenna," *IEEE Antennas Wireless Propag. Lett.*, vol. 16, pp. 1751 – 1754, Feb. 2017.

[371] K. Konstantinidis *et al.*, "Low-THz dielectric lens antenna with integrated waveguide feed," *IEEE Trans. Terahertz Sci. Technol.*, vol. 7, pp. 572 – 581, Sep. 2017.

[372] S. Van Berkel *et al.*, "Wideband double leaky slot lens antennas in CMOS technology at submillimeter wavelengths," *IEEE Trans. Terahertz Sci. Technol.*, vol. 10, pp. 540 – 553, Sep. 2020.

[373] Q. Xiong *et al.*, "A wideband and high-gain fully metallic lens antenna for terahertz applications," *Electronics Lett.*, vol. 58, pp. 337 – 339, Mar. 2022.

[374] L. Lu *et al.*, "An overview of massive MIMO: Benefits and challenges," *IEEE J. Sel. Topics Signal Process.*, vol. 8, pp. 742 – 758, Mar. 2014.

[375] S. Li *et al.*, "Characterization of metasurface lens antenna for sub-6GHz dual-polarization full-dimension massive MIMO and multibeam systems," *IEEE Trans. Antennas Propag.*, vol. 68, pp. 1366 – 1377, Mar. 2020.

[376] J. Lee, H. Kim, and J. Oh, "Large-aperture metamaterial lens antenna for multi-layer MIMO transmission for 6G," *IEEE Access*, vol. 10, pp. 20 486 – 20 495, Feb. 2022.

[377] Y. Chen and C. Han, "Razor-sharp narrowbeam communications and management for terahertz wireless networks (INVITED PAPER)," in *2021 Comput., Commun. and IoT Appl.*, 2021, pp. 335–340.

[378] B. Peng *et al.*, "Power-angular spectra correlation based two step angle of arrival estimation for future indoor terahertz communications," *IEEE Trans. Antennas Propag.*, vol. 67, no. 11, pp. 7097–7105, 2019.

[379] W. Jiang and H. D. Schotten, "Initial beamforming for millimeter-wave and terahertz communications in 6G mobile systems," in *Proc. 2022 IEEE Wireless Commun. and Netw. Conf. (WCNC)*, Austin, USA, Apr. 2022.

[380] ——, "Initial access for millimeter-wave and terahertz communications with hybrid beamforming," in *Proc. 2022 IEEE Int. Commun. Conf. (ICC)*, Seoul, South Korea, May 2022.

[381] Z. Xiao *et al.*, "Hierarchical codebook design for beamforming training in millimeter-wave communication," *IEEE Trans. Wireless Commun.*, vol. 15, no. 5, pp. 3380–3392, 2016.

[382] Y. Chen *et al.*, "Millidegree-level direction-of-arrival estimation and tracking for terahertz ultra-massive MIMO systems," *IEEE Trans. Wireless Commun.*, vol. 21, no. 2, pp. 869–883, 2022.

[383] S. Hur *et al.*, "Millimeter wave beamforming for wireless backhaul and access in small cell networks," *IEEE Trans. Commun.*, vol. 61, no. 10, pp. 4391–4403, 2013.

[384] J. Wang *et al.*, "Beam codebook based beamforming protocol for multi-Gbps millimeter-wave WPAN systems," *IEEE J. Sel. Areas Commun.*, vol. 27, no. 8, pp. 1390–1399, 2009.

[385] IEEE, "IEEE standard for information technology– local and metropolitan area networks– specific requirements– part 15.3: Amendment 2: Millimeter-wave-based alternative physical layer extension," *IEEE Std.*, pp. 1–200, Oct. 2009.

[386] J. Tan and L. Dai, "Wideband beam tracking based on beam zooming for THz massive MIMO," in *IEEE Global Commun. Conf. (GLOBECOM)*, 2020, pp. 1–6.

[387] ——, "Delay-phase precoding for thz massive mimo with beam split," in *IEEE Global Commun. Conf. (GLOBECOM)*, 2019, pp. 1–6.

[388] Y. Ghasempour *et al.*, "Single-shot link discovery for terahertz wireless networks," *Nature Communications*, vol. 11, no. 1, p. 2017, Apr 2020.

[389] S. Noh, M. D. Zoltowski, and D. J. Love, "Multi-resolution codebook and adaptive beamforming sequence design for millimeter wave beam alignment," *IEEE Trans. Wireless Commun.*, vol. 16, no. 9, pp. 5689–5701, 2017.

[390] C. Lin, G. Y. Li, and L. Wang, "Subarray-based coordinated beamforming training for mmwave and sub-thz communications," *IEEE J. Sel. Areas Commun.*, vol. 35, no. 9, pp. 2115–2126, 2017.

[391] R. Zhang *et al.*, "Coordinated subarray based multi-user beam training for indoor sub-THz communications," in *IEEE 88th Veh. Technol. Conf. (VTC-Fall)*, 2018, pp. 1–5.

[392] Y.-R. Tsai and W.-H. Chen, "High efficiency beam alignment based on multi-modal beam patterns for massive mimo antenna systems," *IEEE Trans. Veh. Technol.*, vol. 70, no. 12, pp. 13 035–13 046, 2021.

[393] B. Peng, S. Priebe, and T. Kürner, "Fast beam searching concept for indoor terahertz communications," in *The European conf. Antennas Propag. (EuCAP)*, 2014, pp. 639–643.

[394] G. Stratidakis *et al.*, "A low-overhead hierarchical beam-tracking algorithm for thz wireless systems," in *European Conf. Netw. and Commun. (EuCNC)*, 2020, pp. 74–78.

[395] B. Ning *et al.*, "A unified 3d beam training and tracking procedure for terahertz communication," *IEEE Trans. Wireless Commun.*, vol. 21, no. 4, pp. 2445–2461, 2022.

[396] A. Ahmadi and O. Semiari, "Reinforcement learning for optimized beam training in multi-hop terahertz communications," in *IEEE International Conf. Commun. (ICC)*, 2021, pp. 1–6.

[397] Y. Wu *et al.*, "Hierarchical beam alignment in single-user MIMO single-carrier frequency division multiple access terahertz communication systems," in *IEEE International Conf. Commun. Workshops (ICC Workshops)*, 2021, pp. 1–7.

[398] S. Jayaprakasam *et al.*, "Robust beam-tracking for mmwave mobile communications," *IEEE Commun. Lett.*, vol. 21, no. 12, pp. 2654–2657, 2017.

[399] M. PremKumar *et al.*, "Least squares based channel estimation approach and bit error rate analysis of cognitive radio," in *International Conf. Robot. Autom. Contr. Embedded Syst. (RACE)*, 2015, pp. 1–4.

[400] T. Doeker *et al.*, "Angle of arrival and angle of departure estimation using compressed sensing for terahertz communications," in *The European conf. Antennas Propag. (EuCAP)*, 2021, pp. 1–5.

[401] M. Cui and L. Dai, "Near-field channel estimation for extremely large-scale MIMO with hybrid precoding," in *IEEE Global Commun. Conf. (GLOBECOM)*, 2021, pp. 1–6.

[402] R. Méndez-Rial *et al.*, "Channel estimation and hybrid combining for mmwave: Phase shifters or switches?" in *Inf. Theory and Appl. Workshop (ITA)*, 2015, pp. 90–97.

[403] V. Schram, A. Moldovan, and W. H. Gerstacker, "Compressive sensing for indoor THz channel estimation," in *Asilomar Conf. on Signals Syst. Comput.*, 2018, pp. 1539–1546.

[404] J. Yang *et al.*, "Fast beam training architecture for hybrid mmwave transceivers," *IEEE Trans. Veh. Technol.*, vol. 69, no. 3, pp. 2700–2715, 2020.

[405] X. Gao *et al.*, "Fast channel tracking for terahertz beamspace massive MIMO systems," *IEEE Trans. Veh. Technol.*, vol. 66, no. 7, pp. 5689–5696, 2017.

[406] G. Stratidakis *et al.*, "A cooperative localization-aided tracking algorithm for THz wireless systems," in *IEEE Wireless Commun. and Netw. Conf. (WCNC)*, 2019, pp. 1–7.

[407] A. Liao *et al.*, "2D unitary ESPRIT based super-resolution channel estimation for millimeter-wave massive MIMO with hybrid precoding," *IEEE Access*, vol. 5, pp. 24 747–24 757, 2017.

[408] Y. Chen, L. Yan, and C. Han, "Millidegree-level direction-of-arrival (DoA) estimation and tracking for terahertz wireless communications," in *Annual IEEE International Conf. on Sens. Commun. Netw. (SECON)*, 2020, pp. 1–9.

[409] A. Liao *et al.*, "Angle estimation for terahertz ultra-massive MIMO-based space-to-air communications," in *IEEE/CIC International Conf. Commun. in China (ICCC)*, 2021, pp. 776–781.

[410] Y. Chen and C. Han, "Deep CNN-based spherical-wave channel estimation for terahertz ultra-massive MIMO systems," in *IEEE Global Commun. Conf. (GLOBECOM)*, 2020, pp. 1–6.

[411] S. Nie and I. F. Akyildiz, "Deep kernel learning-based channel estimation in ultra-massive MIMO communications at 0.06-10 THz," in *IEEE Global Commun. Conf. (GLOBECOM)*, 2019, pp. 1–6.

[412] C. Hu *et al.*, "Super-resolution channel estimation for mmwave massive MIMO with hybrid precoding," *IEEE Trans. Veh. Technol.*, vol. 67, no. 9, pp. 8954–8958, 2018.

[413] M. Sánchez-Fernández *et al.*, "Gridless multidimensional angle-of-arrival estimation for arbitrary 3D antenna arrays," *IEEE Trans. Wireless Commun.*, vol. 20, no. 7, pp. 4748–4764, 2021.

[414] Y. J. Cho *et al.*, "RF lens-embedded antenna array for mmwave MIMO: Design and performance," *IEEE Commun. Mag.*, vol. 56, no. 7, pp. 42–48, 2018.

[415] A.-J. van der Veen *et al.*, "Joint angle and delay estimation using shift-invariance techniques," *IEEE Trans. Signal Process.*, vol. 46, no. 2, pp. 405–418, 1998.

[416] T. S. Cousik *et al.*, "Deep learning for fast and reliable initial access in AI-driven 6G mm wave networks," *IEEE Trans. Netw. Sci. & Eng.*, pp. 1–12, 2022.

[417] M. S. Sim, *et al.*, "Deep learning-based mmwave beam selection for 5G NR/6G with sub-6 ghz channel information: Algorithms and prototype validation," *IEEE Access*, vol. 8, pp. 51 634–51 646, 2020.

[418] M. A. Habibi *et al.*, "Towards a Fully Virtualized, Cloudified, and Slicing-aware RAN for 6G Mobile Networks," (2021). pp 327-358. In: Wu Y. et al. (eds) 6G Mobile Wireless Networks. Computer Communications and Networks. Springer, Cham.

[419] ——, "Enabling Network and Service Programmability in 6G Mobile Communication Systems," in *IEEE Future Networks World Forum*, 2022, pp. 320–327.

[420] C. Han, J. M. Jornet, and I. Akyildiz, "Ultra-massive MIMO channel modeling for graphene-enabled terahertz-band communications," in *2018 IEEE 87th vehicular technology conference (VTC Spring)*. IEEE, 2018, pp. 1–5.

[421] S. A. Busari, K. M. S. Huq, S. Mumtaz, and J. Rodriguez, "Terahertz massive MIMO for beyond-5G wireless communication," in *2019 IEEE International Conference on Communications (ICC)*. IEEE, 2019, pp. 1–6.

[422] F. Sheikh, Y. Gao, and T. Kaiser, "A study of diffuse scattering in massive MIMO channels at terahertz frequencies," *IEEE Trans. Antennas Propag.*, vol. 68, no. 2, pp. 997–1008, 2019.

[423] F. Gao *et al.*, "Wideband beamforming for hybrid massive MIMO terahertz communications," *IEEE J. Sel. Areas Commun.*, vol. 39, no. 6, pp. 1725–1740, 2021.

[424] K. Dovelos *et al.*, "Channel estimation and hybrid combining for wideband terahertz massive MIMO systems," *IEEE J. Sel. Areas Commun.*, vol. 39, no. 6, pp. 1604–1620, 2021.

[425] Y. Chen, L. Yan, C. Han, and M. Tao, "Millidegree-level direction-of-arrival estimation and tracking for terahertz ultra-massive MIMO systems," *IEEE Trans. Wireless Commun.*, vol. 21, no. 2, pp. 869–883, 2022.

[426] Z. Wan, Z. Gao, F. Gao, M. D. Renzo, and M.-S. Alouini, "Terahertz massive MIMO with holographic reconfigurable intelligent surfaces," *IEEE Trans. Wireless Commun.*, vol. 69, no. 7, pp. 4732–4750, 2021.

[427] B. Ning, Z. Chen, W. Chen, Y. Du, and J. Fang, "Terahertz multi-user massive MIMO with intelligent reflecting surface: Beam training and hybrid beamforming," *IEEE Trans. Veh. Technol.*, vol. 70, no. 2, pp. 1376–1393, 2021.

[428] W. Jiang and H. Schotten, "Orthogonal and non-orthogonal multiple access for intelligent reflection surface in 6G systems," in *Proc. 2023 IEEE Wireless Commun. and Netw. Conf. (WCNC)*, Glasgow, Scotland, UK, Mar. 2023.

[429] H. Zhang *et al.*, "Energy efficient resource allocation in terahertz downlink NOMA systems," *IEEE Trans. Commun.*, vol. 69, no. 2, pp. 1375–1384, 2021.

[430] S. R. Sabuj *et al.*, "Machine-type communications in NOMA-based terahertz wireless networks," *Int. J. Intell. Syst.*, vol. 3, pp. 31–47, 2022.

[431] Z. Chen *et al.*, "Towards intelligent reflecting surface empowered 6G terahertz communications: A survey," *China Commun.*, vol. 18, no. 5, pp. 93–119, 2021.

[432] X. Xu *et al.*, "Graph-embedded multi-agent learning for smart reconfigurable THz MIMO-NOMA networks," *IEEE J. Sel. Areas Commun.*, vol. 40, no. 1, pp. 259–275, 2022.

[433] M. Shahjalal *et al.*, "User clustering techniques for massive MIMO-NOMA enabled mmwave/THz communications in 6G," in *2021 Twelfth Intl. Conf. Ubiquitous and Future Netw. (ICUFN)*, 2021, pp. 379–383.

[434] ——, "Fuzzy c-means clustering-based mMIMO-NOMA downlink communication for 6G ultra-massive interconnectivity," in *2021 International Conference on Artificial Intelligence in Information and Communication (ICAIIC)*. IEEE, 2021, pp. 421–424.

[435] Z. Ding, M. Peng, and H. V. Poor, "Cooperative non-orthogonal multiple access in 5G systems," *IEEE Commun. Lett.*, vol. 19, no. 8, pp. 1462–1465, 2015.

[436] A. S. Parihar *et al.*, "Performance analysis of SWIPT enabled cooperative-NOMA in heterogeneous networks using carrier sensing," *IEEE Trans. Veh. Technol.*, vol. 70, no. 10, pp. 10 646–10 656, 2021.

[437] H. W. Oleiwi and H. Al-Raweshidy, "Cooperative SWIPT THz-NOMA/6G performance analysis," *Electronics*, vol. 11, no. 6, p. 873, 2022.

[438] W. Jiang and H. Schotten, "Performance impact of channel aging and phase noise on intelligent reflecting surface," *IEEE Commun. Lett.*, vol. 27, no. 1, pp. 347–351, Jan. 2023.

[439] ——, "Intelligent reflecting vehicle surface: A novel IRS paradigm for moving vehicular networks," in *Proc. 2022 IEEE 40th Military Commun. Conf. (MILCOM 2022)*, Rockville, MA, USA, Nov. 2022.

[440] W. Jiang and H. D. Schotten, "Capacity analysis and rate maximization design in RIS-aided uplink multi-user MIMO," in *Proc. 2023 IEEE Wireless Commun. and Netw. Conf. (WCNC)*, Glasgow, Scotland, UK, Mar. 2023.

[441] Y. Pan *et al.*, "Uav-assisted and intelligent reflecting surfaces-supported terahertz communications," *IEEE Wireless Communications Letters*, vol. 10, no. 6, pp. 1256–1260, 2021.

[442] Z. Chen *et al.*, "Terahertz wireless communications for 2030 and beyond: A cutting-edge frontier," *IEEE Communications Magazine*, vol. 59, no. 11, pp. 66–72, 2021.

[443] W. Hao *et al.*, "Ultra wideband thz irs communications: Applications, challenges, key techniques, and research opportunities," *IEEE Network*, vol. 36, no. 6, pp. 214–220, 2022.

[444] F. Yang *et al.*, "Terahertz reconfigurable intelligent surfaces (riss) for 6g communication links," *Micromachines*, vol. 13, no. 2, 2022.

[445] C. Xu *et al.*, "Reconfigurable terahertz metamaterials: From fundamental principles to advanced 6g applications," *iScience*, vol. 25, no. 2, p. 103799, 2022.

[446] H. Sarieddeen *et al.*, "An overview of signal processing techniques for terahertz communications," *Proceedings of the IEEE*, vol. 109, no. 10, pp. 1628–1665, 2021.

[447] G. Geraci *et al.*, "What will the future of UAV cellular communications be? A flight from 5G to 6G," *IEEE Commun. Surveys Tuts.*, vol. 24, no. 3, pp. 1304–1335, 2022.

[448] G. Araniti *et al.*, "Toward 6G non-terrestrial networks," *IEEE Netw.*, vol. 36, no. 1, pp. 113–120, 2022.

[449] K. Y. You, "Propagation channel modeling for low-altitude platform non-terrestrial networks from 275 GHz to 3 THz," *Int. J. Microw. Wirel. Technol.*, vol. 12, no. 3, pp. 1–17, 2022.

[450] S. Aliaga, V. Petrov, and J. M. Jornet, "Cross-link interference modeling in 6G millimeter wave and terahertz LEO satellite communications," *arXiv preprint arXiv:2302.04169*, 2023.

[451] J. Kokkoniemi *et al.*, "Channel modeling and performance analysis of airplane-satellite terahertz band communications," *IEEE Trans. Veh. Technol.*, vol. 70, no. 3, p. 2047–2061, Mar. 2021.

[452] Y. J. Guo *et al.*, "Quasi-optical multi-beam antenna technologies for B5G and 6G mmWave and THz networks: A review," *IEEE Open J. Antennas Propag.*, vol. 2, pp. 807–830, 2021.

[453] A. J. Alqaraghuli, A. Singh, and J. M. Jornet, "Compact two-stage origami horn antenna for terahertz CubeSat networks," in *2022 IEEE International Symposium on Antennas and Propagation and USNC-URSI Radio Science Meeting (AP-S/URSI)*. IEEE, 2022, pp. 1102–1103.

[454] K. Tamesue *et al.*, "Digital predistortion for THz RF power amplifier with 16-APSK modulation in non-terrestrial-networks," *IEICE Proceedings Series*, vol. 72, no. S12-3, 2022.

[455] R. Kumar and S. Arnon, "DNN beamforming for LEO satellite communication at sub-THz bands," *Electronics*, vol. 11, no. 23, p. 3937, 2022.

[456] P. Ramezani, B. Lyu, and A. Jamalipour, "Toward RIS-enhanced integrated terrestrial/non-terrestrial connectivity in 6G," *IEEE Netw.*, pp. 1–9, 2022.

[457] S. Aliaga, A. J. Alqaraghuli, and J. M. Jornet, "Joint terahertz communication and atmospheric sensing in low earth orbit satellite networks: Physical layer design," in *2022 IEEE 23rd International Symposium on a World of Wireless, Mobile and Multimedia Networks (WoWMoM)*. IEEE, 2022, pp. 457–463.

[458] N. P. Kuruvatti and etal., "Empowering 6g communication systems with digital twin technology: A comprehensive survey," *IEEE Access*, vol. 10, pp. 112 158–112 186, 2022.

[459] B. Han *et al.*, "Digital Twins for Industry 4.0 in the 6G Era," https://arxiv.org/abs/2210.08970, accessed on 26 February 2023.

[460] Z. Tao *et al.*, "Optimal control for digital-twin thz/vlc communication networks," in *2022 IEEE Int. Conf. on Comm. Worksh. (ICC Workshops)*, 2022, pp. 910–915.

[461] M. Pengnoo *et al.*, "Digital twin for metasurface reflector management in 6g terahertz communications," *IEEE Access*, vol. 8, pp. 114 580–114 596, 2020.

[462] L. Zhang *et al.*, "Digital-twin prediction of metamorphic object transportation by multi-robots with thz communication framework," *IEEE Transac. on Inte. Trans. Sys.*, pp. 1–9, 2022.

[463] W. Jiang and H. Schotten, "Neural network-based fading channel prediction: A comprehensive overview," *IEEE Access*, vol. 7, pp. 118 112–118 124, Aug. 2019.

[464] W. Jiang and H. D. Schotten, "Deep learning for fading channel prediction," *IEEE Open J. the Commun. Society*, vol. 1, pp. 320–332, Mar. 2020.

[465] ——, "A comparison of wireless channel predictors: Artificial Intelligence versus Kalman filter," in *Proc. 2019 IEEE Int. Commun. Conf. (ICC)*, Shanghai, China, May 2019.

[466] Y. Jiang *et al.*, "Machine learning and application in terahertz technology: A review on achievements and future challenges," *IEEE Access*, vol. 10, pp. 53 761–53 776, 2022.

[467] A. Banerjee, C. Chakraborty, and M. Rathi, "Chapter 8 - medical imaging, artificial intelligence, internet of things, wearable devices in terahertz healthcare technologies," in *Terahertz Biomedical and Healthcare Technologies*. Elsevier, 2020, pp. 145–165.

[468] R. Mitsuhashi *et al.*, "Terahertz tag identifiable through shielding materials using machine learning," *Opt. Express*, vol. 28, no. 3, pp. 3517–3527, Feb 2020.

[469] Z. Koczor-Benda *et al.*, "Molecular screening for terahertz detection with machine-learning-based methods," *Phys. Rev. X*, vol. 11, p. 041035, Nov 2021.

[470] M. M. U. Rahman *et al.*, "Physical layer authentication in nano networks at terahertz frequencies for biomedical applications," *IEEE Access*, vol. 5, pp. 7808–7815, 2017.

[471] Z. Fang and D. M. Mittleman, "Physical-layer security using atmosphere-limited line-of-sight terahertz links," in *Conference on Lasers and Electro-Optics*. Optica Publishing Group, 2021, p. JW1A.18.

[472] V. Petrov *et al.*, "Exploiting multipath terahertz communications for physical layer security in beyond 5g networks," in *IEEE INFOCOM 2019 - IEEE Conf. on Comp. Comm. Worksh.*, 2019, pp. 865–872.

[473] J. Woo *et al.*, "Physical-layer security for thz communications via orbital angular momentum waves," in *2022 IEEE Worksh. on Sign. Process. Systems*, 2022, pp. 1–6.

[474] H. Chen *et al.*, "A tutorial on terahertz-band localization for 6g communication systems," *IEEE Comm. Surv. & Tuto.*, vol. 24, no. 3, pp. 1780–1815, 2022.

[475] S. Fan *et al.*, "A structured bidirectional lstm deep learning method for 3d terahertz indoor localization," in *IEEE INFOCOM 2020 - IEEE Conf. on Comp. Comm.*, 2020, pp. 2381–2390.

[476] ——, "Siabr: A structured intra-attention bidirectional recurrent deep learning method for ultra-accurate terahertz indoor localization," *IEEE Jour. on Select. Areas in Comm.*, vol. 39, no. 7, pp. 2226–2240, 2021.

[477] X. Liu *et al.*, "Performance analysis of multi-connectivity under blockage in terahertz communication system," in *2022 IEEE 33rd Annual International Symposium on Personal, Indoor and Mobile Radio Communications (PIMRC)*. IEEE, 2022, pp. 1146–1152.

[478] A. Shafie, N. Yang, and C. Han, "Multi-connectivity for indoor terahertz communication with self and dynamic blockage," in *2020 IEEE International Conference on Communications (ICC)*, 2020, pp. 1–7.

[479] D. Moltchanov *et al.*, "Uninterrupted connectivity time in THz systems under user micromobility and blockage," in *2021 IEEE Global Communications Conference (GLOBECOM)*. IEEE, 2021, pp. 01–06.

[480] E. Sopin *et al.*, "User association and multi-connectivity strategies in joint terahertz and millimeter wave 6G systems," *IEEE Trans. Veh. Technol.*, vol. 71, no. 12, pp. 12 765–12 781, 2022.
[481] M. F. Özkoç *et al.*, "The impact of multi-connectivity and handover constraints on millimeter wave and terahertz cellular networks," *IEEE J. Sel. Areas Commun.*, vol. 39, no. 6, pp. 1833–1853, 2021.
[482] A. A. Dowhuszko *et al.*, "Distance-aware coordinated multi-point transmission for terahertz band communication," in *2017 IEEE 18th Intl. Workshop Signal Process. Advances Wireless Commun. (SPAWC)*. IEEE, 2017, pp. 1–5.
[483] O. Abbasi and H. Yanikomeroglu, "A cell-free scheme for UAV base stations with HAPS-assisted backhauling in terahertz band," in *2022 IEEE Intl. Conf. Commun. (ICC)*. IEEE, 2022, pp. 249–254.
[484] M.-T. Suer *et al.*, "Multi-connectivity as an enabler for reliable low latency communications—an overview," *IEEE Commun. Surv. Tutor.*, vol. 21, no. 1, pp. 156 – 169, 2020, first Quarter.
[485] P. Zhang *et al.*, "Out-of-band information aided mmwave/thz beam search: A spatial channel similarity perspective," *IEEE Commun. Mag.*, pp. 1–7, 2022.
[486] P. Kyösti *et al.*, "On the feasibility of out-of-band spatial channel information for millimeter-wave beam search," *IEEE Trans. Antennas Propag.*, pp. 1–1, 2023.
[487] B. Peng, S. Priebe, and T. Kürner, "Fast beam searching concept for indoor terahertz communications," in *The 8th European Conference on Antennas and Propagation (EuCAP 2014)*, 2014, pp. 639–643.
[488] B. Peng *et al.*, "Power-angular spectra correlation based two step angle of arrival estimation for future indoor terahertz communications," *IEEE Trans. Antennas Propag.*, vol. 67, no. 11, pp. 7097–7105, 2019.
[489] J. Yang *et al.*, "Integrated communication and localization in millimeter-wave systems," *Frontiers of Information Technology & Electronic Engineering*, vol. 22, no. 4, pp. 457–470, 2021.
[490] X. Li *et al.*, "Integrated sensing and communication in 6G: The deterministic channel models for THz imaging," in *Proc. IEEE 32nd Int. Symp. Pers. Indoor Mobile Radio Commun. (PIMRC)*, 2021, pp. 1–6.
[491] A. M. Elbir *et al.*, "Terahertz-band integrated sensing and communications: Challenges and opportunities," *arXiv preprint arXiv:2208.01235*, 2022.
[492] H. Chen *et al.*, "A tutorial on terahertz-band localization for 6G communication systems," *IEEE Commun. Surveys Tuts.*, 2022.
[493] S. Nie and I. F. Akyildiz, "Three-dimensional dynamic channel modeling and tracking for terahertz band indoor communications," in *Proc. IEEE 28th Int. Symp. Pers. Indoor Mobile Radio Commun. (PIMRC)*, 2017, pp. 1–5.
[494] Z. Chen *et al.*, "A survey on terahertz communications," *China Commun.*, vol. 16, no. 2, pp. 1–35, 2019.
[495] H. Sarieddeen, M.-S. Alouini, and T. Y. Al-Naffouri, "An overview of signal processing techniques for terahertz communications," *Proceedings of the IEEE*, vol. 109, no. 10, pp. 1628–1665, 2021.
[496] H. Wymeersch *et al.*, "Radio localization and mapping with reconfigurable intelligent surfaces: Challenges, opportunities, and research directions," *IEEE Veh. Technol. Mag.*, vol. 15, no. 4, pp. 52–61, 2020.
[497] D. K. P. Tan *et al.*, "Integrated sensing and communication in 6G: Motivations, use cases, requirements, challenges and future directions," in *Proc. IEEE Int. Online Symp. on Joint Commun. & Sens. (JC&S)*, 2021, pp. 1–6.
[498] D. Moltchanov *et al.*, "A tutorial on mathematical modeling of 5G/6G millimeter wave and terahertz cellular systems," *IEEE Commun. Surveys Tuts.*, 2022.
[499] J. A. Zhang *et al.*, "Enabling joint communication and radar sensing in mobile networks—a survey," *IEEE Commun. Surveys Tuts.*, vol. 24, no. 1, pp. 306–345, 2021.
[500] I. F. Akyildiz *et al.*, "Terahertz band communication: An old problem revisited and research directions for the next decade," *IEEE Trans. Commun.*, vol. 70, no. 6, pp. 4250–4285, 2022.
[501] Y. Wu *et al.*, "Sensing integrated DFT-spread OFDM waveform and deep learning-powered receiver design for terahertz integrated sensing and communication systems," *IEEE Trans. Commun.*, 2022.
[502] Y. Wu, C. Han, and Z. Chen, "DFT-spread orthogonal time frequency space system with superimposed pilots for terahertz integrated sensing and communication," *arXiv preprint arXiv:2202.10035*, 2022.
[503] J. Yang *et al.*, "Integrated sensing and communication with multi-domain cooperation," *arXiv preprint arXiv:2105.03065*, 2021.
[504] S. Helal *et al.*, "Signal processing and machine learning techniques for terahertz sensing: An overview," *IEEE Signal Process. Mag.*, vol. 39, no. 5, pp. 42–62, 2022.
[505] J. M. Mateos-Ramos *et al.*, "Model-driven end-to-end learning for integrated sensing and communication," *arXiv preprint arXiv:2212.10211*, 2022.
[506] Z.-M. Jiang *et al.*, "Intelligent reflecting surface aided dual-function radar and communication system," *IEEE Syst. J.*, vol. 16, no. 1, pp. 475–486, 2021.
[507] X. Wang *et al.*, "Joint waveform and discrete phase shift design for RIS-assisted integrated sensing and communication system under Cramér-Rao bound constraint," *IEEE Trans. Veh. Technol.*, vol. 71, no. 1, pp. 1004–1009, 2021.
[508] ——, "Joint waveform design and passive beamforming for RIS-assisted dual-functional radar-communication system," *IEEE Trans. Veh. Technol.*, vol. 70, no. 5, pp. 5131–5136, 2021.
[509] Z. Wang *et al.*, "Simultaneously transmitting and reflecting surface (STARS) for terahertz communications," *arXiv preprint arXiv:2212.00497*, 2022.
[510] C. Han *et al.*, "THz ISAC: A physical-layer perspective of terahertz integrated sensing and communication," *arXiv preprint arXiv:2209.03145*, 2022.
[511] V. Petrov *et al.*, "On unified vehicular communications and radar sensing in millimeter-wave and low terahertz bands," *IEEE Wireless Commun. Mag.*, vol. 26, no. 3, pp. 146–153, 2019.
[512] Z. Zhang *et al.*, "6G wireless networks: Vision, requirements, architecture, and key technologies," *IEEE Veh. Technol. Mag.*, vol. 14, no. 3, pp. 28–41, 2019.
[513] C. Chaccour *et al.*, "Joint sensing and communication for situational awareness in wireless THz systems," *arXiv preprint arXiv:2111.14044*, 2021.
[514] T. Wild, V. Braun, and H. Viswanathan, "Joint design of communication and sensing for beyond 5G and 6G systems," *IEEE Access*, vol. 9, pp. 30 845–30 857, 2021.
[515] C. Chaccour *et al.*, "Seven defining features of terahertz (THz) wireless systems: A fellowship of communication and sensing," *IEEE Commun. Surveys Tuts.*, vol. 24, no. 2, pp. 967–993, 2022.
[516] Y. Wu, C. Han, and Z. Chen, "THz ISCI: Terahertz integrated sensing, communication and intelligence," in *Proc. Int. Conf. on Infr., Mill. and Ter. Waves (IRMMW-THz)*, 2021, pp. 1–2.
[517] Y. Wu *et al.*, "A sensing integrated DFT-spread OFDM system for terahertz communications," in *Proc. IEEE 93rd Veh. Technol. Conf. (VTC2021-Spring)*, 2021, pp. 1–5.
[518] Y. Wu, C. Han, and T. Yang, "DFT-spread orthogonal time frequency space modulation design for terahertz communications," in *Proc. IEEE Global Commun. Conf. (GLOBECOM)*, 2021, pp. 01–06.
[519] J. Ma and L. Ping, "Data-aided channel estimation in large antenna systems," *IEEE Trans. Signal Process.*, vol. 62, no. 12, pp. 3111–3124, 2014.
[520] W. Cui *et al.*, "Low complexity DOA estimation for wideband off-grid sources based on re-focused compressive sensing with dynamic dictionary," *IEEE J. Sel. Topics Signal Process.*, vol. 13, no. 5, pp. 918–930, 2019.
[521] M. L. Rahman *et al.*, "Joint communication and radar sensing in 5G mobile network by compressive sensing," *IET Commun.*, vol. 14, no. 22, pp. 3977–3988, 2020.
[522] J. He, H. Wymeersch, and M. Juntti, "Channel estimation for RIS-Aided mmWave MIMO systems via atomic norm minimization," *IEEE Trans. Wireless Commun.*, vol. 20, no. 9, pp. 5786–5797, 2021.
[523] J. He, A. Fakhreddine, and G. C. Alexandropoulos, "Joint channel and direction estimation for ground-to-UAV communications enabled by a simultaneous reflecting and sensing RIS," *arXiv preprint arXiv:2210.15238*, 2022.
[524] S. P. Chepuri *et al.*, "Integrated sensing and communications with reconfigurable intelligent surfaces," *arXiv preprint arXiv:2211.01003*, 2022.
[525] J. He *et al.*, "Beyond 5G RIS mmwave systems: Where communication and localization meet," *IEEE Access*, vol. 10, pp. 68 075–68 084, 2022.
[526] J. He, A. Fakhreddine, and G. C. Alexandropoulos, "Simultaneous indoor and outdoor 3D localization with STAR-RIS-Assisted millimeter wave systems," in *Proc. IEEE 96th Veh. Technol. Conf. (VTC2022-Fall)*, 2022, pp. 1–6.
[527] ——, "STAR-RIS-Enabled simultaneous indoor and outdoor 3D localization: Theoretical analysis and algorithmic design," *arXiv preprint arXiv:2302.03342*, 2023.
[528] Q. Gao *et al.*, "Joint location and beamforming design for STAR-RIS assisted NOMA systems," *arXiv preprint arXiv:2206.12836*, 2022.
[529] Z. Wang, X. Mu, and Y. Liu, "STARS enabled integrated sensing and communications," *arXiv preprint arXiv:2207.10748*, 2022.

[530] L. Dai *et al.*, "Delay-phase precoding for wideband THz massive MIMO," *IEEE Trans. Wireless Commun.*, vol. 21, no. 9, pp. 7271–7286, 2022.
[531] W. Chen *et al.*, "An ISAC-based beam alignment approach for enhancing terahertz network coverage," *arXiv preprint arXiv:2212.01728*, 2022.
[532] L. Moeller, J. Federici, and K. Su, "2.5 gbit/s duobinary signalling with narrow bandwidth 0.625 terahertz source," *Electronics letters*, vol. 47, pp. 856 – 858, Jul. 2011.
[533] S. Koenig *et al.*, "Wireless sub-THz communication system with high data rate," *Nature photonics*, vol. 7, pp. 977 – 981, Oct. 2013.
[534] I. Kallfass *et al.*, "64 gbit/s transmission over 850 m fixed wireless link at 240 GHz carrier frequency," *J. Infrared, millimeter, and terahertz waves*, vol. 36, pp. 221 – 233, Jan. 2015.
[535] W. Qiuyu *et al.*, "Design and tests of 21 km, 5 Gbps, 0.14 THz wireless communication system," *High Power Laser and Particle Beams*, vol. 29, p. 060101, Jun. 2017.
[536] X. Li *et al.*, "120 Gb/s wireless terahertz-wave signal delivery by 375 GHz-500 GHz multi-carrier in a 2 × 2 MIMO system," *J. Lightwave Technology*, vol. 37, pp. 606 – 611, Jan. 2019.
[537] S. Jia *et al.*, "2 × 300 Gbit/s line rate PS-64QAM-OFDM THz photonic-wireless transmission," *J. Lightwave Technology*, vol. 38, pp. 4715 – 4721, Sep. 2020.
[538] T. Harter *et al.*, "Generalized kramers–kronig receiver for coherent terahertz communications," *Nature Photonics*, vol. 14, pp. 601 – 606, Sep. 2020.
[539] W. Li *et al.*, "54/104 meters terahertz wireless delivery of 124.8/44.8 Gbit/s signals without terahertz amplifier," in *Asia Commun. and Photonics Conf.*, Shanghai, China, Oct. 2021, pp. 1 – 3.
[540] Y. Horst *et al.*, "Transparent Optical-THz-Optical link transmission over 5/115 m at 240/190 Gbit/s enabled by plasmonics," in *2021 Optical Fiber Commun. Conf. and Exhibition (OFC)*, San Francisco, USA, Jun. 2021, pp. 1 – 3.
[541] J. Zhang *et al.*, "Real-time demonstration of 100 GbE THz-wireless and fiber seamless integration networks," *J. Lightwave Technology*, vol. 14, pp. 1 – 10, Sep. 2022.
[542] M. Zhu *et al.*, "Ultra-wideband fiber-THz-fiber seamless integration communication system toward 6G: architecture, key techniques, and testbed implementation," *Science China Information Sciences*, vol. 66, pp. 1 – 18, Jan. 2023.
[543] O. Li *et al.*, "Integrated sensing and communication in 6G a prototype of high resolution THz sensing on portable device," in *2021 Joint Eur. Conf. on Netw. and Commun. & 6G Summit (EuCNC/6G Summit)*, Porto, Portugal, Jul. 2021, pp. 544 – 549.

Appendix B
Biography Section

Wei Jiang (M'09-SM'19) received a Ph.D. degree in Computer Science from Beijing University of Posts and Telecommunications (BUPT) in 2008. From 2008 to 2012, he was with the 2012 Laboratory, HUAWEI Technologies. From 2012 to 2015, he was with the Institute of Digital Signal Processing, University of Duisburg-Essen, Germany. Since 2015, he has been a Senior Researcher with German Research Center for Artificial Intelligence (DFKI), the biggest European AI research institution and the birthplace of the "Industry 4.0" strategy. Meanwhile, he was a Senior Lecturer with the University of Kaiserslautern, Germany, from 2016 to 2018. He has a monograph titled *6G Key Technologies: A Comprehensive Guide (Wiley&IEEE Press, Nov. 2022)* and contributed three book chapters about 5G and machine-learning-based communications. He has over 90 conference and journal papers, holds around 30 granted patents, and participated in a number of EU and German research projects: *ABSOLUTE*, *5G COHERENT*, *5G SELFNET*, *5G-ACIA*, *AI@EDGE*, *TACNET4.0*, *KICK*, *AI-NET-ANTELLAS*, and *Open6GHub*. He received the best paper award in IEEE CQR 2022 and the best presentation award in IEEE CCAI 2023. He was the Guest Editor for the Special Issue on "Computational Radio Intelligence: A Key for 6G Wireless" in *ZTE Communications* (December 2019). He serves as an Associate Editor for *IEEE Access* (2019 2023), an Editor for *IEEE Communications Letters*, and a Moderator for *IEEE TechRxiv*. He served as a member of the organizing committee or technical committee for many conferences such as IEEE ICASSP 2022, CCS 2014, PIMRC 2020, ICCC 2017/2021/2022, HP3C 2022, icWCSN 2022/2023, Globecom 2022/2023, and ICC 2023. He was the founder and vice chair of the special interest group (SIG) "Cognitive Radio in 5G" under IEEE Technical Committee on Cognitive Networks.

Qiuheng Zhou received his B.Sc degree in Electronics and Information Engineering from Tianjin University of Technology, China, in 2015. He obtained his M.Sc. degree in autonomous and networked driving from the University of Stuttgart, Germany, in 2020. Since April 2020, he has been working as a researcher in the intelligent networks of German Research Center for Artificial Intelligence (DFKI). His main research interests include channel measurement, software-defined radio networks, machine learning, channel prediction, and resource allocation.

Jiguang He (M'20-SM'22) received the Ph.D. degree from the University of Oulu, Finland, in 2018 on communications engineering. He is now a senior researcher at Technology Innovation Institute, Abu Dhabi, United Arab Emirates, and holds Docentship (adjunct professor) at the University of Oulu. From September 2013 to March 2015, he was with the State Key Laboratory of Terahertz and Millimeter Waves at the City University of Hong Kong, working on beam tracking over millimeter wave MIMO systems. From June 2015 to August 2021, he has been with the Centre for Wireless Communications (CWC), University of Oulu, Finland, first as a doctoral candidate, and then a postdoctoral researcher. He was an assistant professor at Macau University of Science and Technology from August 2021 to March 2022. He has participated in many international and national projects, e.g., EU FP7 RESCUE, EU H2020 ARIADNE, 6G Flagship, and received one FDCT-GDST joint research project from Macau Science and Technology Development Fund. He is an Exemplary Reviewer for IEEE Transactions on Communications as well as IEEE Communications Letters and a TPC member for various prestigious IEEE conferences. His research interests span millimeter wave MIMO communications, reconfigurable intelligent surfaces for simultaneous localization and communications (SLAC), and advanced signal processing techniques.

Mohammad Asif Habibi received his B.Sc. degree in Telecommunications Engineering from Kabul University, Afghanistan, in 2011. He obtained his M.Sc. degree in Systems Engineering and Informatics from the Czech University of Life Sciences, Czech Republic, in 2016. Since January 2017, he has been working as a research fellow and Ph.D. candidate at the Division of Wireless Communications and Radio Navigation, Rheinland-Pfälzische Technische Universität (previously known as Technische Universität Kaiserslautern), Germany. From 2011 to 2014, he worked as a radio access network engineer for HUAWEI. His main research interests include network slicing, network function virtualization, resource allocation, machine learning, and radio access network architecture.

Sergiy Melnyk received his Dipl.-Ing degree in Electronics and Information Engineering from Technische University Munich in 2012. Since April 2015, he has been working as a researcher in the Intelligent Networks Group of German Research Center for Artificial Intelligence (DFKI). His main research interests include industrial communications systems, software-defined radio networks, and lower-layer protocol design.

Mohammed El-Absi is currently working as a Senior Researcher at Digital Signal Processing Institute at University of Duisburg-Essen, Duisburg, Germany, where he received his Ph.D. degree (Summa Cum Laude) in electrical engineering in 2015. He received the M.S. degree in electrical engineering in 2008 from Jordan University of Science and Technology and the B.E. degree in electrical engineering in 2005 from Islamic University of Gaza, Gaza, Palestine. He received a Mercator fellow at the Collaborative Research Center ”Mobile Material Characterization and Localization by Electromagnetic Sensing” (MARIE) in the period of 2017-2018. He received the German Academic Exchange Service Fellowship in 2006 and 2011. He is currently contributing in 6G research hub for open, efficient and secure mobile radio systems (6GEM) and Collaborative Research Center ”Mobile Material Characterization and Localization by Electromagnetic Sensing” (MARIE). He is a principal investigator in the excellent terahertz research for communication, localization, material characterization, medical technology and environmental monitoring (terahertz.NRW). His research interests are in the area of communications and signal processing.

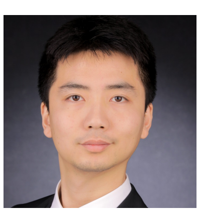

Bin Han (M’15-SM’21) received his B.E. degree in 2009 from Shanghai Jiao Tong University, M.Sc. in 2012 from the Technical University of Darmstadt, and a Ph.D. degree in 2016 from Karlsruhe Institute of Technology. Since July 2016 he has been with the Division of Wireless Communications and Radio Positioning, RPTU Kaiserslautern-Landau (formerly: Technical University of Kaiserslautern) as a Postdoctoral Researcher and Senior Lecturer. His research interests are in the broad area of wireless communications and networking, with the current focus on B5G/6G and MEC. He is the author of one book, five book chapters, and over 50 research papers. He has participated in multiple EU research projects. He is Editorial Board Member for Network, Guest Editor for Electronics, and has served as Organizing Committee Member and/or TPC Member for GLOBECOM, ICC, EuCNC, EW, and ITC. He is a voting member of the IEEE Standards Association Working Groups P2303 and P3106.

Marco Di Renzo (Fellow, IEEE) received the Laurea (cum laude) and Ph.D. degrees in electrical engineering from the University of L’Aquila, Italy, in 2003 and 2007, respectively, and the Habilitation à Diriger des Recherches (Doctor of Science) degree from University Paris-Sud (currently Paris-Saclay University), France, in 2013. Currently, he is a CNRS Research Director (Professor) and the Head of the Intelligent Physical Communications group in the Laboratory of Signals and Systems (L2S) of Paris-Saclay University – CNRS and CentraleSupelec, Paris, France. At Paris-Saclay University, he serves as the Coordinator of the Communications and Networks Research Area of the Laboratory of Excellence DigiCosme, as a Member of the Admission and Evaluation Committee of the Ph.D. School on Information and Communication Technologies, and as a Member of the Evaluation Committee of the Graduate School in Computer Science. He is a Founding Member and the Academic Vice Chair of the Industry Specification Group (ISG) on Reconfigurable Intelligent Surfaces (RIS) within the European Telecommunications Standards Institute (ETSI), where he serves as the Rapporteur for the work item on communication models, channel models, and evaluation methodologies. He is a Fellow of the IEEE, IET, and AAIA; an Ordinary Member of the European Academy of Sciences and Arts, an Ordinary Member of the Academia Europaea; and a Highly Cited Researcher. Also, he holds the 2023 France-Nokia Chair of Excellence in ICT, and was a Fulbright Fellow at City University of New York, USA, a Nokia Foundation Visiting Professor, and a Royal Academy of Engineering Distinguished Visiting Fellow. His recent research awards include the 2021 EURASIP Best Paper Award, the 2022 IEEE COMSOC Outstanding Paper Award, the 2022 Michel Monpetit Prize conferred by the French Academy of Sciences, the 2023 EURASIP Best Paper Award, the 2023 IEEE COMSOC Fred W. Ellersick Prize, and the 2023 IEEE COMSOC Heinrich Hertz Award. He serves as the Editor-in-Chief of IEEE Communications Letters.

Hans D. Schotten (S’93-M’97) received the Ph.D. degree from the RWTH Aachen University of Technology, Germany, in 1997. From 1999 to 2003, he worked for Ericsson. From 2003 to 2007, he worked for Qualcomm. He became manager of a R&D group, Research Coordinator for Qualcomm Europe, and Director for Technical Standards. In 2007, he accepted the offer to become a full professor at the University of Kaiserslautern. In 2012, he - in addition - became the scientific director of the German Research Center for Artificial Intelligence (DFKI) and head of the Department for Intelligent Networks. Professor Schotten served as dean of the Department of Electrical Engineering of the University of Kaiserslautern from 2013 until 2017. Since 2018, he is chairman of the German Society for Information Technology and a member of the Supervisory Board of the VDE. He is the author of more than 200 papers and participated in 30+ European and national collaborative research projects.

Fa-Long Luo (SM'95-F'16) has served as a Board Member of both the Conference Board and the Membership Board of the IEEE Signal Processing Society (SPS) as well as an IEEE Fellow Committee Member. Dr. Luo served as the Society Representative of SPS in the IEEE TAB Committee on Standards. He was the Chairman of the Industry DSP Technology Standing Committee (IDSP-SC) and a Technical Directions Board Member of IEEE SPS as well as a founding member of the IoT SIG of SPS. He was the founding Editor-in-Chief of the International Journal of Digital Multimedia Broadcasting. He has 39 years of academic, industry, and research experience with an emphasis on translating adaptive signal processing techniques to practical applications and commercial products related to multimedia, wireless communications, and digital broadcasting. Including his well-received books: "Applied Neural Networks for Signal Processing" (1997, Cambridge University Press) and "Signal Processing for 5G: Algorithms and Implementations" (2016, Wiley-IEEE), Dr. Luo has published 7 books and more than 100 technical papers in the related fields. Dr. Luo has also contributed 115 USA patents (issued or pending) which have successfully resulted in a number of new or improved commercial products in mass production.

Tarek S. El-Bawab (Fellow, IEEE) is the Dean of the School of Engineering and Professor of Electrical and Computer Engineering at the American University of Nigeria. Before this, he was Professor and Dean of Engineering and Applied Sciences at Nile University (Egypt), Professor of Electrical and Computer Engineering at Jackson State University (USA), and Project Manager with the Network Strategy Group of Alcatel-Lucent USA (now Nokia). Earlier, he assumed research roles with Alcatel-Lucent, Colorado State University (USA), and the University of Essex (UK). Before this he led large-scale international telecommunication projects in the Middle East and Africa for 10 years.

Dr. El-Bawab research interests include telecommunications, network architectures, performance analysis, and Discipline Based Education Research (DBER). He has more than 80 scholarly journal/conference papers and patents. His book Optical Switching is one of the most comprehensive references in its subject. He is the Series Editor of Springer's Textbooks in Telecommunication Engineering, the Editor in Chief of the IEEE Communications Magazine (2017-2021), IEEE Distinguished Lecturer (2016-2019), Eta Kappa Nu (HKN) member, and NSF Review Panelist. Tarek led the Telecommunication Engineering Education (TEE) initiative and movement (2008-2014), which resulted in recognition of network/telecommunication engineering as distinct ABET-accreditable education discipline. He is the first recipient of the IEEE Communications Society's (ComSoc) Education Award due to this work (2015).

He has served IEEE and ComSoc in numerous capacities. He serves/served as Board Member of the IEEE Educational Activities Board, EAB (2016-2017), as Board Member of the IEEE PSPB's Thesaurus Editorial Board (2021-2023), as Board Member of the ComSoc Board of Governors (2014-2015, 2018-2019, and 2020-2021), and Board Member of the ComSoc Educational Services Board (2012-2019). He served as the ComSoc Director of Industry Communities (2020-2021), Director for Standards Development (2018-2019) and Director of Conference Operations (2014-2015). He was elected as Chair of the Transmission, Access, and Optical Systems (TAOS) Technical Committee for two terms, and as chair in several ICC/Globecom Conferences. Dr. El-Bawab has B.Sc. in electrical engineering from Ain Shams University (Egypt), M.Sc. in solid state science from the American University in Cairo, M.Sc. in telecommunications and information systems from the University of Essex (UK), and Ph.D. in electrical engineering from Colorado State University (USA).

Markku Juntti (Fellow, IEEE) received his M.Sc. (EE) and Dr.Sc. (EE) degrees from University of Oulu, Oulu, Finland in 1993 and 1997, respectively. Dr. Juntti was with University of Oulu in 1992–98. In academic year 1994–95, he was a Visiting Scholar at Rice University, Houston, Texas. In 1999–2000, he was a Senior Specialist with Nokia Networks in Oulu, Finland. Dr. Juntti has been a professor of communications engineering since 2000 at University of Oulu, Centre for Wireless Communications (CWC), where he leads the Communications Signal Processing (CSP) Research Group. He also serves as Leader of CWC – Radio Technologies (RT) Research Unit. His research interests include signal processing for wireless networks as well as communications and information theory. He is an author or co-author in almost 500 papers published in international journals and conference records as well as in books *Wideband CDMA for UMTS* in 2000–2010, *Handbook of Signal Processing Systems* in 2013 and 2018 and *5G Wireless Technologies* in 2017. Dr. Juntti is also an Adjunct Professor at Department of Electrical and Computer Engineering, Rice University, Houston, Texas, USA.

Dr. Juntti is an Editor of IEEE TRANSACTIONS ON WIRELESS COMMUNICATIONS, and served previously in a similar role in IEEE TRANSACTIONS ON COMMUNICATIONS and IEEE TRANSACTIONS ON VEHICULAR TECHNOLOGY. He was Secretary of IEEE Communications Society Finland Chapter in 1996–97 and the Chairman for years 2000–01. He has been Secretary of the Technical Program Committee (TPC) of the 2001 IEEE International Conference on Communications (ICC), and the Chair or Co-Chair of the Technical Program Committee of several conferences including 2006 and 2021 IEEE International Symposium on Personal, Indoor and Mobile Radio Communications (PIMRC), the Signal Processing for Communications Symposium of IEEE Globecom 2014, Symposium on Transceivers and Signal Processing for 5G Wireless and mm-Wave Systems of IEEE GlobalSIP 2016, ACM NanoCom 2018, and 2019 International Symposium on Wireless communications Systems (ISWCS). He has also served as the General Chair of 2011 IEEE communications Theory Workshop (CTW 2011) and 2022 IEEE Workshop on Signal Processing Advances in Wireless Communications (SPAWC).

Mérouane Debbah (Fellow, IEEE) is Professor at Khalifa University of Science and Technology in Abu Dhabi. He received the M.Sc. and Ph.D. degrees from the Ecole Normale Supérieure Paris-Saclay, France. He was with Motorola Labs, Saclay, France, from 1999 to 2002, and then with the Vienna Research Center for Telecommunications, Vienna, Austria, until 2003. From 2003 to 2007, he was an Assistant Professor with the Mobile Communications Department, Institut Eurecom, Sophia Antipolis, France. Since 2007, he is Full Professor at CentraleSupelec, Gif-sur-Yvette, France. From 2007 to 2014, he was the Director of the Alcatel-Lucent Chair on Flexible Radio. From 2014 to 2021, he was Vice-President of the Huawei France Research Center. He was jointly the director of the Mathematical and Algorithmic Sciences Lab as well as the director of the Lagrange Mathematical and Computing Research Center. From 2021 to 2023, he was Chief Researcher at the Technology Innovation Institute and leading the AI & Digital Science Research centers at the Technology Innovation Institute. He was also Adjunct Professor with the Department of Machine Learning at the Mohamed Bin Zayed University of Artificial Intelligence in Abu Dhabi. Since 2023, he is Professor at at Khalifa University of Science and Technology in Abu Dhabi and founding director of the 6G center. He has managed 8 EU projects and more than 24 national and international projects. His research interests lie in fundamental mathematics, algorithms, statistics, information, and communication sciences research. He holds more than 40 patents. He is an IEEE Fellow, a WWRF Fellow, a Eurasip Fellow, an AAIA Fellow, an Institut Louis Bachelier Fellow and a Membre émérite SEE. He was a recipient of the ERC Grant MORE (Advanced Mathematical Tools for Complex Network Engineering) from 2012 to 2017. He was a recipient of the Mario Boella Award in 2005, the IEEE Glavieux Prize Award in 2011, the Qualcomm Innovation Prize Award in 2012, the 2019 IEEE Radio Communications Committee Technical Recognition Award and the 2020 SEE Blondel Medal. He received more than 30 best paper awards, among which the 2007 IEEE GLOBECOM Best Paper Award, the Wi-Opt 2009 Best Paper Award, the 2010 Newcom++ Best Paper Award, the WUN CogCom Best Paper 2012 and 2013 Award, the 2014 WCNC Best Paper Award, the 2015 ICC Best Paper Award, the 2015 IEEE Communications Society Leonard G. Abraham Prize, the 2015 IEEE Communications Society Fred W. Ellersick Prize, the 2016 IEEE Communications Society Best Tutorial Paper Award, the 2016 European Wireless Best Paper Award, the 2017 Eurasip Best Paper Award, the 2018 IEEE Marconi Prize Paper Award, the 2019 IEEE Communications Society Young Author Best Paper Award, the 2021 Eurasip Best Paper Award, the 2021 IEEE Marconi Prize Paper Award, the 2022 IEEE Communications Society Outstanding Paper Award, the 2022 ICC Best paper Award, the 2022 IEEE GLOBECOM Best Paper Award, 2022 IEEE TAOS TC Best GCSN Paper Award, the 2022 IEEE International Conference on Metaverse Best Paper Award, the 2023 IEEE Communications Society Fred W. Ellersick Prize, the 2023 ICC best paper award as well as the Valuetools 2007, Valuetools 2008, CrownCom 2009, Valuetools 2012, SAM 2014, and 2017 IEEE Sweden VT-COM-IT Joint Chapter best student paper awards. He is an Associate Editor-in-Chief of the journal Random Matrix: Theory and Applications. He was an Associate Area Editor and Senior Area Editor of the IEEE TRANSACTIONS ON SIGNAL PROCESSING from 2011 to 2013 and from 2013 to 2014, respectively. From 2021 to 2022, he served as an IEEE Signal Processing Society Distinguished Industry Speaker.

VICTOR C. M. LEUNG (Life Fellow, IEEE) is a Distinguished Professor of Computer Science and Software Engineering at Shenzhen University, China. He is also an Emeritus Professor of Electrical and Computer Engineering and Director of the Laboratory for Wireless Networks and Mobile Systems at the University of British Columbia (UBC), Canada. His research is in the broad areas of wireless networks and mobile systems, and he has published widely in these areas. His published works have together attracted more than 50,000 citations. He is named in the current Clarivate Analytics list of "Highly Cited Researchers". Dr. Leung is serving on the editorial boards of the IEEE Transactions on Green Communications and Networking, IEEE Transactions on Cloud Computing, IEEE Transactions on Computational Social Systems, IEEE Access, and several other journals. He received the 1977 APEBC Gold Medal, 1977-1981 NSERC Postgraduate Scholarships, IEEE Vancouver Section Centennial Award, 2011 UBC Killam Research Prize, 2017 Canadian Award for Telecommunications Research, 2018 IEEE TCGCC Distinguished Technical Achievement Recognition Award, and 2018 ACM MSWiM Reginald Fessenden Award. He co-authored papers that won the 2017 IEEE ComSoc Fred W. Ellersick Prize, 2017 IEEE Systems Journal Best Paper Award, 2018 IEEE CSIM Best Journal Paper Award, and 2019 IEEE TCGCC Best Journal Paper Award. He is a Life Fellow of IEEE, and a Fellow of the Royal Society of Canada (Academy of Science), Canadian Academy of Engineering, and Engineering Institute of Canada.